M 2021

U.PORTO
FEUP FACULDADE DE ENGENHARIA
UNIVERSIDADE DO PORTO

A NEW APPROACH ON THE PREDICTION OF DISSOCIATION OF IONIC LIQUIDS

HUGO DA SILVA MARQUES

DISSERTAÇÃO DE MESTRADO APRESENTADA
À FACULDADE DE ENGENHARIA DA UNIVERSIDADE DO PORTO EM
MIEQ – MESTRADO INTEGRADO EM ENGENHARIA QUÍMICA

Master's in Chemical Engineering

A new approach on the prediction of dissociation of ionic liquids

Master dissertation

of

Hugo da Silva Marques

Developed within the course of dissertation

held at



Supervisor at FEUP: **Prof. Elena Gómez Costas**

Joint supervisor at FEUP: **Prof. Maria Eugénia Macedo**





July 2021

CLASSIFIED DOCUMENT. USE ONLY FOR EVALUATION PURPOSES

Acknowledgments

First of all, I would like to express how the elaboration of this thesis has changed my perspective of an academic career for the better. I feel that I have learned so much, acquired so many skills and even improved others that will be useful in my future from a general point of view and not only at work.

Hence, there are many people that I would like to thank. To start, I would like to thank my supervisors, Prof. Maria Eugénia Macedo and Prof. Elena Costas. Without them none of this work would have been possible, since the idea of this thesis was offered to me by them. For that, I am eternally thankful, not only for giving me the opportunity to work on this novelty, but also for being beacons of confidence and optimism. As I stated before, this work was truly a life changing experience and most of it is due to these two amazing people. I would also want to express my gratitude to my colleague Pedro Velho, someone that I can look up as a friend and a reliable teammate that will always be pushing me to keep going forward and improving.

A sincere thank you to all the members of LSRE -LCM that have crossed paths with me, specially to Prof. Madalena Dias, who always demonstrated genuine interest and concern for my academic ventures.

A special thank you to my parents that have made everything that has been to their disposable in order for me to be where I am today. Thank you to my oldest, dearest and best friend, my brother André, who has taught me so much in life that I will never be able to repay. To the rest of my family, my soon-to-be sister-in-law, my sister and stepmother, thank you for all the help and support. Thank you for all the unconditional love and support you have given me in all these years.

I would also want to thank some professors that have left their mark on me through my academic pathway. To Prof. Joana Peres, Prof. Joaquim Faria, Prof. José Orfão, Prof. Fernão Magalhães, Prof. Adrián Silva, Prof., Fernando Pereira, Prof. Mafalda Ribeiro, Prof. Alexandre Ferreira, Prof. Manuel Alves, Prof. Miguel Loureiro and Prof. Mário Rui. Lastly, but not least important, I would like to specially thank Prof. Ricardo Santos for believing in me until the end and being an incredible professor.

Finally, I would like to give a big thank you to all my friends from FEUP (Eva, Ana, Manuel, Gonçalo, Beatriz, Helena, Rui, Pedro, Nuno and Ana Sousa) and to my other friends from different parts of my life (Vânia, Ana Rita and Rui). Thank you for being here for me, for pulling me to the ground when got too much over my head, for all your support and, most importantly, for making me who I am today.

To all the incredible people in my life, thank you.

Abstract

Ionic liquids (ILs) are ionic compounds that are liquids at room temperature. These have increased in interest since the beginning of the millennium. These are a new class of solvents that can replace the volatile organic compounds (VOCs) due to a large array of properties, such as negligible vapor pressure, thermal stability and high solubility for a wide variety of compounds, which makes them attractive for several applications (chemical synthesis, catalysis, liquid-liquid separation processes). Therefore, it is needed to understand the behavior of equilibrium of mixtures containing ionic liquids in order to design process units and operation processes. Moreover, thermodynamic models are required to describe the behavior and the properties of ionic liquids in liquid-liquid equilibria (LLE).

In this work, the main goal was to study the LLE of ionic liquids in water systems concerning the degree of dissociation that occurs as well as how this phenomenon is affected by the structural properties, such as the length of the alkyl chain in the cation, the cation and the anion of the ionic liquids. For this purpose, an extensive review of the LLE of ionic liquid/water systems available in literature was carried out and selected equilibria data were compiled in a database. Additionally, appropriate thermodynamic models were used to study the existence of dissociation and its extent: no dissociation, partial dissociation and total dissociation. Besides finding appropriate models, the influence of the closest approach parameter in the Pitzer-Debye-Hückel (PDH) equation was also studied.

Three values of the closest approach parameter (a minimum, an average and a maximum value) were obtained for fourteen aqueous systems of the scope of this work (ionic liquid/water). Afterwards, LLE data was modeled for the systems mentioned above applying the UNIQUAC model, that only accounts for short-range interactions, and the PDH + UNIQUAC model, that accounts for short and long-range interactions, with different values of the closest approach parameter. These thermodynamic models provided results which agreed with the extent of dissociation of each type of system found in the literature. Afterwards, an evaluation of the influence of the cation's alkyl chain length, the cation and the anion of ionic liquids on the interaction parameters was performed. Based on these conclusions with was possible to reduce the number of parameters of the PDH + UNIQUAC model. All the calculations were performed in the same manner for these new thermodynamic models and all the conclusions found previously were still valid. Finally, this work allowed to predict the dissociation of ionic liquids in water only based on the results of the application of thermodynamic models from LLE data, giving a fundamental importance to the closest approach parameter, which is the principal novelty of this work.

Keywords: Ionic liquids, LLE, UNIQUAC, Pitzer-Debye-Hückel, closest approach parameter

Resumo

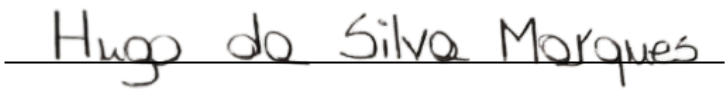
Líquidos iónicos são compostos iónicos que existem em fase líquida à temperatura ambiente. O seu interesse tem vindo a crescer desde o início do milénio. Estes são uma nova classe de solventes que pretendem substituir os compostos orgânicos voláteis (COVs) devido a uma variedade de propriedades, como a sua pressão de vapor desprezável, estabilidade térmica e elevada solubilidade para um elevado número de compostos, que os torna atrativos para diversas aplicações (síntese química, catálise, separações liquido-líquido). Desta forma, é necessário compreender o equilíbrio de misturas que contenham líquidos iónicos para que se possam projetar unidades e operações processuais. Para além disto, são necessários modelos termodinâmicos que descrevam o comportamento e propriedades dos líquidos iónicos em equilíbrio líquido-líquido (ELL).

Neste trabalho, o principal objetivo foi estudar o ELL de líquidos iónicos em sistemas com água, tendo em conta o grau de dissociação que ocorre assim como de que forma este fenómeno é afetado pelas propriedades estruturais, como o comprimento da cadeia alquílica no catião, o catião em si, assim como o anião presente no líquido iónico. Para este objetivo, realizou-se uma revisão extensa dos sistemas líquido iónico/água existentes na literatura. Adicionalmente, modelos termodinâmicos apropriados foram usados para estudar a existência de dissociação, assim como a sua extensão, podendo esta ser nula, parcial ou total. Para além da seleção de modelos apropriados, foi também estudada a influência do parâmetro de aproximação iónica da equação de Pitzer-Debye-Hückel.

Obtiveram-se três valores do parâmetro de aproximação (um mínimo, um médio e um máximo), para catorze sistemas aquosos de líquido iónico/água. Em seguida, diagramas de ELL foram modelados para os sistemas mencionados acima aplicando o modelo UNIQUAC, que apenas considera interações de curto alcance, e para o modelo PDH+ UNIQUAC, que considera interações de curto e longo alcance. Este último modelo foi testado com diferentes valores do parâmetro de aproximação. Os modelos termodinâmicos usados geraram resultados concordantes com a extensão de dissociação de cada tipo de sistema encontrada na literatura. Em seguida, fez se uma avaliação da influência do comprimento da cadeia alquílica do catião, do catião em si, e do anião, e de como estes afetavam os parâmetros de interação. Com estas conclusões foi possível diminuir o número de parâmetros do modelo PDH+ UNIQUAC. Todos os cálculos foram realizados da mesma forma para este novo modelo termodinâmico e todas as conclusões se mantiveram igualmente válidas. Por fim, este trabalho permitiu prever a dissociação de líquidos iónicos em água, baseando-se apenas nos resultados da aplicação de modelos termodinâmicos a partir de dados de equilíbrio líquido-líquido, dando uma importância nova ao parâmetro de aproximação, sendo essa a principal inovação contida neste trabalho.

Declaration

I hereby declare, under word of honor, that this work is original and that all non-original contributions are indicated and due reference is given to the author and source



Hugo da Silva Marques, 5 July, 2021

Index

1 Introduction 1
1.1 Framing and presentation of the work 1
1.2 Presentation of the company 2
1.3 Author's contribution 3
1.4 Organization of the dissertation 4
2 Context and state of the art 5
2.1 Ionic liquids: an overview 5
2.2 Applications 7
2.3 Phase equilibria for ionic liquids and water system 9
3 Computational applications 13
3.1 Microsoft Excel 13
3.2 MATLAB 13
3.3 CurveExpert Professional 14
4 Theory and modeling approach 15
4.1 Liquid-liquid equilibrium criterion 15
4.2 Thermodynamic models used in this work 16
4.3 Closest approach parameter 20
5 Results and discussion 25
5.1 Ionic liquids selected 25
5.2 Thermodynamic models used in this work 28
5.3 Modeling results obtained in this work 28
6 Conclusions 41
7 Assessment of the work done 43
7.1 Objectives achieved 43
7.2 Suggestions of future work 43
7.3 Final assessment 44
8 References 45
Appendixes 51

List of figures

Figure 2.1 - Most common cations and anions found in ionic liquids' families 5

Figure 2.2 – Number of Web of Science publications per year since 1990 on ionic liquids..... 6

Figure 2.3 – Conventional applications of ionic liquids..... 8

Figure 4.1 - Representation of the hard-core collision diameter in ionic liquids.....21

Figure 5.1 –Some examples for calculated solubility curves for the binary system ionic liquid/water at atmospheric pressure... 30

Figure 5.2 - Influence of alkyl chain length, cation and anion in ionic liquid/water systems for the UNIQUAC model 32

Figure 5.3 – UNIQUAC interaction parameters for PDH + UNIQUAC model for the influence of the alkyl chain length in ionic liquid/water systems.... 34

Figure 5.4 - UNIQUAC interaction parameters for PDH + UNIQUAC model for the influence of the cation in ionic liquid/water systems... 35

Figure 5.5 - UNIQUAC interaction parameters for PDH + UNIQUAC model for the influence of the anion in ionic liquid/water systems.....36

Figure 5.6 – Some examples for calculated solubility curves for the binary system ionic liquid/water at atmospheric pressure considering the PDH + UNIQUAC model with 4 parameters... 37

Figure 5.7 - Deviations for the studied ionic liquids in this work... 39

List of tables

Table 4.1 - Constants used in the Pitzer-Debye-Hückel term. 19

Table 4.2 - Calculated values for the minimum, medium and maximum closest approach parameter at 40 ºC for the ionic liquids used in this work.. 23

Table 5.1 - Ionic liquids selected in this work.....26

Table 5.2 -Dissociation ranges for ionic liquids of the dicyanamide family.. 27

Table 5.3 - Dissociation degree for the selected ionic liquids/water systems.....27

Table 5.4 - UNIQUAC and PDH + UNIQUAC deviations obtained from LLE modeling. 31

Table 5.5 - PDH + UNIQUAC with 4 parameters deviation obtained from LLE modeling 38

Notation and Glossary

T	Temperature	K
a_{i}	Activity of species i	
x_{i}	Mole fraction of species i	
G^{E}	Excess Gibbs energy	J
r_{i}	Molecular van der Waals volume	
q_{i}	Molecular van der Waals surface area	
l_{i}	UNIQUAC's combinatorial term parameter	
Δu_{ij}	UNIQUAC interaction parameter	K
a_{ij}	UNIQUAC interaction parameter	K
b_{ij}	UNIQUAC interaction parameter	
I_{x}	Ionic strength	
$I_{\mathrm{x}}{}^{\nabla}$	PDH parameter computed from ionic charges	
$A_{\mathrm{DH,x}}$	PDH parameter computed from physical constants and temperature	
z_{i}	Ionic charge of species i	
a	Hard-core collision diameter	m
M_{i}	Molecular mass of species i	$g \cdot mol^{-1}$
R_{IL}	Ionic liquid ionic radius	m
R_{W}	Water molecular radius	m
N_{spec}	Number of species in solution	
N_{ion}	Number of ions in solution	
n	Number of experimental points	
R_{i}	Arbitrary alkyl group	
R	Ideal gas constant	$J \cdot mol^{-1} \cdot K^{-1}$
N_{A}	Avogadro's number	mol^{-1}
e	Electronic charge	C
k	Boltzmann constant	$J \cdot K^{-1}$
r	Hydrodynamic radius of particle	m
D	Diffusion coefficient of particle	$m^2 \cdot s^{-1}$

Greek Letters

μ	Chemical potential	$J \cdot mol^{-1}$
α	Phase α	
β	Phase β	
γ_i	Activity coefficient of species i	
ϕ_i	Volume fraction of species i	
θ_i	Surface area fraction of species i	
τ_{ij}	UNIQUAC's residual term parameter	
ρ	Closest approach parameter	
ρ_0	Density of solvent	$kg \cdot m^{-3}$
ρ_i	Density of species i	$kg \cdot m^{-3}$
ε	Dielectric constant of solvent	
ε_0	Vacuum permittivity	$C^2 \cdot J^{-1} \cdot m^{-1}$
η	Viscosity of particle	$Pa \cdot s$
σ	Deviation of composition	

Indexes

i	Species i
o	Adopted standard state
UNIQUAC	UNIversal QUAsiChemical model
PDH	Pitzer-Debye-Hückel equation
C	Combinatorial term
R	Residual term
min	Minimum value for the closest approach parameter
med	Average value for the closest approach parameter
max	Maximum value for the closest approach parameter
exp	Experimental value
calc	Calculated value
IL	Ionic liquid-rich phase
W	Water-rich phase

List of Acronyms

VOC	Volatile organic compound
LLE	Liquid-liquid equilibrium/equilibria
EoS	Equation of state
CPA	Cubic Plus Association
PC-SAFT	Perturbed Chain Statistical Associating Fluid Theory
NRTL	Non-Random-Two-Liquid
UNIQUAC	UNIversal QUAsiChemical
COSMO-RS	Conductor like Screening Model for Real Solvents
QSPR	Quantitative structure-property relationship
PDH	Pitzer-Debye-Hückel
VBA	Visual Basic for Applications

1 Introduction

1.1 Framing and presentation of the work

Electrolyte solutions are present in several branches of daily life and find numerous applications in physical sciences including chemistry, geology, material science, medicine, biochemistry as well as in many engineering fields, especially, chemical, biochemical, electrical and petroleum engineering. In all these applications, Thermodynamics plays a crucial role in the understanding of the behavior of phase equilibria and physical properties.

Ionic liquids (ILs) are compounds composed of ions that are liquid at temperatures close to room temperature and they are called "green" because of their negligible vapor pressure and their general non-toxicity. They are considered as alternative solvents to the traditional volatile organic compounds (VOCs). Another important characteristic is that an ionic liquid suitable for a specific application can be synthesized by adequate combination of the anion and cation. Moreover, other well-known properties are: thermal stability and high solubility for a wide variety of compounds.

The overall aim of this project is to evaluate and assess the dissociation of ionic liquids in binary aqueous solutions based on liquid-liquid equilibria (LLE) data from the literature. For this purpose, two thermodynamic models will be applied to predict the degree of dissociation (none, partial or total): the conventional UNIversal QUAsiChemical (UNIQUAC) model for short-range interactions and the Pitzer-Debye-Hückel (PDH) equation, to account for the long-range interactions, combined with the UNIQUAC model (PDH + UNIQUAC). For the first time, one of the parameters in the PDH equation (the closest approach parameter) will be calculated accounting for all the different dissociation extent, enhancing its physical meaning.

This was a risky, ambitious and crucial task, but a successful completion will have significant impact in the scientific community. The proposed research will significantly have contributed considerably to the comprehension of the behavior of the ionic liquids. Although the difficulties mentioned before, the main goal was fully achieved.

1.2 Presentation of the company

The Associate Laboratory LSRE-LCM is a partnership between LSRE - Laboratory of Separation and Reaction Engineering and LCM - Laboratory of Catalysis and Materials. Promoting the advance of scientific and technological know-how in the Chemical Engineering areas of Separation and Reaction Processes, Product Engineering, Catalysis and Carbon Materials, Thermodynamics and Environmental Engineering.

The research interests of the Thermodynamics and Environmental group fall into four scientific sub-areas: Chemical Engineering Thermodynamics, Water Management, Processes for Pollution Control and Waste Reuse, Recycling and Valorization. Efficient and environmentally friendly technologies aiming at pollution abatement, waste valorization and products recovery as well as thermodynamic modeling are the major concerns of this group.

The Chemical Engineering Thermodynamics group is a research line which uses the general concepts of Applied Thermodynamics for different separation and reaction processes. The main focus is on the application to Biotechnology and Pharmaceutical industries. The team has a very extensive and high merit expertise in both experimental measurements of different types of phase equilibria (vapor-liquid, liquid-liquid, solid-liquid equilibria and Aqueous Two-Phase Systems) and modeling with excess Gibbs energy models and equations of state, being internationally recognized. Research activities are targeted to the development of new predictive methodologies that will enable to support the design of new and green separation processes using environmental benign solvents (e.g., ionic liquids, deep eutectic solvents). The characterization of these solvents is a fundamental task for the purposes to be achieved.

1.3 Author's contribution

The work was started by searching all the available liquid-liquid equilibria (LLE) data of binary ionic liquid/water systems in the literature. After a thorough search, a database of the LLE data was built in the Microsoft Excel application. From this database some ionic liquids with features of interest were selected and another database was developed with the solubility experimental data for the aforementioned systems. This last database functioned as an input file for the MATLAB program that was developed from scratch afterwards. Another task was to relocate the knowledge of different programing languages for the MATLAB programing language in order to make the code consisting of the before mentioned input Excel file, all the calculation mechanisms, the optimization subroutines that made physical sense in the context of this work and the output files, also known as the results. These results consisted of the calculation of several properties, optimized parameters and values of the objective function. The code was also programed to display the results in the form of graphs and tables. Lastly, the understanding of the results and conclusions of this thesis were performed by the author. In summary, the author's contribution was to carry out all the presented work, under the guidance of the supervisors.

1.4 Organization of the dissertation

Including this introductory chapter, this work is divided into eight chapters.

Chapter 1: **Introduction**. The first chapter entitled Introduction is devoted to the presentation of the addressed problem and to the work carried out.

Chapter 2: **State of the art**. This chapter describes shortly the background on ionic liquids, their properties, applications and the reason behind their rise of interest since the 2000s. Following, a summary for the liquid-liquid equilibria with ionic liquid/water systems is carried out as well as a report of the key points on the modeling of ionic liquids equilibria throughout the years, giving special focus to the modeling of ionic liquids as electrolytes.

Chapter 3: **Computational applications**. This chapter provides a brief context of which informatic tools were used in the elaboration of this work and also which features they have and how they were used.

Chapter 4: **Theory and modeling approach**. In this chapter, the fundamental equations and thermodynamic models used are introduced, which include the liquid-liquid equilibrium criterion, the UNIQUAC model and the PDH + UNIQUAC model. These are presented with their physical background, giving special focus on the closest approach parameter.

Chapter 5: **Results and discussion.** The results are presented in graphs and tables with exhaustive explanation. In further detail, plots of the modeling results of this work are compared to the experimental data from literature, together with the deviation values and the optimized UNIQUAC interaction parameters for the general dissociation behavior of some ionic liquids in water systems.

Chapter 6: **Conclusions**. the main highlights of this work are assessed in this chapter, while paving the way for a further reflection on which goals of the work were fulfilled.

Chapter 7: **Assessment of work done**. As the previous chapter indicates, a reflection of the work carried out is made.

Chapter 8: **References**. The last chapter includes the References, where all the bibliography used is present.

2 Context and state of the art

2.1 Ionic liquids: an overview

Ionic liquids are chemical compounds with a melting temperature below 100 ºC, at atmospheric pressure[1,2]. Ionic liquids are composed of one anion and one cation. Generally, the cation is larger than the anion and presents reduced degree of symmetry[3]. Most ionic liquids are based on cations such as imidazoliums, pyridiniums, pyrrolidiniums, ammoniums and phosphoniums[3,4]. Regarding the anions, the most common are halides (e.g., chloride, Cl^-, and bromide, Br^-), fluorinated anions (tetrafluoroborate, $[BF_4]^-$, and hexafluorophosphate, $[PF_6]^-$), bis(trifluoromethylsulfonyl)imide, $[NTf_2]^-$, trifluoromethanesulfonate, $[TFO]^-$, and others such as acetate, dicyanamide, alkyl phosphate and alkyl sulfate[3,4]. Figure 2.1 presents the most common cation and anion families of ionic liquids. The R_i groups in the figure correspond to some arbitrary alkyl groups.

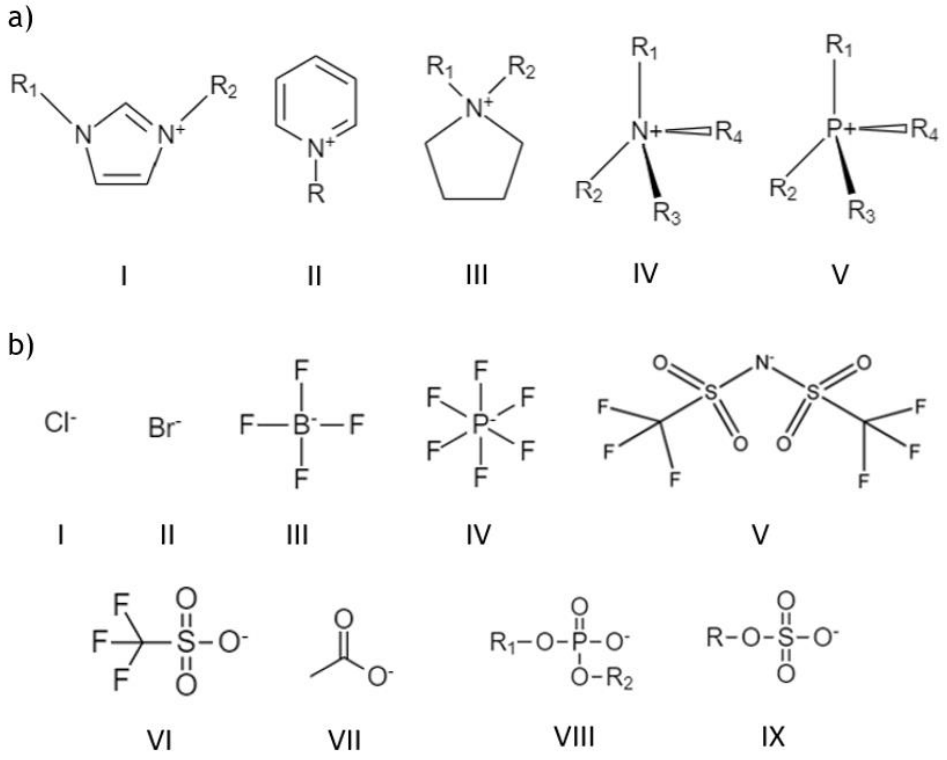


Fig. 2.1: Most common a) cations and b) anions found in ionic liquids' families. a) I – imidazolium, II – pyridinium, III – pyrrolidinium, IV – ammonium, V – phosphonium. b) I – chloride, II – bromide, III – tetrafluoroborate, V – hexafluorophosphate, V - bis(trifluoromethylsulfonyl)imide, VI – trifluoromethanesulfonate, VII – acetate, VII – dicyanamide, VIII – alkyl phosphate, IX – alkyl sulfate.

The first work reporting the synthesis of an ionic liquid - ethylammonium nitrate, ($[C_2NH_3][NO_3]$) – was published in 1914 by Walden[5,6]. This ionic liquid presented a melting temperature of 12 ºC at atmospheric pressure[7]. At this time, some of the studied ionic liquids were considered very reactive with water[8]. Therefore, only with the discovery of new ionic liquids, more stable with water, the interest of these compounds increased again[9,10]. Since then, the interest of the scientific community on these compounds has been increasing for different purposes, such as chemical synthesis, extraction processes, catalysis among many others[1,11]. Moreover, the number of publications concerning ionic liquids has increased exponentially since 2000, as Figure 2.2 shows.

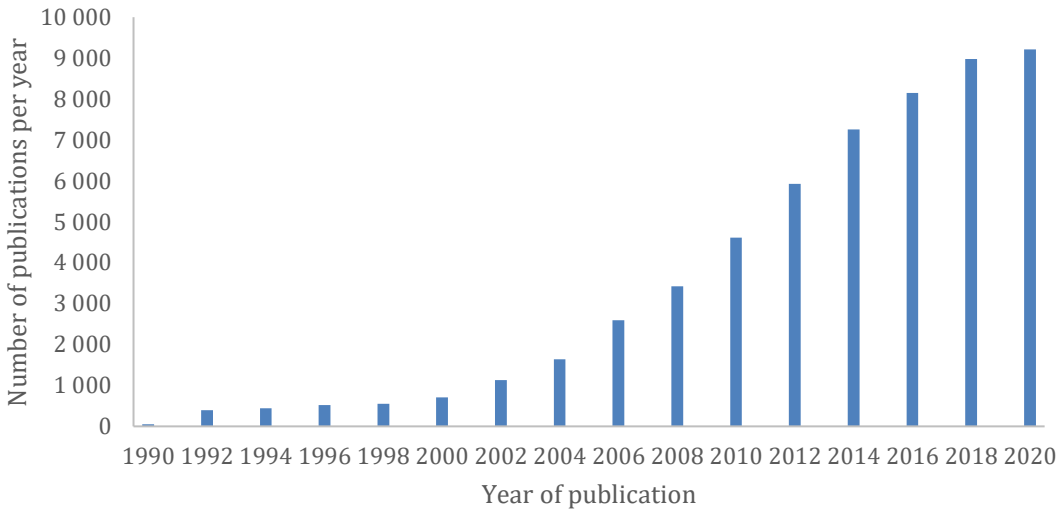


Fig. 2.2: Number of Web of Science publications per year since 1990 on ionic liquids. Data taken from Web of Science (accessed in May 2021). Topic of search: ionic liquids.

Ionic liquids have several physical-chemical properties that make them highly interesting, such as being liquids over a large range of temperatures. Some of them can even be in the liquid state from below 0 ºC to 300 ºC[10]. In general, they have low flammability, high chemical and thermal stability, high selectivity and solvation capability for organic, inorganic and organometallic compounds. Moreover, they have high ionic conductivity[12,13]. From an environmental point of view, it must be referred that their vapor pressure is often negligible and that they usually have low toxicity, which makes them ecofriendly substitutes for volatile organic compounds (VOCs)[1,2,3,11,12,13], and their study is considered priority by the United States Environmental Protection Agency[14]. Although many of these characteristics are found in several ionic liquids, not all present the mentioned properties, since it is a very broad family of chemical species. However, ionic liquids present some drawbacks, such as their high cost and low flexibility[15].

It is possible to synthesize an enormous amount of ionic liquids, with different physical-chemical properties according to the final desired applications. Therefore, they are often called “designer solvents” or “tunable materials”, which makes them very appealing compounds and have been successfully used in a wide range of industries[1,10,16]. The main applications for ionic liquids are discussed in the following section.

2.2 Applications

Ionic liquids have been investigated for applications in many different fields, such as chemical synthesis[13,17-20], catalysis[18,21,22], electrochemistry[10,12,13,23,24], analytical chemistry[16,24], liquid-liquid extraction[25-27], nanotechnology[24] and biotechnology[28]. They can act as solvent and can be used as additives to change properties of mixtures.

Some other applications of ionic liquids include recovery of polar compounds, like acetone, ethanol and butanol from fermentation processes[11,12], removal of organic contaminants and ionic metals from aqueous waste streams[11] and demulsification processes[2]. Another use of ionic liquids is in homogeneous and biphasic transfer catalysis[12,13,17,24,25,29,30]. The most important applications of ionic liquids can be found in Figure 2.3.

The areas of biochemistry, pharmacy and biology have also achieved very relevant results with the implementation of these compounds as solvents, since, as earlier stated they are biocompatible[13,24], which is a requirement to ensure the stability and activity of enzymes and proteins in the bioindustry. Further, the use of ionic liquids in the extraction and purification of several biomolecules such as amino acids, proteins, antibiotics, hormones, DNA, biofuels and opium alkaloids, among others, has been successful[13].

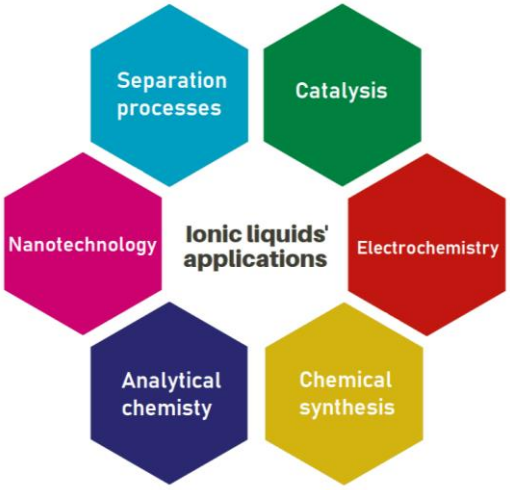


Fig. 2.3: Conventional applications of ionic liquids.

The first patent involving an industrial application of ionic liquids dates from 1934 and is related to cellulose solutions[15,30]. Ionic liquids are used as catalyst by Eastman chemical company since 1996[15]. They are also used as a mercury removal solvent from oil streams in hydrocarbon production facilities by Petronas since 2012[32] and by some other companies such as SASOL (South Africa), BP (United Kingdom), Evonik Degussa (Germany), ExxonMobil (United States), Petro China (China)[15]. However, the most successful industrial application involving ionic liquids is the BASIL process, implemented by BASF (Germany), since 2002[15].

2.3 Phase equilibria for ionic liquids and water systems

One of the areas in which research on ionic liquids has been carried out extensively is in extraction processes. For this, the behavior of liquid-liquid equilibria (LLE) of systems with water or organic solvents with ionic liquids must be known[33].

In this context, LLE data for binary ionic liquid/water systems is reported in the literature for different ionic liquids. It is important to highlight that ionic liquid/water systems are widely found in several industrial processes[12]. In literature there are, at least, 108 229 publications (Web of Science) focused on ionic liquids, but when this search is restricted to LLE only 1 584 results are obtained. A narrower interval is found for the topic "ionic liquid water liquid-liquid equilibria", with 761 publications.

This knowledge of the behavior of the LLE is important to design extraction units, so as to reduce the number of experiments and it is crucial to develop thermodynamic models to accurately represent and predict this kind of data. Otherwise, it would become a very expensive and time-consuming task, since the determination of the LLE data is usually obtained using gravimetric methods[1,13,34], refractometric techniques[34,35], static methods[36] and conductivity methods[36,37].

2.3.1 Modeling of ionic liquids and water systems

Since it is time-consuming to undergo the experimental determinations of phase equilibria, one convenient tool is the thermodynamic modeling. By definition, there are two types of models: equations of state (EoS), that are used to calculate fugacity coefficients[38] (such as the Cubic Plus Association (CPA)[39] and the Perturbed Chain Statistical Associating Fluid Theory (PC-SAFT), an EoS that is based on the Statistical Associating Fluid Theory[40]) and models based on equations for the excess Gibbs energy, used to calculate activity coefficients (such as the Non-Random-Two-Liquid (NRTL) model and the Universal Quasichemical (UNIQUAC) model).

The majority of publications involving LLE data of ionic liquids/water only report experimental data. The few that present thermodynamic modeling only applied the NRTL model[1,2,35-37,41] and the Conductor like Screening Model for Real Solvents (COSMO-RS) model[11,12,42-44].

Some other approaches included the PC-SAFT EoS, for example, for the fitting of the LLE data for several ionic liquid/water systems. These included the work of Domanska *et al.* (2016)[45], where the 1-hexyl-1-methylpyrrolidinium, $[C_6C_1pyr]^+$, the 1-hexyl-1,4-diaza-[2.2.2]-bicyclooctanium, $[C_6DABCO]^+$, the 1-(2-methoxyethyl)-3-methylimidazolium, $[C_{201}C_1im]^+$ and the 1-(2-methoxethyl)-1-methylpyrrolidinium, $[C_{201}C_1pyr]^+$, cations were used combined with the bis(trifluoromethylsulfonyl)imide anion, $[NTf_2]^-$, in water systems. The authors used the NRTL model and the PC-SAFT equation. The NRTL model was applied in a purely correlative way while the PC-SAFT EoS was used as a predictive tool for the LLE.

Freire *et al.* (2010)[46] used a quantitative structure-property relationship (QSPR) model to predict the mutual solubilities of ionic liquids and water. The ionic liquids studied in this work were composed by hexafluorophosphate and bis(trifluoromethylsulfonyl)imide anions combined with imidazolium and pyridinium cations.

2.3.2 Modeling of ionic liquids as electrolytes in water systems

Most of the works published so far considered the ionic liquids as a "neutral" species, but since the early 2000s that discussion about considering ionic liquids in solution as neutral in the entire composition range or if they can dissociate has arisen. Therefore, this question concerning the possibility of total or partial dissociation of ionic liquids in solution is emerging.

Some publications focused on measurements of conductivities of ionic liquids[47-49] suggest that the ionic liquid could be dissociated and there are some works which report the dissociation constants and the ionicity of ionic liquid solutions[50-53]. Nordness *et al.* (2019)[54] calculated the ionicity of some ionic liquids (mostly based on $[NTf_2]^-$ anion), using experimental density, viscosity and conductivity of ionic liquids available in the literature. Then, the values of ionicity were related to degrees of dissociation.

Nordness and Brennecke (2020)[4] suggested the ionic liquid dissociation under some conditions. Since several solutions of ionic liquids with solvents, not only water, present conductivity, as shown in literature, it is hinted that there are ions in the solution prevenient of the dissociation of the ionic liquid.

From a scientific and industrial point of view, the extent to which cations and anions in ionic liquids solutions are dissociated is of fundamental importance since its dissociation affects viscosity, density, solubility, among other important physical-chemical properties[4]. On the other hand, considering ionic liquids as electrolytes requires thermodynamic models that account for long-range interactions, and these were scarcely used so far. An earlier effort was reported by Maia *et al.* (2010)[1] who applied a modification of the NRTL model which included a Debye-Hückel term that takes into consideration the long-range forces, more suitable for systems containing electrolytes: the electrolyte-NRTL model (eNRTL). The results were compared with the conventional NRTL equation. Both models yielded results that agreed with the experimental data for low temperatures, while near the critical region the NRTL model performed better, for the systems $[C_6mim][BF_4]$/water and $[C_8mim][BF_4]$/water.

Recently, Lin *et al.* (2021)[55] reported that some of the prior works assuming either no dissociation or complete dissociation were not consistent with experimental observations. In this publication, the partial dissociation of three ionic liquids (1-ethyl-3-methylimidazolium ethylsulfate, $[C_2mim][EtSO_4]$, 1-ethyl-3-methylimidazolium trifluoroacetate, $[C_2mim][TFA]$, and 1-ethyl-3-methylimidazolium trifluoromethanesulfonate, $[C_2mim][TFO]$), using vapor-liquid equilibria (VLE) data, was considered and the dissociation equilibria was described using the values of dissociation constants. The authors used the Redlich-Kwong equation of state for the vapor phase and the eNRTL model for the liquid phase.

Having this in mind, the aim of this project is to evaluate and assess the dissociation of ionic liquids in aqueous solutions based on LLE data from the literature[1,2,11,12,13]. For this purpose, two thermodynamic models will be applied to predict the extent of dissociation (none, partial or total): the conventional UNIversal QUAsiChemical (UNIQUAC) model and the Pitzer-Debye-Hückel (PDH) equation for the long-range interactions combined with the UNIQUAC model (PDH + UNIQUAC). For the first time, one of the parameters in the PDH equation (the closest approach parameter) will be calculated accounting for all the different dissociation extent, enhancing its physical meaning.

3 Computational applications

3.1 Microsoft Excel

Microsoft Excel is a program developed by Microsoft for analysis and storage of data in spreadsheet form. Its features include calculation, graphing tools, pivot tables and a macro programing language: Visual Basic for Applications (VBA). Excel is part of the Microsoft Office suite of software and has been extensively used for data treatment in a variety of fields.

In this work, it was used as a database tool, as calculation instrument and as an input file for the MATLAB program.

3.2 MATLAB

MATLAB is a programming and numeric computing platform used by engineers and researchers to analyze data, develop algorithms, and create models. It is used worldwide for a range of applications, in industry and academia, including deep learning and machine learning, signal processing and communications, image and video processing, control systems, test and measurement, computational finance, and computational biology.

For this project, MATLAB was employed as the selected tool to program the two distinct thermodynamic models used. It was used for to build a code that could run the calculations for the required properties, while finding the optimal values for the designated model. The core of this code has 4 main branches. The first is in the structure of the code containing variables that do not depend on the equilibria data from the Microsoft Excel database and the equations that rule the thermodynamic computations required to achieve the modeling results. The second feature of this program is its ability to receive an input, where all the information related to the studied system are transferred into the program from an external source, e.g., an Excel spreadsheet. The following element is its optimization routine, where several iterations are made to obtain the minimum value possible for the objective function, specified for the goal of this work. Finally, the last component of the program is the output. In the output, the optimized results are displayed and combined with the value of the objective function. Graphics comparing the experimental and modeling data were displayed as outputs including parity plots. The deviations were also displayed in the results window. These outputs could also be externally saved to another source for further processing.

3.3 CurveExpert Professional

CurveExpert Professional is a cross-platform solution for curve fitting and data analysis. CurveExpert Professional is intended for heavy duty nonlinear regression analysis (curve fitting) and smoothing of data. This program gives for a level of detail and convenience not possible by a basic fitting program, allowing for multiple custom models for a single dataset, as well as the direct application of these same models on multiple datasets, which can be visualized and analyzed simultaneously.

This program was essential in the fitting of the MATLAB results. With it, the best adjusted curve was obtained.

4 Theory and modeling approach

In this chapter the main concepts of phase equilibria and the equations of the adopted thermodynamic models are presented. It is worth to remark that special focus is given to liquid-liquid equilibrium (LLE) of binary systems of ionic liquid/water. The reason is due mainly to the fact that this kind of information will be used for the studies of the dissociation of ionic liquids.

4.1 Liquid-liquid equilibrium criterion

Modeling phase equilibria data is crucial to develop and design processes and operation units based on equilibrium stages, such as distillation, liquid-liquid extraction or crystallization[1].

The general phase equilibrium condition is the equality of chemical potential, μ, of a given species i in all phases. This criterion is depicted by eq.(4.1), for a two phase system composed of phases α and β.

$$\mu_i^{\alpha} = \mu_i^{\beta} \tag{4.1}$$

Assuming a pure liquid state at the system temperature and pressure as the standard state for all components of the solution, the chemical potential of a species i may be written as eq.(4.2):

$$\mu_i = \mu_i^{\circ} + RT \ln(a_i) \tag{4.2}$$

where μ_i° is the chemical potential at the adopted standard state, R is the ideal gas constant, T is the absolute temperature and a_i is the activity of species i.

Combining eq.(4.1) and eq.(4.2) the liquid-liquid equilibria (LLE) criteria reduces to an activity equality for each species i in the solution. This result is shown by eq.(4.3).

$$a_i^{\alpha} = a_i^{\beta} \tag{4.3}$$

Activity is defined according to eq.(4.4).

$$a_i = \gamma_i x_i \tag{4.4}$$

where x_i is the mole fraction of species i in the solution and γ_i is the activity coefficient for that specific species i.

Therefore, the phase equilibria condition can be written using eq.(4.5), where activities are expressed according to eq.(4.4).

$$\gamma_i^{\alpha} x_i^{\alpha} = \gamma_i^{\beta} x_i^{\beta} \tag{4.5}$$

The activity coefficients need to be obtained from a thermodynamic model. An expression for the excess Gibbs energy must be employed. The two thermodynamic models used in this work, the UNIQUAC model and the PDH + UNIQUAC model, are discussed in the next section.

4.2 Thermodynamic models used in this work

Having defined the LLE equilibrium criterion it is needed to select a thermodynamic model to estimate the values of the activity coefficients.

In this work, one of the considered models is the UNIQUAC equation[56,57]. The UNIQUAC model has proven to provide accurate results for the description of short-range interactions in non-electrolyte systems[56,57], as well as for electrolyte systems[58].

Furthermore, to evaluate the extent of dissociation of the ionic liquids in water systems considered in this project, which is it main goal, the Pitzer-Debye-Hückel equation for the long-range interactions coupled with the UNIQUAC equation was also studied.

4.2.1 UNIQUAC model

The UNIQUAC model is an excess Gibbs energy equation, which accounts for short-range interactions. This equation, which is a local composition model, is the sum of two contributions: the combinatorial term, $G^{\mathrm{E,C}}$, which takes into account differences in size and shape of molecules, and the residual term, $G^{\mathrm{E,R}}$, which is the enthalpic contribution where the interaction parameters are included. Therefore, for the UNIQUAC model, the molar excess Gibbs energy is given by eq.(4.6).

$$G^{\mathrm{E}} = G^{\mathrm{E,UNIQUAC}} = G^{\mathrm{E,C}} + G^{\mathrm{E,R}} \tag{4.6}$$

Deriving eq.(4.6) allows to obtain the activity coefficient of species i. Thus, the activity coefficient for any species i is given by eq.(4.7).

$$\ln(\gamma_{\mathrm{i}}) = \ln\left(\gamma_{\mathrm{i}}^{\mathrm{UNIQUAC}}\right) = \ln\left(\gamma_{\mathrm{i}}^{\mathrm{C}}\right) + \ln\left(\gamma_{\mathrm{i}}^{\mathrm{R}}\right) \tag{4.7}$$

where $\gamma_{\mathrm{i}}^{\mathrm{C}}$ is the combinatorial term and $\gamma_{\mathrm{i}}^{\mathrm{R}}$ is the residual term.

Regarding the combinatorial term, $\gamma_{\mathrm{i}}^{\mathrm{C}}$, which represents the differences in size and shape of molecules in the system, it can be calculated through eq.(4.8).

$$\ln\left(\gamma_{\mathrm{i}}^{\mathrm{C}}\right) = \ln\left(\frac{\phi_{\mathrm{i}}}{x_{\mathrm{i}}}\right) + 5q_{\mathrm{i}}\ln\left(\frac{\theta_{\mathrm{i}}}{\phi_{\mathrm{i}}}\right) + l_{\mathrm{i}} - \frac{\phi_{\mathrm{i}}}{x_{\mathrm{i}}}\sum_{j=1}^{N_{\mathrm{spec}}} x_{\mathrm{j}} l_{\mathrm{j}} \tag{4.8}$$

where the parameter l_i can be obtained through eq.(4.9).

$$l_i = 5(r_i - q_i) - (r_i - 1) \quad (4.9)$$

and the volume fraction, ϕ_i, and the surface area fraction, θ_i, of i component are calculated with eq.(4.10) and eq.(4.11).

$$\phi_i = \frac{x_i r_i}{\sum_{j=1}^{N_{spec}} x_j r_j} \quad (4.10)$$

$$\theta_i = \frac{x_i q_i}{\sum_{j=1}^{N_{spec}} x_j q_j} \quad (4.11)$$

where N_{spec} is the number of species in solution and r_i and q_i are the molecular van der Waals volumes and molecular surface areas, respectively. These values can be found in Appendix A, together with the IUPAC names and structures for all ionic liquids used in this work[59-66].

The residual term, γ_i^R, is related to the short-range molecular energetic interactions between species in solution. It can be expressed through eq.(4.12).

$$\ln(\gamma_i^R) = q_i \left[1 - \ln\left(\sum_{j=1}^{N_{spec}} \theta_j \tau_{ji}\right) - \sum_{j=1}^{N_{spec}} \frac{\theta_j \tau_{ij}}{\sum_{k=1}^{N_{spec}} \theta_k \tau_{kj}}\right] \quad (4.12)$$

The parameter τ_{ij} is given by eq.(4.13).

$$\tau_{ij} = \exp\left(-\frac{\Delta u_{ij}}{T}\right) \quad (4.13)$$

where Δu_{ij} is the UNIQUAC interaction parameter. For some applications, these parameters present some type of dependence with temperature, for example, linear or quadratic[1]. In this study, a linear dependency of the UNIQUAC interaction parameter with temperature was used. It is employed to achieve more accurate results.

$$\Delta u_{ij} = a_{ij} + b_{ij} T \quad (4.14)$$

where a_{ij} and b_{ij} are the parameters between species i and j that will be optimized.

Thus, from eq.(4.14) there are 4 parameters for each binary mixture. These will be estimated based on experimental data.

4.2.2 PDH + UNIQUAC model

According to the literature, when ions are present in solution, the Pitzer-Debye-Hückel equation is amongst the most popular ones. It is one equation specially developed for systems with long-range forces.

The Pitzer-Debye-Hückel (PDH) equation has been used by Pitzer (1980)[67] and Pitzer and Simonson (1986)[68] with great success for aqueous systems composed of common ions (mainly nitrate). Moreover, it has also been adopted for many common salt systems (e.g., systems with sodium chloride, NaCl, sodium bromide, NaBr, potassium bromide, KBr, and potassium chloride, KCl) with very satisfactory results.

It is worth mentioning that this model will be used within the scope of this thesis, for the first time, to evaluate the degree of dissociation of different ionic liquids in water. The Pitzer-Debye-Hückel (PDH) equation is usually combined with a model for short-range interactions. In this study, the UNIQUAC model was chosen. Consequently, the molar excess Gibbs energy, G^{E}, is the sum of the UNIQUAC model and the PDH equation.

$$G^{\mathrm{E}} = G^{\mathrm{E,UNIQUAC}} + G^{\mathrm{E,PDH}} \tag{4.15}$$

For the activity coefficient, eq.(4.15) can be derived to yield eq.(4.16).

$$\ln(\gamma_{\mathrm{i}}) = \ln\left(\gamma_{\mathrm{i}}{}^{\mathrm{UNIQUAC}}\right) + \ln\left(\gamma_{\mathrm{i}}{}^{\mathrm{PDH}}\right) \tag{4.16}$$

Regarding the UNIQUAC term, it was already detailed in Section 4.2.1. and the only difference is that, when dissociation of ionic liquids in water exists, there are 3 different species in solution (cation, anion and solvent), which leads to 6 different UNIQUAC interaction parameters, Δu_{ij}. However, since each UNIQUAC interaction parameter will also follow a linear temperature fitting, 12 parameters (a_{ij} and b_{ij}) will have to be optimized.

Concerning the Pitzer-Debye-Hückel term, the general form of its contribution, for each species, is given by eq.(4.17), when considering the symmetrical convention for the activity coefficients[67].

$$\ln\left(\gamma_{\mathrm{i}}{}^{\mathrm{PDH}}\right) = -{z_{\mathrm{i}}}^2 A_{\mathrm{DH,x}} \left[\frac{2}{\rho}\ln\left(\frac{1+\rho\sqrt{I_{\mathrm{x}}}}{1+\rho\sqrt{{I_{\mathrm{x}}}^{\nabla}}}\right) + \sqrt{I_x}\,\frac{1-{I_{\mathrm{x}}}/{{I_{\mathrm{x}}}^{\nabla}}}{1+\rho\sqrt{I_{\mathrm{x}}}}\right] \tag{4.17}$$

I_{x} is the ionic strength, in mole fraction basis, given by eq.(4.18).

$$I_{\mathrm{x}} = 0.5\sum_{l=1}^{N_{\mathrm{ion}}} {z_{\mathrm{l}}}^2 x_{\mathrm{l}} \tag{4.18}$$

where N_{ion} is the number of ions in the solution and z_{l} is the ionic charge of the ion l.

For electrolytes with a unitary charge for each ion, like the ones in this work, the parameter ${I_x}^{\nabla}$ is given by eq.(4.19).

$${I_x}^{\nabla} = \frac{{z_i}^2}{2} \tag{4.19}$$

with the parameter $A_{DH,x}$ being defined as,

$$A_{DH,x} = \frac{1}{3}\frac{\sqrt{2N_A}}{8\pi}\left(\frac{e^2}{\varepsilon_0 k}\right)^{1.5}\frac{{\rho_0}^{0.5}}{(\varepsilon T)^{1.5}} \tag{4.20}$$

where N_A is the Avogrado's number, e is the electronic charge, ε_0 is the vacuum permittivity, k is the Boltzmann constant, ρ_0 is the solvent's density and ε is the solvent's dielectric constant. These first 4 parameters are constants which are displayed in Table 4.1[69].

Table 4.1: Constants used in the Pitzer-Debye-Hückel term.

Avogadro's number / mol^{-1}	$6.0238 \cdot 10^{23}$
Electronic charge / C	$1.6022 \cdot 10^{-19}$
Vacuum permittivity / $C^2 \cdot J^{-1} \cdot m^{-1}$	$8.8542 \cdot 10^{-12}$
Boltzmann constant / $J \cdot K^{-1}$	$1.3803 \cdot 10^{-23}$

As for the properties of the solvent, such as the density, ρ_0, and the dielectric constant, ε, these properties were investigated for the only solvent present in the mixtures of this work: water. Firstly, from the literature, it was possible to observe that the water's dielectric constant did not change significantly with the studied temperatures, which allowed to use an average value of 80[70]. For the water density, since there are numerous published works on this topic, a fitted function based on experimental data[71] was chosen. The parameters for this fitting and corresponding plot can be found in Appendix A.

For the solvent, eq.(4.17) can be reduced to eq.(4.21) for a non-charged species.

$$\ln\left({\gamma_i}^{PDH}\right) = A_{DH,x}\frac{2I_x\sqrt{I_x}}{1+\rho\sqrt{I_x}} \tag{4.21}$$

where the parameter ρ is the ionic closest approach parameter. Further explanation on this parameter ρ will be given in Section 4.3.

4.3 Closest approach parameter

The closest approach parameter, ρ, is related to the closest approach of the ions. The concepts of closest approach parameter and hard-core collision diameter have been reported by Pitzer in 1980[67] and the values established have been used until the present.

Many authors have assumed ρ between 8 to 15 but use a fixed value of 14.9[67,72,73]. Although initially these values were only valid for nitrates, until nowadays they have been used for a wider variety of salts. Achard *et al.* (1994)[74] used a higher value than 15 for the fitted value of the parameter (ρ = 17.1). Despite existing literature available reporting the mentioned values for the parameter ρ, none of these works were focused on ionic liquids.

Pitzer and Simonson (1986)[68] also proposed an equation to calculate the parameter ρ related to the approximate theory.

$$\rho = a\left(\frac{2e^2 N_{\mathrm{A}}\rho_{\mathrm{i}}}{M_{\mathrm{i}}\varepsilon_0 k\varepsilon T}\right)^{1/2} \tag{4.24}$$

where ρ_{i} is the density of the species i, M_{i} is molecular mass of the species i and a is the hard-core collision diameter. These molecular mass and density for each ionic liquid studied in this work can be found in Appendix A[75-82].

Since the hard-core collision diameter depends on the degree of dissociation of any electrolyte in solution (if no dissociation occurs there would be no solvent molecules between the ions, while if there is total dissociation two solvent molecules between the ions can exist - one surrounding each of them), the closest approach parameter should be calculated in function of the degree of dissociation of the electrolyte. Figure 4.1 shows the underlying theory supporting the calculation of this parameter, for the aqueous systems, ionic liquid/water, presented in this work. One of the main goals of this work is a novel approach to obtain the closest approach parameter, based on theoretical considerations.

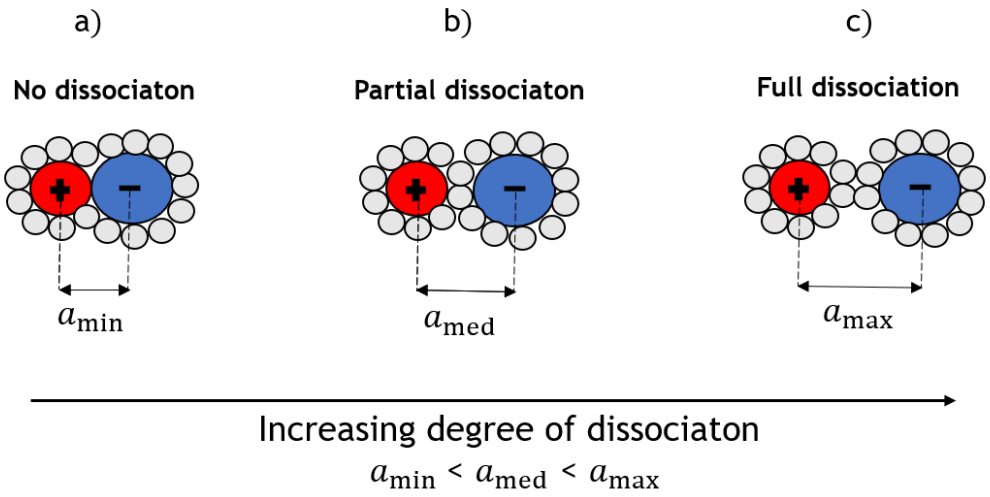


Fig. 4.1: Representation of the hard-core collision diameter in ionic liquids. The red spheres (+) represent the cation, the blue spheres (-) represent the anion and the grey spheres (O) represent the water molecules. a) No dissociation, there are no water molecules between the ions, the distance is minimum. b) Partial dissociation, there is one water molecule between the ions. c) Full dissociation, both ions are solvated, there is two water molecules and the distance is maximum.

Figure 4.1 a) refers to the absence of dissociation. In this situation, the distance between the ions can be considered minimum, resulting in the minimum hard-core collision diameter, $a_{\min}$, and the minimum ionic closest approach parameter, $\rho_{\min}$.

Figure 4.1 b) shows the condition when there is partial dissociation. Some average distance between the maximum and minimum value should be assumed. For this case, it is considered that only one water molecule is among the ions and that this corresponds to an average value of the hard-core collision diameter, a_{med}, and a corresponding medium value of the ionic closest approach parameter, ρ_{med}.

Lastly, Figure 4.1 c) presents the full dissociation scenario of the ionic liquid in water and, by assumption, both ions are solvated by water molecules. This results in having two water molecules between the ions. For this, the distance between the ions is deemed maximum, resulting in the maximum hard-core collision diameter, $a_{\max}$, and in the maximum ionic closest approach parameter, $\rho_{\max}$.

Accordingly, the ionic hard-core collision diameter used in this work for each situation can be obtained from eq.(4.23) to eq.(4.25).

$$a_{\min} = R_{\mathrm{IL}} \tag{4.23}$$

$$a_{\max} = R_{\mathrm{IL}} + 2R_{\mathrm{W}} \tag{4.24}$$

$$a_{\mathrm{med}} = \frac{a_{\min} + a_{\max}}{2} \tag{4.25}$$

where R_{IL} is the ionic radius of the ionic liquid and R_{W} is the radius of the water molecule.

Due to the lack of data available in the literature concerning the ionic radii of ionic liquids, the computation of these values was based on the Stokes-Einstein equation. This equation is as follows:

$$r = \frac{kT}{6\pi\eta D} \tag{4.26}$$

where r is the hydrodynamic radius of the particle, η is the viscosity of the particle and D is the diffusion coefficient of the particle in the solution. The r in equation (4.26) can be approximated to R_{IL} in equation (4.23).

Based on the conclusions of Mclaughlin (1958)[83], Green *et al.* (2017)[84] simplified the above equation. The simplified expression for a temperature of 40 ºC is presented in eq.(4.27). This temperature is the one selected by Green *et al.* (2017)[84] in their work and it is also an average value for the range of temperatures used in this work.

$$r = \frac{1}{2}\left(\frac{M_{\mathrm{i}}}{\rho_{\mathrm{i}} N_{\mathrm{A}}}\right) \tag{4.27}$$

Zhang *et al.* (2006)[85] reports data for the bond distance and angles of some ionic liquids. In this publication data are available for one of the ionic liquids used in this work (1-butyl-3-methylimidazolium hexafluorophosphate, $[C_4mim][PF_6]$). Combining the bound distance and angles data from that paper and the law of cosines it is possible to estimate the distance between the anion and the cation to the value of 3.230 Å, while the value calculated with eq.(4.27) is 3.519 Å. Since these values are similar, it is possible to highlight the reliability of the new approach adopted using eq.(4.27) to calculate all the radius for other ionic liquids used in this work. The values of R_{IL} for the ionic liquids from this work are given in Appendix A.

Since the closest approach parameter does not change significantly with temperature, especially in the temperature range used in this study a value of ρ was calculated for each ionic liquid, and for each situation mentioned above (no dissociation, partial dissociation and full dissociation) at 40 ºC. The values of the 3 closest approach parameters for each ionic liquid are presented in Table 4.2.

Table 4.2: Calculated values for the minimum, medium and maximum closest approach parameter at 40 °C for the ionic liquids used in this work.

Ionic liquid	$\rho_{\min}$	ρ_{med}	$\rho_{\max}$
$[C_2mim][NTf_2]$	8.95	12.63	16.31
$[C_3mim][NTf_2]$	9.17	12.85	16.53
$[C_4mim][NTf_2]$	9.33	13.01	16.69
$[C_5mim][NTf_2]$	9.52	13.20	16.88
$[C_6mim][NTf_2]$	9.68	13.36	17.04
$[C_7mim][NTf_2]$	9.87	13.55	17.22
$[C_8mim][NTf_2]$	10.01	13.69	17.36
$[C_4py][NTf_2]$	9.29	12.97	16.65
$[C_4mim][PF_6]$	8.33	12.01	15.69
$[C_6mim][PF_6]$	8.76	12.44	16.11
$[C_8mim][PF_6]$	9.15	12.83	16.50
$[C_6mim][BF_4]$	8.56	12.23	15.91
$[C_8mim][BF_4]$	8.93	12.60	16.28
$[C_{10}mim][BF_4]$	9.30	12.98	16.66

5 Results and discussion

In this chapter, results on the dissociation of some selected ionic liquids in aqueous systems are presented. These were obtained from the modeling of liquid-liquid equilibria (LLE) data of systems ionic liquid/water using the PDH equation + UNIQUAC model that accounts for long-range and short-range interactions. A comparison with the modeling using only the UNIQUAC model is also performed to better evaluate the degree of dissociation of these binary systems composed of ionic liquids and water. The former thermodynamic model takes into account the existence of 3 species in the solution since the ionic liquid dissociates into an anion and a cation, while the latter takes only into account the existence of 2 species, since the ionic liquid is treated as a neutral molecule.

5.1 Ionic liquids selected

The selection of the ionic liquids in this work was performed based on the ionic liquids studied by Nordness and Brennecke (2020)[4], since, at the time this work was suggested, it was the only publication considering the degree of dissociation of ionic liquids. Moreover, the selected ionic liquids allow the study of the influence of the cation alkyl chain length, the cation and the anion on the dissociation of the ionic liquid. The chosen ionic liquids are presented in Table 5.1. Their IUPAC names and chemical structures can be found in Appendix A, as mentioned in Chapter 4.

Liquid-liquid equilibria data for binary systems, ionic liquid/water, from literature, will be used for the study of dissociation of the selected ionic liquids. Ionic liquids containing the $[NTf_2]^-$ anion in the imidazolium cation with different alkyl chain length will be compared to evaluate the influence of the alkyl chain length in the dissociation of these ionic liquids. These ionic liquids are $[C_2mim][NTf_2]$, $[C_3mim][NTf_2]$, $[C_4mim][NTf_2]$, $[C_5mim][NTf_2]$, $[C_6mim][NTf_2]$, $[C_7mim][NTf_2]$ and $[C_8mim][NTf_2]$. Regarding the influence of the cation on the dissociation of the ionic liquids, the imidazolium cation ($[C_4mim][NTf_2]$) is compared with the pyridinium cation ($[C_4py][NTf_2]$) with the same anion and alkyl chain length. Lastly, the study of the impact of the anions of the ionic liquids on dissociation is carried out using three different ionic liquids with the same cation. These anions are $[NTf_2]^-$, $[PF_6]^-$ and $[BF_4]^-$ and the cation is $[C_6mim]^+$.

Table 5.1: Ionic liquids selected in this work.

$[NTf_2]^-$ family		$[PF_6]^-$ family	$[BF_4]^-$ family
$[C_2mim][NTf_2]$	-	-	-
$[C_3mim][NTf_2]$	-	-	-
$[C_4mim][NTf_2]$	$[C_4py][NTf_2]$	$[C_4mim][PF_6]$	-
$[C_5mim][NTf_2]$	-	-	-
$[C_6mim][NTf_2]$	-	$[C_6mim][PF_6]$	$[C_6mim][BF_4]$
$[C_7mim][NTf_2]$	-	-	-
$[C_8mim][NTf_2]$	-	$[C_8mim][PF_6]$	$[C_8mim][BF_4]$
-	-	-	$[C_{10}mim][BF_4]$

It is important to mention that the publication of Nordness and Brennecke (2020)[4] did not contain data of dissociation for all the ionic liquids shown in the above table. Therefore, some assumptions had to be made regarding the degree of the dissociation in the whole composition range of the ionic liquids in this work.

Firstly, it was observed that for the dicyanamide family, $[DCA]^-$, when the cation is pyridinium, its dissociation in water does not change significantly while increasing the alkyl chain length of the $[DCA]^-$-based ionic liquids[4]. The ionic liquids that illustrate this behavior are shown in the first four rows of Table 5.2. Moreover, it is also evident that when the anion is the same, but the pyridinium cation is changed to an imidazolium cation, the range of dissociation increases considerably, which indicates that different assumptions must be made for pyridiniums and imidazoliums-based ionic liquids. This phenomenon is also noticeable in Table 5.2, where it can be seen that the increase of alkyl chain length of the cation does not influence significatively the dissociation ranges, as stated above, whereas the cation used plays a major role on the ionic liquid dissociation in water.

Table 5.2: Dissociation ranges for ionic liquids of the dicyanamide family.

Ionic liquid	Dissociation Lower-Bound	Dissociation Upper-Bound
1-propylpyridinium dicyanamide [C_3py][DCA]	0.9303	0.9882
1-butylpyridinium dicyanamide [C_4py][DCA]	0.9189	0.9806
1-pentylpyridinium dicyanamide [C_5py][DCA]	0.9198	0.9854
1-hexylpyridinium dicyanamide [C_6py][DCA]	0.9075	0.9762
1-butyl-3-methylimidazolium dicyanamide [C_3mim][DCA]	0.0096	1.0000

Moreover, since there is at least one dissociation measurement in the work of Nordness and Brennecke (2020)[4] for each of the different anions selected in this work, it is possible to predict the composition range where dissociation occurs for each ionic liquid used in this work, while assuming a narrower range for the ionic liquid that contains pyridinium. These results are presented in Table 5.3.

Table 5.3: Dissociation degree for the selected ionic liquids/water systems.

Ionic liquid family	Dissociation Lower-Bound	Dissociation Upper-Bound	Degree of dissociation
[$C_n$mim][NTf_2][a]	0.0012	0.9998	Partial dissociation
[C_4py][NTf_2]	0.9000	0.9999	No dissociation
[$C_n$mim][PF_6][b]	0.7854	1.0000	No dissociation
[$C_n$mim][BF_4][c]	0.0009	1.0000	Full dissociation

[a] n = 2, 3, 4, 5, 6, 7, 8. [b] n = 4, 6, 8. [c] n = 6, 8, 10.

Experimental LLE data for ionic liquids/water systems will be used to evaluate the degree of dissociation of some ionic liquids in aqueous solution in function of structures of ionic liquids, such as the influence of the cation alkyl chain length, of the cation and of the anion. For this purpose, the experimental data for binary mixtures of ionic liquid/water were collected from literature. This data can be found in Appendix B.

5.2 Thermodynamic models used in this work

The two thermodynamic models used for calculations with the aim of studying the ionic liquid dissociation in water have been described in Chapter 4 of this work. The UNIQUAC model does not consider the ionic liquid as an electrolyte and, therefore, assumes that the only interactions that take place are short-range between the ionic liquid and the solvent, in this case water. The PDH equation + UNIQUAC model assumes dissociation and there are 3 species in solution, the cation and the anion of the ionic liquid and the solvent (water). In this case there are long-range interactions that are described by the Pitzer-Debye-Hückel equation and the short-range interactions are expressed by the UNIQUAC model.

Three values of the closest approach parameter in the PDH equation are considered in this work, one for no dissociation, another for partial dissociation and a third one for full dissociation. This topic has been further explained in Section 4.3.

5.3 Modeling results obtained in this work

In this work, results from the UNIQUAC model and from the PDH + UNIQUAC equation using three different values of the closest approach parameter are compared. For each ionic liquid/water system, these values are given in Section 4.3. The results of this comparison are shown in Figure 5.1 for some ionic liquids that represent the three studied situations: no dissociation, partial dissociation and total dissociation.

Figure 5.1 presents solubility curves of a) water-rich phase and b) ionic liquid-rich phase for the binary system $[C_4mim][PF_6]$/water. For this ionic liquid in water, it is expected that it does not dissociate. Thus, this can be considered as a neutral molecule and the distance between its ions is considered to be minimum (see Figure 4.1 a)). Hence, there are no long-range interactions in solution when considering this case, which is indicative that the thermodynamic models with no long-range interactions will outperform the remaining thermodynamic models. Therefore, it is expected that the UNIQUAC model and the PDH + UNIQUAC model using the minimum closest approach parameter present the best and similar results. For the $[C_4mim][PF_6]$/water displayed in Figures 5.1 a) and b) can be seen as the aforementioned models describe the experimental data with more accuracy than the others. The results for an average value for the closest approach parameter provide an intermediate result, while for the maximum value of ρ the results present significant deviations from the experimental data. Regarding the other ionic liquids studied in this work without dissociation in water, the corresponding results are illustrated in Appendix C and their trends follow the same behavior observed for the $[C_4mim][PF_6]$/water system.

Concerning partial dissociation, when there is dissociation at low ionic liquid mole fraction in the binary mixture ionic liquid/water and there is no dissociation at high ionic liquid mole fraction in the binary mixture ionic liquid/water, Figure 5.1 represents as example the calculated solubility curves with thermodynamic models for c) water-rich phase and d) ionic liquid-rich phase for the binary system $[C_4mim][NTf_2]$/water. This is an intermediate case between full dissociation and no dissociation, so the average value for the closest approach parameter would yield the best results for both phases, while a more detailed analysis is required for each phase regarding the thermodynamic models performance. On one hand, for the water-rich phase, where there is dissociation, it is expected that after the average value for the closest approach parameter, the best model is the one using the maximum value for ρ, since it assumes dissociation. On the other hand, the worst performing models for this case would be the UNIQUAC model and the PDH + UNIQUAC model with a minimum ρ, since these assume no dissociation whatsoever. For the ionic liquid-rich phase, where there is no dissociation, the results should be opposite from the above: since there is no dissociation, the UNIQUAC model and the PDH + UNIQUAC model with a minimum ρ will yield the best results after the average value for ρ, followed by the maximum value of ρ. The result for the $[C_4mim][NTf_2]$/water system present the anticipated results: the average value for the closest approach parameter produced the best results in the whole composition range, while the maximum value for ρ followed for the water-rich phase, whereas the UNIQUAC model and the PDH + UNIQUAC model with a minimum ρ provided better results for the ionic liquid-rich phase. The ionic liquids composed of the $[NTf_2]^-$ anion in this work, ionic liquids which present partial dissociation in water, also follow these trends in both phases as can be seen in Appendix C.

Finally, Figure 5.1 shows the solubility curves for e) water-rich phase and f) ionic liquid-rich phase for the binary system $[C_6mim][BF_4]$/water. Since this is an ionic liquid with full dissociation in the whole composition range, it is expected that the best model is the PDH + UNIQUAC with a maximum value for the closest approach parameter. With the average value for ρ intermediate results are attained, while the UNIQUAC model and the PDH + UNIQUAC model with a minimum value for ρ provide the worst results, since these stray farther from the reality for this ionic liquid due to assuming a low distance between the ions, whereas it is considered to be the opposite for these type of ionic liquids. The results show exactly what is calculated below, since the maximum value for ρ yields the best results, followed by the intermediate value and last the UNIQUAC model and the PDH + UNIQUAC model with a minimum ρ. The ionic liquids containing the $[BF_4]^-$ anion in this work also have total dissociation and follow this trend as can be noticed in Appendix C.

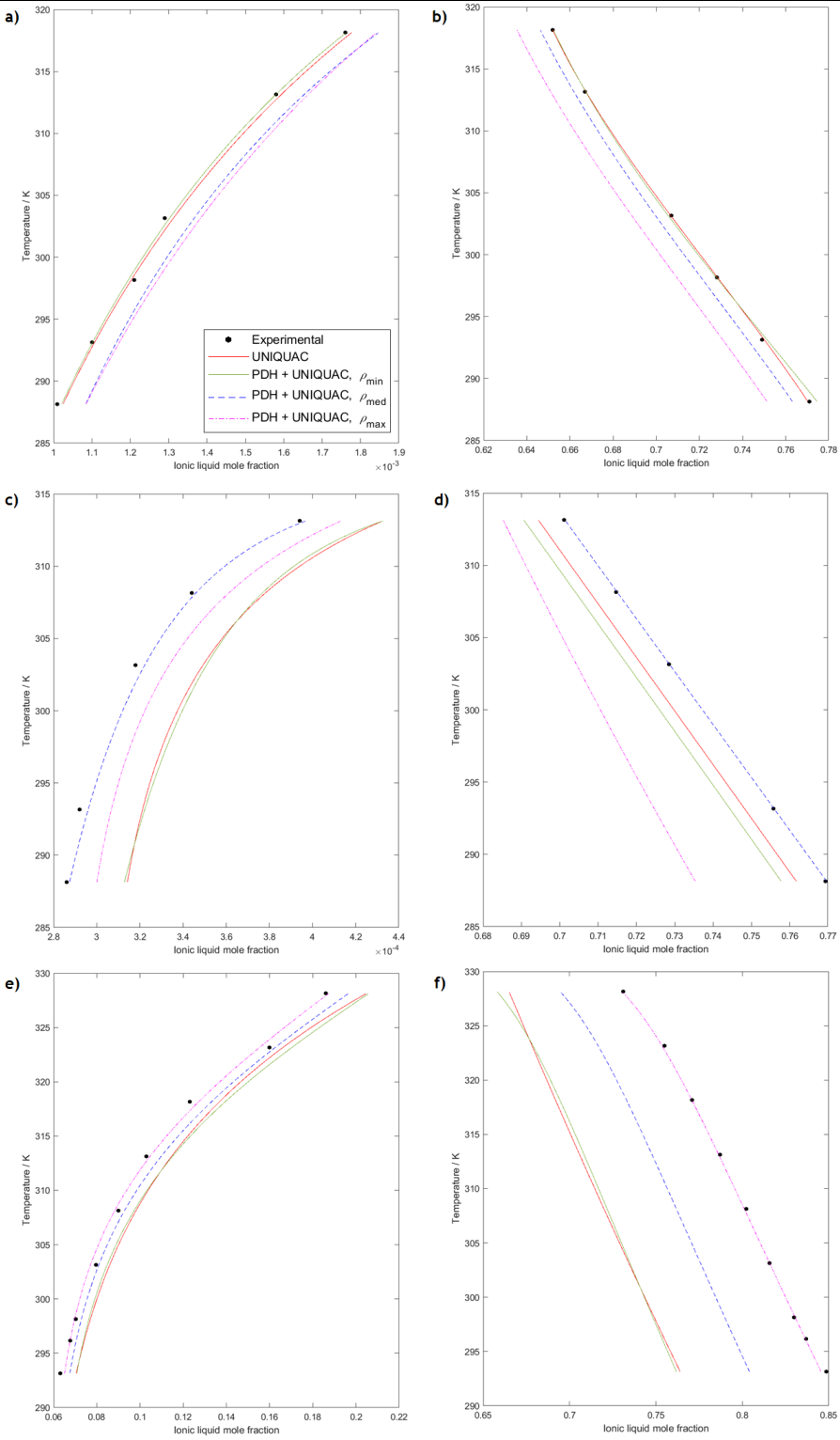


Fig. 5.1: Some examples for calculated solubility curves for the binary system ionic liquid/water at atmospheric pressure. a) water-rich phase for $[C_4mim][PF_6]$/water; b) ionic liquid-rich phase for $[C_4mim][PF_6]$/water; c) water-rich phase for $[C_4mim][NTf_2]$/water; d) ionic liquid-rich phase for $[C_4mim][NTf_2]$/water; e) water-rich phase for $[C_6mim][BF_4]$/water; f) ionic liquid-rich phase for $[C_6mim][BF_4]$/water. The black dots represent the experimental points[1,2,11,12,13], the red lines correspond to the results from the UNIQUAC model, the green lines correspond to the results from the PDH + UNIQUAC model for a minimum closest approach parameter, the blue lines for a medium closest approach parameter and the pink lines for a maximum closest approach parameter.

In Appendix D the calculated mole fraction from the two thermodynamic models with three closest approach parameters for all studied ionic liquids in this work are presented. The deviation of the composition, σ, obtained from the LLE modeling is presented in Table 5.4 for the ionic liquids mentioned in this section, [C_4mim][PF_6], [C_4mim][NTf_2] and [C_6mim][BF_4], while for the other ionic liquids the deviations obtained in this work can be found in Appendix D. This deviation, is calculated from eq.(5.1).

$$\sigma = \frac{1}{2n}\sum_{i=1}^{n}\left[\frac{|x_{\text{exp}}{}^{\text{IL}} - x_{\text{calc}}{}^{\text{IL}}|}{x_{\text{exp}}{}^{\text{IL}}} + \frac{|x_{\text{exp}}{}^{\text{W}} - x_{\text{calc}}{}^{\text{W}}|}{x_{\text{exp}}{}^{\text{W}}}\right] \times 100 \qquad (5.1)$$

where n is the number of experimental points, x_{exp} is the experimental ionic liquid mole fraction in the binary mixture and x_{calc} is the calculated one.

Table 5.4: UNIQUAC and PDH + UNIQUAC deviation of composition obtained from LLE modeling.

Ionic liquid	σ_{UNIQUAC} %	$\sigma_{\rho_{\text{min}}}$ %	$\sigma_{\rho_{\text{med}}}$ %	$\sigma_{\rho_{\text{max}}}$ %
[C_4mim][PF_6]	0.4419	0.1775	3.1798	4.2668
[C_4mim][NTf_2]	5.4392	5.7512	0.5102	4.1768
[C_6mim][BF_4]	9.6865	9.8251	4.8264	0.0565

The conclusions from Figures 5.1 can also be observed from the values of the deviations of the mole fraction of ionic liquid in the mixtures. Ionic liquids that do not dissociate present similar deviations for the UNIQUAC and the PDH + UNIQUAC model with minimum ρ, while displaying higher deviations with the increase degree of dissociation. For the ionic liquids that present partial dissociation, the PDH + UNIQUAC model with the average value for the ρ is performing better while the other thermodynamic models reach similar deviations globally. For the fully dissociated ionic liquids the best model is the one that considers a maximum ρ value. After that, the deviation increases with the degree of dissociation decreases. The deviations of the compositions for the remaining studied ionic liquids in water are presented in Appendix D, as already mentioned above.

To abridge, for the UNIQUAC model there are 2 UNIQUAC interaction parameters (which corresponds to 4 parameters to optimize) and for the PDH + UNIQUAC model there are 6 UNIQUAC interaction parameters (which corresponds to 12 parameters to optimize). The values of these parameters are found in Appendix E.

In Figure 5.2 the UNIQUAC interaction parameters for the UNIQUAC model that represent the influence of the alkyl chain length, cation and anion of the ionic liquid on the degree of ionic liquid dissociation in water systems are represented.

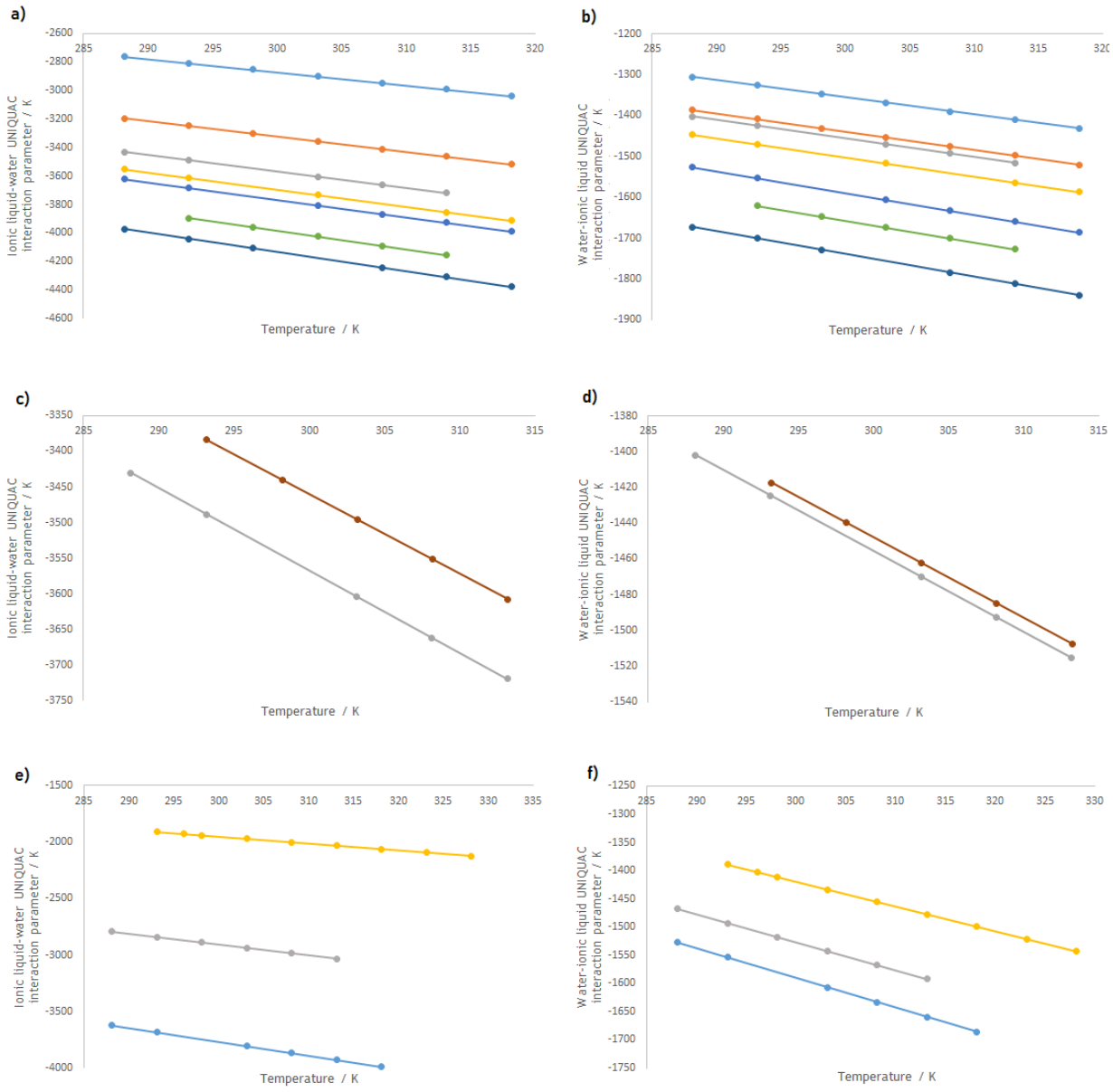


Fig. 5.2: Influence of a) alkyl chain length in the ionic liquid-water interactions, b) alkyl chain length in the water-ionic liquid interactions, c) cation in the ionic liquid-water interactions, d) cation in the water-ionic liquid interactions e) anion in the ionic liquid-water interactions and f) anion in the water-ionic liquid interactions on the dissociation for the UNIQUAC model. In a) and b), the light blue line is the [C_2mim][NTf_2]/water, the orange line corresponds to the [C_3mim][NTf_2]/water, the grey line represents the [C_4mim][NTf_2]/water, the yellow line refers to the [C_5mim][NTf_2]/water, the blue line displays the [C_6mim][NTf_2]/water, the green line presents the [C_7mim][NTf_2]/water and the dark blue line shows the [C_8mim][NTf_2] /water. In c) and d), the brown line is the [C_4py][NTf_2]/water and the grey line represents the [C_4mim][NTf_2]/water. In e) and f), the yellow line is the [C_6mim][BF_4]/water, the grey line represents [C_6mim][PF_6]/water and the light blue line displays the [C_6mim][NTf_2]/water.

As can be observed from the results of Figure 5.2, there are several trends in the effect of the alkyl chain length, cation and anion of ionic liquids on the dissociation in water systems. Firstly, in Figures 5.2 a) and b), it can be seen that when the alkyl chain increases the interaction parameters become more negative. This effect of increasing the alkyl chain length with the UNIQUAC interaction parameters becoming higher in absolute value is also a trend visible for the other two families studied in this work, $[PF_6]^-$ and $[BF_4]^-$, which are displayed in Appendix E. Regarding the influence of different cations, the impact of the imidazolium and the pyridinium cation with $[NTf_2]^-$ anion was assessed. Figures 5.2 c) and d) indicate that the values of UNIQUAC interaction parameters are similar for the different cations. The difference of anions combined with the same cation ($[C_6mim]^+$) is visualized from Figures 5.2 e) and f). In these figures it is possible to observe that the trend of the UNIQUAC interaction parameters follows $[BF_4]^- < [PF_6]^- < [NTf_2]^-$. These conclusions can be applied for the same anions with different alkyl chain length, $[C_8mim]^+$, in Appendix E.

The trends detailed above are identical to the ionic liquid-water interactions and the water-ionic liquid interactions, although their magnitude is lower for the water-ionic liquid interaction.

Respect to the PDH + UNIQUAC model, the tendencies in the UNIQUAC interaction parameters are very similar independently of which closest approach parameter. Likewise, the results from the average value for ρ were chosen. In Figure 5.3 it is possible to observe the influence of the alkyl chain length, in Figure 5.4 the impact of the cation and in Figure 5.5 the effect of the anion of the ionic liquid on the dissociation in water systems.

Figure 5.3 presents several behaviors when considering that there are three species in solution. Regarding the cation and anion interactions (Figures 5.3 a) and c)), these have positive values and decrease when the alkyl chain length's increases. Concerning the water and cation interactions (Figures 5.3 b) and e)), these are of much higher magnitude than the cation and anion interactions and have negative values. Furthermore, they decrease in absolute value as the alkyl chain length increases. The interaction between the anion and water molecules (Figures 5.3 d) and f)) show similar values and in these cases the alkyl chain length has no effect in the interactions. These trends also match with the results for the other two families studied in this work. Results can be found in Appendix E.

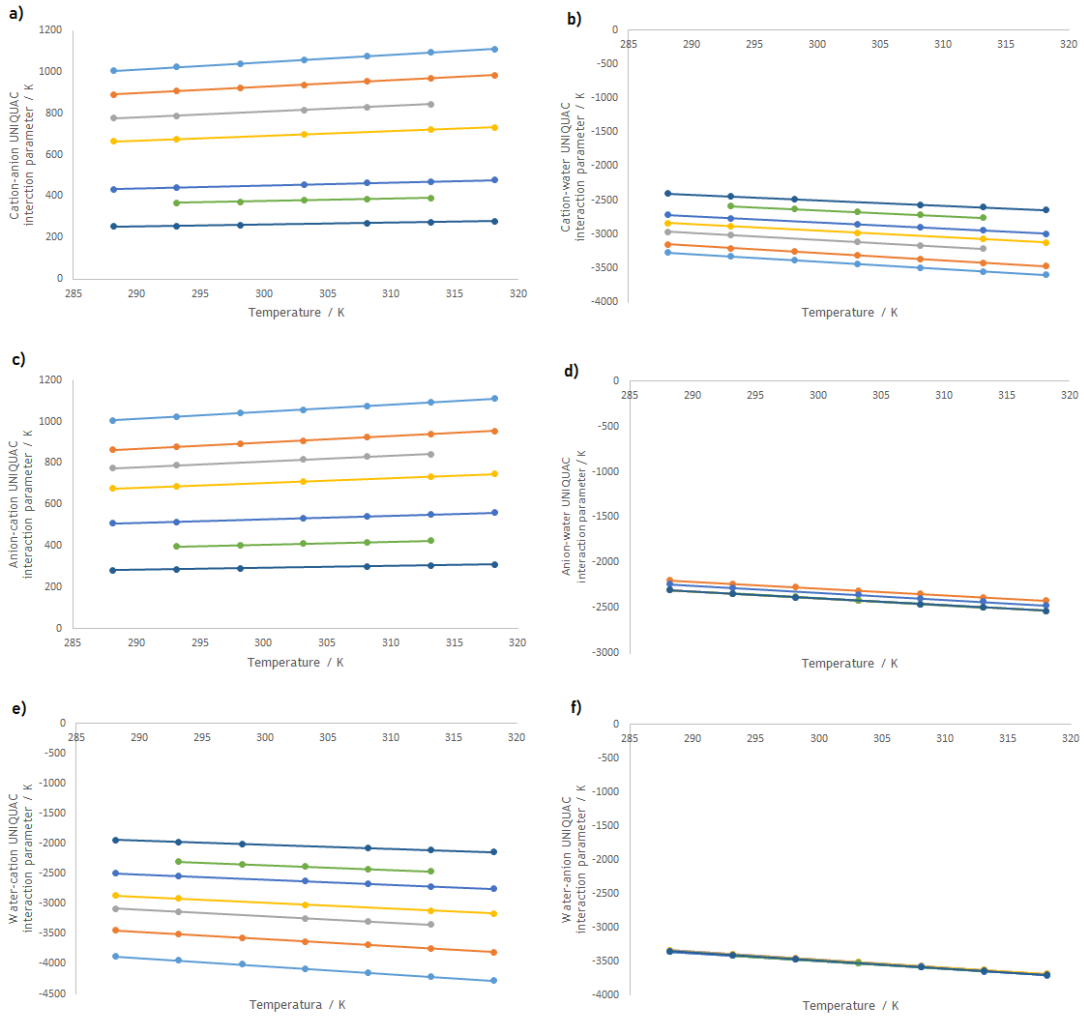


Fig. 5.3: UNIQUAC interaction parameters for PDH + UNIQUAC model for the influence of the alkyl chain length on the dissociation in water systems. a) cation-anion interactions, b) cation-water interactions, c) anion-cation interactions, d) anion-water interactions, e) water-cation interactions and f) water-anion interactions. The light blue line is the $[C_2mim][NTf_2]$/water, the orange line represent the $[C_3mim][NTf_2]$/water, the grey line displays the $[C_4mim][NTf_2]$/water, the yellow line portrays the $[C_5mim][NTf_2]$/water, the blue line shows the $[C_6mim][NTf_2]$/water, the green line presents the $[C_7mim][NTf_2]$/water and the dark blue line denotes the $[C_8mim][NTf_2]$/water.

When comparing two different cations with similar alkyl chain length and the same anion, it was shown that the values of the interaction parameters using the UNIQUAC model do not differ significantly. When considering long-range forces, the results are the same. Figures 5.4 d) and f) point out the same conclusions: the alkyl chain length influence, since the cation would have no effect in the anion and water interactions. Regarding the other figures, Figures 5.4 a), b), c) and e), there are no relevant differences in the interactions parameters for the three ionic liquids/water systems analyzed in this study.

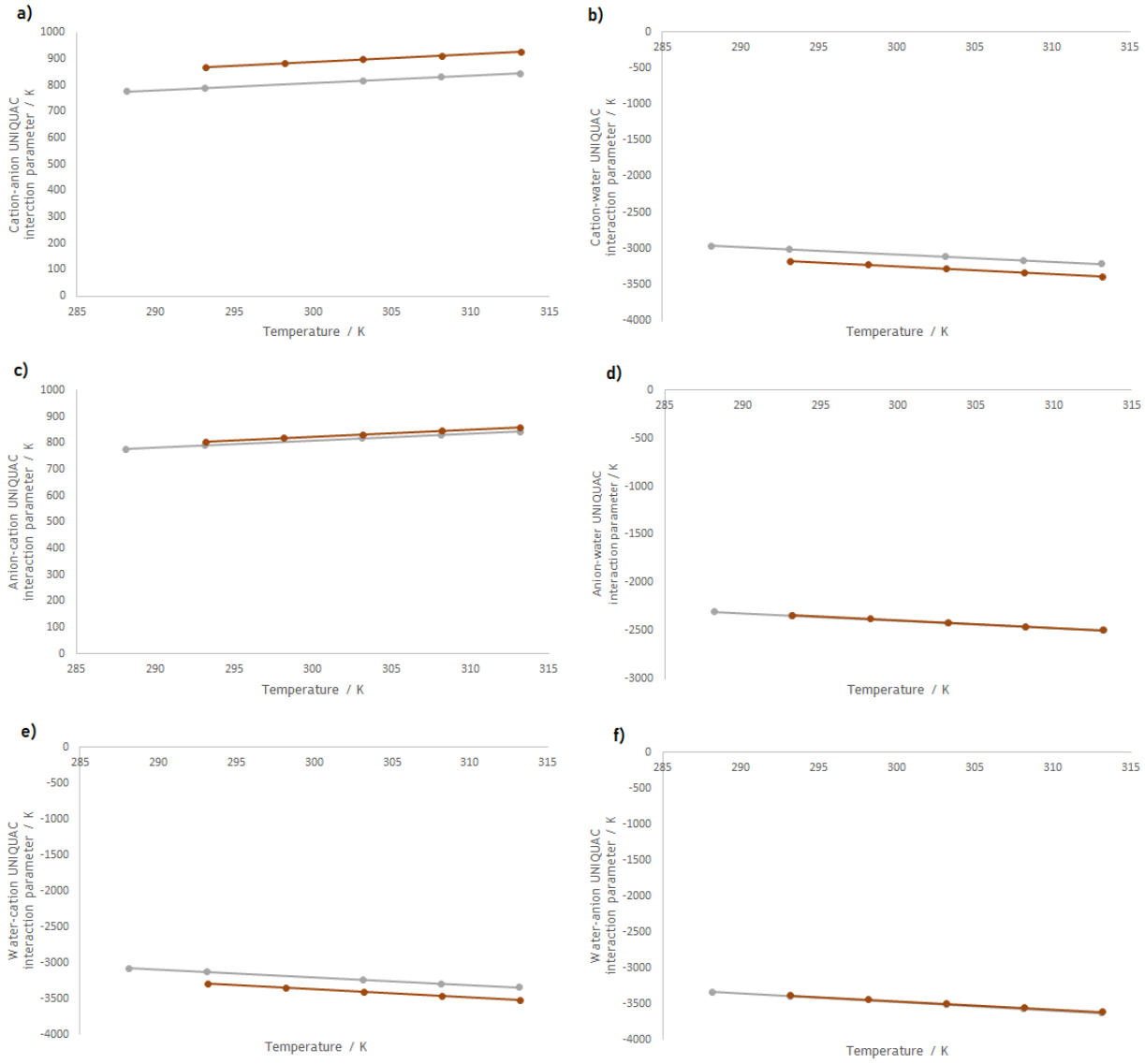


Fig. 5.4: UNIQUAC interaction parameters for PDH + UNIQUAC model for the influence of the cation on the dissociation in water systems. a) cation-anion interactions, b) cation-water interactions, c) anion-cation interactions, d) anion-water interactions, e) water-cation interactions and f) water-anion interactions. The brown line is the $[C_4py][NTf_2]$/water and the grey line displays the $[C_4mim][NTf_2]$/water.

In the same way some conclusions of the UNIQUAC model applied for the evaluation of the cation influence on the dissociation of ionic liquids in aqueous solution, others can also be made for the study of the effect of the anion in water systems. The major highlight obtained before was that the interactions parameters for the UNIQUAC model followed the trend $[BF_4]^-$< $[PF_6]^-$< $[NTf_2]^-$. This tendency is also visible in Figures a), c), d) and f), in absolute value. The sign of the interaction parameters depends on whether the interaction is among the cation and anion or anion and water. Regarding Figures 5.5 b) and e), this is a similar case to Figure 5.3 d) and f), since the cation in this study is always the same, which would mean that the interactions between the cation and water molecules do not depend on the anion.

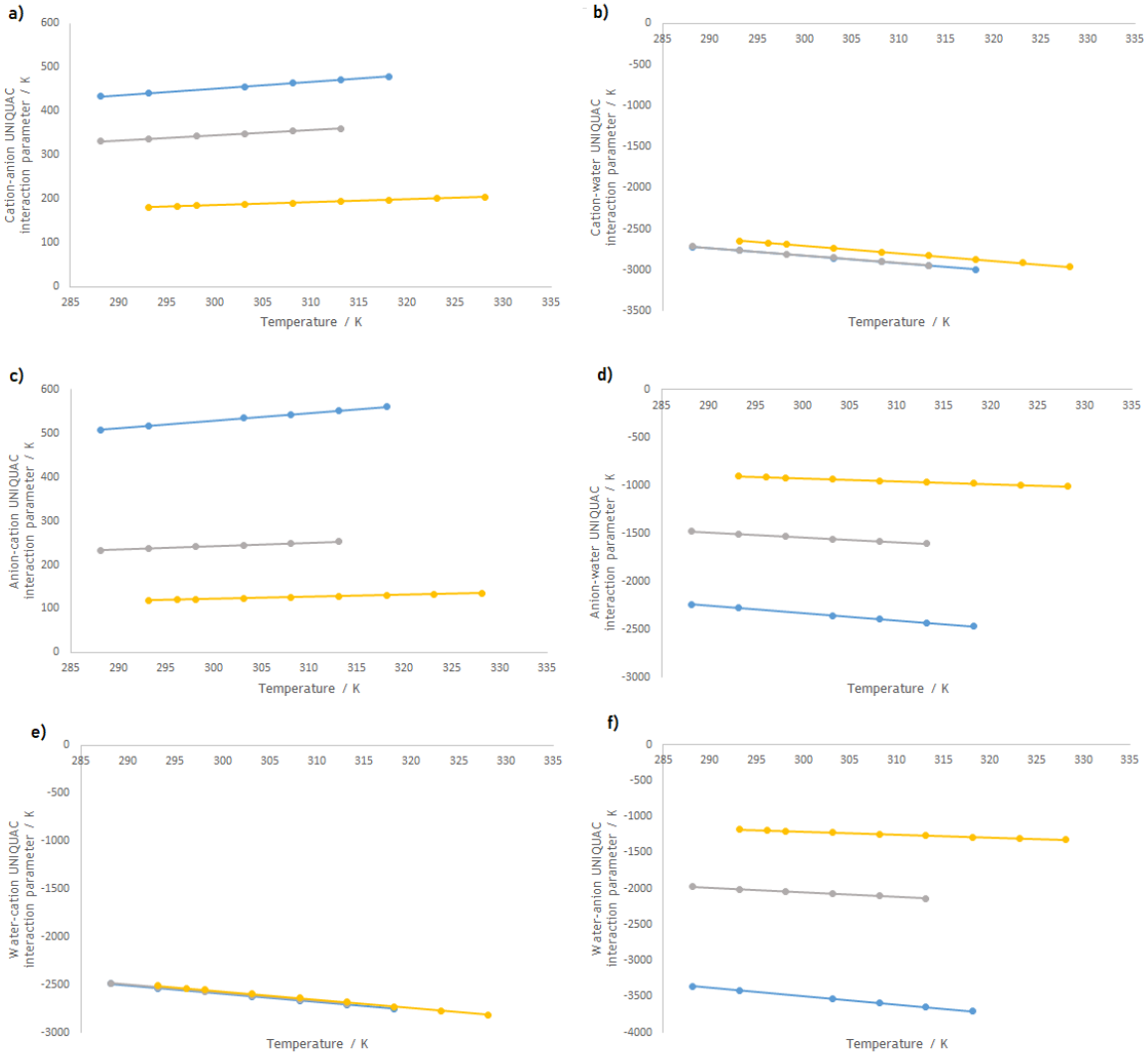


Fig. 5.5: UNIQUAC interaction parameters for PDH + UNIQUAC model for the influence of the anion on the dissociation in water systems. a) cation-anion interactions, b) cation-water interactions, c) anion-cation interactions, d) anion-water interactions, e) water-cation interactions and f) water-anion interactions. The yellow line is the $[C_6mim][BF_4]$/water, the grey line represent the $[C_6mim][PF_6]$/water and the light blue line displays the $[C_6mim][NTf_2]$/water.

An attempt to reduce the number of parameters of the PDH + UNIQUAC model (the interactions for the anion-water and water-anion are similar in each family when studying the influence of the alkyl chain length) was performed, thus resulting in a total of 4 UNIQUAC interaction parameters (8 parameters to optimize). Since the number of parameters in the model decreased, it is expected a worse performance than with 6 parameters, although the important contribution is to observe if the trends obtained before are still valid. The modeling results for the ionic liquids mentioned before with the 4-parameter model are presented in Figure 5.6. The achieved results for other ionic liquids studied in this work are in Appendix F.

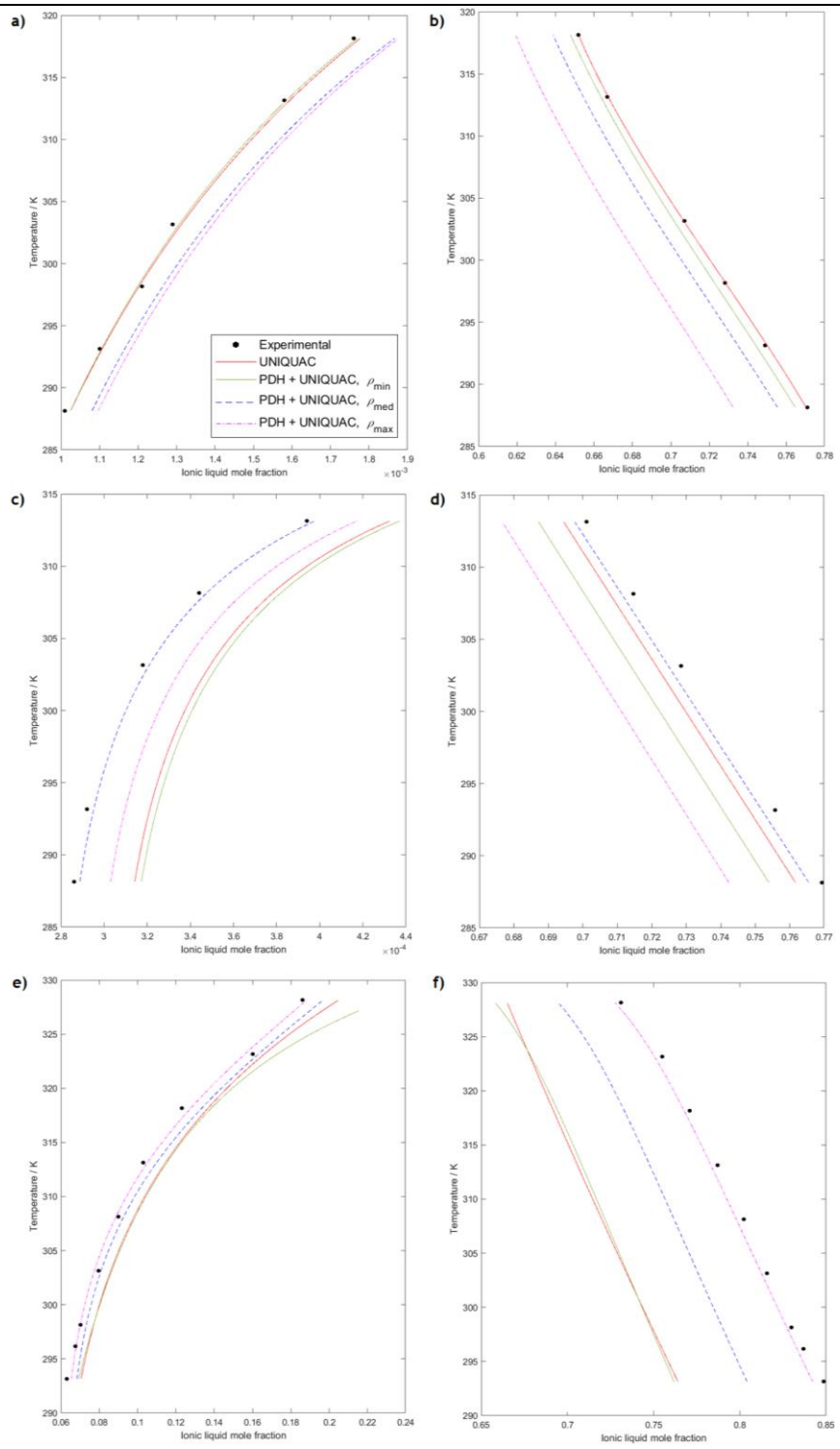


Fig. 5.6: Some examples for calculated solubility curves for the binary system ionic liquid/water at atmospheric pressure considering the 4-parameter PDH + UNIQUAC model. a) water-rich phase for $[C_4mim][PF_6]$/water; b) ionic liquid-rich phase for $[C_4mim][PF_6]$/water; c) water-rich phase for $[C_4mim][NTf_2]$/water; d) ionic liquid-rich phase for $[C_4mim][NTf_2]$/water; e) water-rich phase for $[C_6mim][BF_4]$/water; f) ionic liquid-rich phase for $[C_6mim][BF_4]$/water. The black dots represent the experimental points[1,2,11,12,13], the red lines correspond to the results from the UNIQUAC model, the green lines correspond to the results from the PDH + UNIQUAC model for a minimum closest approach parameter, the blue lines for a medium closest approach parameter and the pink lines for a maximum closest approach parameter.

As expected, the results present higher deviations for ionic liquid mole fraction in the mixture when compared to the 6-parameter model. Despite of that, the trends of UNIQUAC model and PDH + UNIQUAC model with a minimum ρ model being the best options for the ionic liquids that do not dissociate, the PDH + UNIQUAC with an average ρ corresponding the greatest choice for ionic liquids with partial degree of dissociation and PDH + UNIQUAC with a maximum ρ matching the top possibility for ionic liquid that fully dissociate in all their composition range, are still the same. These trends hold for all the other ionic liquids studied in this work, as can be seen in Appendix F.

The deviations of compositions, calculated with eq.(5.1), from the thermodynamic models with 4 parameters are presented in Table 5.5. The deviations of compositions for the other ionic liquids studied in this work obtained with all the modeled solubility are visualized in Appendix G, as well as the calculated ionic liquid composition for both phases.

Table 5.5: UNIQUAC and PDH + UNIQUAC with 4 parameters deviation of composition obtained from LLE modeling.

Ionic liquid	$\sigma_{\mathrm{UNIQUAC}}$ %	$\sigma_{\rho_{\mathrm{min}}}$ %	$\sigma_{\rho_{\mathrm{med}}}$ %	$\sigma_{\rho_{\mathrm{max}}}$ %
$[C_4mim][PF_6]$	0.4419	0.5952	3.9920	6.0763
$[C_4mim][NTf_2]$	5.4392	6.4979	0.7497	4.7500
$[C_6mim][BF_4]$	9.6865	9.9941	4.9940	0.4737

As mentioned above, the deviations increase when compared with the thermodynamic models with 6 parameters. The UNIQUAC model deviations were kept to compare the performance of the 4 models. Again, when there is no dissociation, the UNIQUAC model and the PDH + UNIQUAC model with minimum ρ perform better, despite UNIQUAC always functioning better for all ionic liquids that dissociate, which was not true when using the thermodynamic models with 6 parameters, as can be checked by Figure 5.7. For the ionic liquids where dissociation occurs, either partial or total, the corresponding prior best model (PDH + UNIQUAC model with average ρ for partial dissociation and PDH + UNIQUAC model with maximum ρ for full dissociation) still performs better than the UNIQUAC model, despite the increased deviations, for the ionic liquids in Table 5.5 and other ionic liquids studied in this work, as can be seen in Figure 5.7.

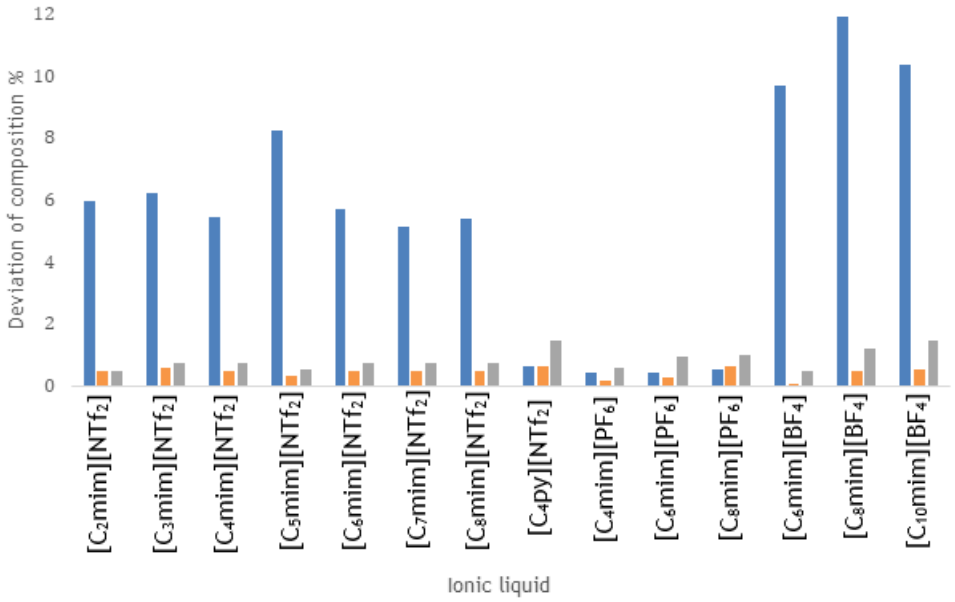


Fig. 5.7: Deviations of composition, σ, for the studied ionic liquids in this work. Blue presents the UNIQUAC model, orange is the best performing model from the PDH + UNIQUAC with 6 parameters and grey shows the best performing model from the PDH + UNIQUAC with 4 parameters.

The UNIQUAC interaction parameters for the thermodynamic models with 4 parameters for all ionic liquids studied in this work are presented in Appendix H. As previously, the effect of the increase of the alkyl chain length and the effect of both the cation and the anion on the dissociation of ionic liquids in water systems was evaluated. Since the obtained trends are the same as displayed in Figures 5.3, 5.4 and 5.5, these were allocated in Appendix H regarding the value of the average value for the closest approach parameter, since the other two closest approach parameters (minimum and maximum closest) presented the same tendencies, identical to the 6-parameter approach.

Finally, all the results from the thermodynamic models used in this work agree with the experimental LLE data available in literature. This allows us to safely say that this work is an efficient tool to predict the dissociation of ionic liquids in water systems based only on the results of application of thermodynamic models regarding liquid-liquid equilibria data.

6 Conclusions

The main objective of this work was to use two thermodynamic models to predict the degree of dissociation of ionic liquids in water. For this purpose, the Pitzer-Debye-Hückel was applied since it has yielded good results on other studies related to electrolytes. In this work three states of dissociation were considered in aqueous binary mixtures containing ionic liquids: no dissociation, partial dissociation (where it is assumed one water molecule among the cation and the anion of ionic liquid) and total dissociation (where each of the ions that compose the ionic liquid are fully solvated, corresponding to existing two water molecules between them). Modeling work of phase equilibria of the ionic liquid/water systems was carried out using the PDH equation to describe the long-range interactions in solution, combined with the UNIQUAC model to account for the short-range forces. This thermodynamic model, which is self-sufficient to describe the three degrees of dissociation assumed in this work was compared to another thermodynamic model, the UNIQUAC equation, in which the ionic liquid is not considered an electrolyte. This model only accounts for the short-range interactions considering the ionic liquid in water systems as a neutral molecule.

For the LLE data of ionic liquid/water systems, the UNIQUAC model and the PDH equation + UNIQUAC model (with three different closest approach parameters) were applied using LLE data from literature. For the ionic liquids $[C_4py][NTf_2]$, $[C_4mim][PF_6]$, $[C_6mim][PF_6]$ and $[C_8mim][PF_6]$ in which there is no dissociation in water the UNIQUAC model and the PDH equation + UNIQUAC model with a minimum closest approach parameter achieved the best results, since these assume that the anion and the cation are close to each other like in a neutral molecule. The differences for calculated compositions in these two thermodynamic models are not significant and can be considered to yield the same results. For this type of systems (systems without dissociation) the average value for the closest approach parameter provided larger deviation than the aforementioned, but better results than using the maximum closest approach parameter, due to this assuming total dissociation. For the ionic liquids $[C_6mim][BF_4]$, $[C_8mim][BF_4]$ and $[C_{10}mim][BF_4]$ in which there is total dissociation in aqueous solution, the maximum value for the closest approach parameter yields the best results, followed by the average value and by the minimum value for the closest approach parameter in the PDH equation + UNIQUAC model, while the latter presents similar results to the UNIQUAC model. The remaining ionic liquids described in this work $[C_2mim][NTf_2]$, $[C_3mim][NTf_2]$, $[C_4mim][NTf_2]$, $[C_5mim][NTf_2]$, $[C_6mim][NTf_2]$, $[C_7mim][NTf_2]$ and $[C_8mim][NTf_2]$ present partial dissociation in water. For both phases of the LLE the average value for the closest approach parameter obtained the best results. For the water-rich phase there is dissociation and, as predicted, the maximum value for the closest approach parameter outperformed the others (the UNIQUAC model and the PDH equation + UNIQUAC model for the minimum value of the

closest approach parameter). For the ionic liquid-rich phase there is no dissociation and, as expected, after the average value for the closest approach parameter, the UNIQUAC model and the PDH equation + UNIQUAC model with a minimum value for the closest approach parameter described the phase equilibria more accurately than the maximum value for the closest approach parameter. The three thermodynamic models that did not use the average closest approach parameter display similar performance.

Regarding the influence of the structure of the ionic liquids in the interaction parameters of the thermodynamic models, the alkyl chain length, the cation and the anion were evaluated. The increase of the alkyl chain length was proven to increment, in absolute value, the interactions of the ionic liquid with water molecules for the UNIQUAC model, while for the interactions of the three species in solution (cation, anion and water) in the PDH + UNIQUAC model it was found that as the length increases the interactions become less significative except when these interactions are between the anion and water molecules. In this case, the interactions were independent of the alkyl chain length. For the cation dependency, it was demonstrated for both thermodynamic models that the change of the cation does not influence the interactions in the mixture. Concerning the anion, a trend was found, for both the UNIQUAC model and the PDH equation + UNIQUAC model, $[BF_4]^-$< $[PF_6]^-$< $[NTf_2]^-$: the change in the anion did not have any relevant impact in the interactions between the cation and the water molecules.

After the work carried out with the thermodynamic model using 6 parameters, the number of parameters was reduced based on the conclusions of the interactions in the different families of ionic liquids in water. This resulted in a thermodynamic model with only 4 parameters. All previous calculations were performed once again yielding extra results. Although the deviations increased, the above-described phase behaviors and structural influences were kept, since the results were the same as for the thermodynamic model with 6 parameters.

The degree of dissociation of different ionic liquid in aqueous systems was successfully studied in this work. The understanding of the physical meaning of the closest approach parameter was improved. It was shown how this closest approach parameter can be used as a powerful tool on the description of the dissociation of ionic liquids in aqueous binary mixtures. Finally, it was possible to reduce the number of parameters in the thermodynamic models used which is a fundamental feature in the modeling of equilibria in general as it is a way to reduce the number of calculations necessary and the time spent on this task.

7 Assessment of the work done

7.1 Objectives achieved

In this work, two thermodynamic models were proposed to predict the extend of dissociation of ionic liquids in water: one thermodynamic model that assumed ionic liquids as neutral species, the UNIQUAC equation, and the other, the PDH + UNIQUAC model, which considers ionic liquids as electrolytes. The latter explores the different possible degrees of dissociation of ionic liquids in aqueous mixtures: no dissociation, partial dissociation or total dissociation. This objective was fully achieved and, for the first time, the physical meaning of the closest approach parameter in the PDH equation was addressed with a theoretical background, and, therefore, the distinct degrees of dissociation in ionic liquid/water systems.

Another objective was the study of the influence of the structure of ionic liquids on the interaction parameters of the UNIQUAC model and the PDH + UNIQUAC model. This secondary goal was also very successful, since it was possible to reduce the number of binary interaction parameters of the UNIQUAC model from 6 to 4, only based on the conclusions obtained from the study of the influence of the alkyl chain length of ionic liquids.

The results from the modeling with the thermodynamic models with 4 parameters presented the same tendencies as the first approach since the results were very similar. This was a very positive outcome due to being a new model with less parameters, which is less time-consuming and easier to work with.

To summarize, all the objectives proposed were accomplished and the additional report of the different values and corresponding physical meaning of the closest approach parameter was done in a way that aims to be a reference key for further works on ionic liquids' dissociation.

7.2 Suggestions of future work

Having enhanced the idea that the ionic liquids could dissociate in water, many opportunities may arise from this conclusion. Firstly, there are millions of possible ionic liquids to be synthesized, which opens the door to many routes. Secondly, another branch that can be followed on the topic of ionic liquids' dissociation is different solvents. The studied solvent in this work is water, as it is the most widely used solvent in industrial processes together with organic solvents such as alcohols. Hence, the next step forward is, understandably, the study of conductivities and LLE data of different ionic liquids in other solvents different from the one reported in this work.

7.3 Final assessment

This work presented itself as a difficult task due to scarcely available literature on ionic liquids' dissociation. It required a very intense research to learn to program in MATLAB, since this programing language is not taught throughout our formation in the previous years, which required much self-learning.

On a final (and good) note, I enjoyed working on this topic. Modeling has its difficulties but can be seen as a very rewarding task if the operator has enough patience. I think this work was a well-crafted theme and fits in the present-day idea of the ionic liquids, which is also another key point for me to have valued having the opportunity to work on it. For me, the best part of end-result of this thesis is that is not a dead-end on ionic liquids: there are many fields that can be explored from now on regarding ionic liquids' dissociation, as mentioned in Subchapter 7.2.

8 References

[1] Maia, F. M., Rodríguez, O., Macedo, E. A. 2010. LLE for (water + ionic liquid) binary systems using [$C_x$mim][BF_4] (x=6,8) ionic liquids. *Fluid Phase Equilibr.*, 296, 184-191.

[2] Santos, D., Góes, M., Franceschi, E., Santos, A., Dariva, C., Fortuny, M., Mattedi, S. 2015. Phase Equilibria for Binary Systems Containing Ionic Liquid with Water or Hydrocarbons. *Braz. J. Chem. Eng.*, 32, 967-974.

[3] Brown, T. L., Lemay, H. E., Burstein, B. E., Murphy, C. J., Woodward, P. M. 2012. *Chemistry: The Central Science*, 12th ed., Prentice Hall.

[4] Nordness, O., Brennecke, J. F. 2020. Ion Dissociation in Ionic Liquids and Ionic Liquid Solutions. *Chem. Ver.*, 120, 12873-12902.

[5] Walden, P. 1914. Über die molekulargrösse und elektrische leitfähigkeit einiger gesehmolzenen salze. *Bull. Aced. Imperr. Sci. St. Petersbourg*, 8, 405-422.

[6] Galinski, M., Lewandowski, A., Stepniak, I. 2006. Ionic liquids as electrolytes. *Electrochim. Acta*, 51, 5567-5580.

[7] Earle, M. J., Seddon, K. R. 2000. Ionic liquids. Green solvents for the future. *Pure Appl. Chem.*, 72, 1391-1398.

[8] Blanchard, L. A., Brennecke, J. F. 2001. Recovery of organic products from ionic liquids using supercrital carbon dioxide. *Ind. Eng. Chem. Res.*, 40, 287-292.

[9] Wilkes, J. S., Zaworotko, M. J. 1992. Air and water stable 1-ethyl-3-methylimidazolium based ionic liquids. *J. Chem. Soc., Chem. Commun.*, 13, 965-967.

[10] Han, X., Armstrong, D. W. 2007. Ionic liquids in separations. *Acc. Of Chem. Res.*, 40, 1079-1086.

[11] Freire, M. G., Neves, C. M. S. S., Carvalho, P. J., Gardas, R. L., Fernandes, A. M., Marrucho, I. M., Santos, L. M. N. B. F., Coutinho, J. A. P. 2007. Mutual Solubilities of Water and Hydrophobic Ionic Liquids. *J. Phys. Chem. B*, 111, 13082-13089.

[12] Freire, M. G., Carvalho, P. J., Gardas, R. L., Marrucho, I. M., Santos, L. M. N. B. F., Coutinho, J. A. P. 2008. Mutual Solubilities of Water and the [$C_n$mim][Tf_2N] Hydrophobic Ionic Liquids. *J. Phys. Chem. B*, 112, 1604-1610.

[13] Maia, F. M., Rodríguez, O., Macedo, E. A. 2012. Relative hydrophobicity of equilibrium phases in biphasic systems (ionic liquid + water). *J. Chem. Thermodyn.*, 48, 221-228.

[14] EPA, United States Environmental Protection Agency (2005, December 15). Novel Strategies for the Synthesis of Ionic Liquids in an Environmentally Friendly Manner. Retrieved from cfpub.epa.gov/si/si_public_record_Report.cfm?Lab=NRMRL&dirEntryID=131443.

[15] Plechkova, N. V., Seddon, K. R. 2008. Applications of ionic liquids in the chemical industry. *Chem. Soc. Rev.*, 37, 123-150.

[16] Anderson, J. L., Armstrong, D. W., Wei, G. T. 2006. Ionic liquids in analytical chemistry. *Anal. Chem.*, 78, 2892-2902.

[17] Seddon, K. R. 1997. Ionic liquids for clean technology. *J. Chem. Technol. Biotechnol.*, 68, 351-356.

[18] Welton, T. 1999. Room-Temperature Ionic Liquids. Solvents for Synthesis and Catalysis. *Chem. Rev.*, 99, 2071-2083.

[19] Favre, F., Olivier-Bourbigou, H., Commereuc, D., Saussine, L. 2001. Hydroformylation of 1-hexene with rhodium in non-aqueous ionic liquids: how to design the solvent and the ligand to the reaction. *Chem. Commun.*, 15, 1360-1361.

[20] Wasserscheid, P., Welton, T. 2007. *Ionic liquids in Synthesis*, 2nd ed., Wiley-VCH, Weinheim.

[21] Dupont, J., Souza, R. F., Suarez, P. A. Z. 2002. Ionic liquid (molten salt) phase organometallic catalysis. *Chem. Rev.*, 102, 3667-3692.

[22] Rantwijk, F. v., Sheldon, R. 2007. Biocatalysis in ionic liquids. *Chem Rev.*, 107, 2757-2785.

[23] Gorlov, M., Kloo, L. 2008. Ionic liquid electrolytes for dye-sensitized solar cells. *Dalton Trans.*, 20, 2655-2666.

[24] Mecerreyes, D. 2011. Polymeric ionic liquids: Broadening the properties and applications of polyelectrolytes. *Prog. Polym. Sci.*, 36, 1629-1648.

[25] Huddleston, J. G., Willauer, H. D., Swatloski, R. P., Visser, A. E., Rogers, R. D. 1998. Room temperature ionic liquids as novel media for clean liquid-liquid extraction. *Chem. Commun.*, 16, 1765-1766.

[26] Wei, G., Chen, J. C., Yang, Z., 2003. Studies on liquid/liquid extraction of copper ion with room temperature ionic liquid. *J. Chin. Chem. Soc.*, 50, 1123-1130.

[27] Han, D., Row, K. H. 2010. Recent Applications of Ionic Liquids in Separation Technology. *Molecules*, 15, 2405-2426.

[28] Roosen, C., Müller, P., Greiner, L. 2008. Ionic liquids in biotechnology: applications and perspectives for biotransformations. *Appl. Microbiol. Biotechnol.*, 81, 607-614.

[29] Hallett, J. P., Welton, T. 2011. Room-Temperature Ionic Liquids: Solvents for Synthesis and Catalysis. 2. *Chem. Rev.*, 111, 3508-3576.

[30] Zhang, Q. H., Zhang, S. G., Deng, Y. Q. 2011. Recent advances in ionic liquid catalysis. *Green Chem.*, 13, 2619-2637.

[31] Graenacher, C. 1934. *Cellulose solution*. US Patent 1943176.

[32] Abai, M., Atkins, M. P., Cheun, K. Y., Holbrey, J., Nockemann, P., Seddon, K., Srinivasan, G., Zou, Y. 2012. *Process for removing metals from hydrocarbons*. Patent WO2012046057.

[33] Chang, C. K., Ling, S. T. 2020. Extended Pitzer-Debye-Hückel Model for Long-Range Interactions in Ionic Liquids. *J. Chem. Eng. Data*, 65, 1019-1027.

[34] Wertz, C., Lehmann, J. K., Heintz, A. 2013. Liquid−Liquid Phase Equilibria of the Binary Ionic Liquid Systems [C_n MIM][NTf_2] + *n*-Butanol, + *n*-Pentanol, + H_2O Using UV Spectroscopic and Densimetric Analytical Methods. *J. Chem. Eng. Data*, 58, 2375-2380.

[35] Teixeira, F. S., Vieira, N. S. M., Cortes, O. A., Araújo, J. M. M., Marrucho, I. M., Rebelo, L. P. N., Pereiro, A. B. 2015. Phase equilibria and surfactant behavior of fluorinated ionic liquids with water. *J. Chem. Thermodyn.*, 82, 99-107.

[36] Domanska, U., Królikowski, M., Zawadzki, M., Wróblewska, A. 2016. Phase equilibrium investigation with ionic liquids and selectivity in separation of 2 phenylethanol from water. *J. Chem. Thermodynamics*, 102, 357-366.

[37] Domanska, U., Okuniewska, P., Królikowski, M. 2016. Separation of 2-phenylethanol (PEA) from water using ionic liquids. *Fluid Phase Equilibr.*, 423, 109-119.

[38] Velho, P., Liang, X., Macedo, E. A., Gómez, E., Kontogeorgis, G. M. 2021. Towards a predictive Cubic Plus Association equation of state. *Fluid Phase Equilibr.*, 540, 113045.

[39] Jog, P. K., Chapman, W. G. 1999. Application of Wertheim's thermodynamic perturbation theory to dipolar hard sphere chains. *Mol. Phys.*, 97, 307-319.

[40] Gross, J., Sadowski, G. 2001. Perturbed-Chain SAFT: An Equation of State Based on a Perturbation Theory for Chain Molecules. *Ind. Eng. Chem. Res.*, 40, 1244-1260.

[41] Li, Y., Wang, L., Cai, S. 2010. Mutual Solubility of Alkyl Imidazolium Hexafluorophosphate Ionic Liquids and Water. *J. Chem. Eng. Data*, 55, 5289-5293.

[42] Neves, C. M. S. S., Batista, M. L. S., Cláudio, A. F. M., Santos, L. M. N. B. F., Marrucho, I. M., Coutinho, J. A. P. 2010. Thermophysical Properties and Water Saturation of $[PF6]^-$ Based Ionic Liquids. *J. Chem. Eng. Data*, 55, 5065-5073.

[43] Neves, C. M. S. S., Rodrigues, A. R., Kurnia, K. A., Esperança, J. M. S. S., Freire, M. G., Coutinho, J. A. P. 2013. Solubility of non-aromatic hexafluorophosphate-based salts and ionic liquids in water determined by electrical conductivity. *Fluid Phase Equilibr.*, 358, 50-55.

[44] Martins, M. A. R., Neves, C. M. S. S., Kurnia, K. A., Santos, L. M. N. B. F., Freire, M. G., Pinho, S. P., Coutinho, J. A. P. 2014. Analysis of the isomerism effect on the mutual solubilities of bis(trifluoromethylsulfonyl)imide-based ionic liquids with Water. *Fluid Phase Equilibr.*, 381, 28-35.

[45] Domanska, U., Paduszynski, K., Królikowski, M., Wróblewska, A. 2016. Separation of 2-Phenylethanol from Water by Liquid−Liquid Extraction with Ionic Liquids: New Experimental Data and Modeling with Modern Thermodynamic Tools. *Ind. Eng. Chem. Res.*, 55, 5736-5747.

[46] Freire, M. G., Neves, C. M. S. S., Ventura, S. P. M., Pratas, M. J., Marrucho, I. M., Oliveira, J., Coutinho, J. A. P., Fernandes, A. M. 2010. Solubility of non-aromatic ionic liquids in water and correlation using a QSPR approach. *Fluid Phase Equilibr.*, 294, 234-240.

[47] Rupp, A., Roznyatovskaya, N., Scherer, H., Beichel, W., Klose, P., Sturm, C., Hoffmann, A., Tübke, J., Koslowski, T., Krossing, I. 2014. Size Matters! On the Way to Ionic Liquid Systems without Ion Pairing. *Chem. Eur. J.*, 20, 9794–9804.

[48] Harris, K. R., Kanakubo, M. 2015. Self-Diffusion, Velocity Cross-Correlation, Distinct Diffusion and Resistance Coefficients of the Ionic Liquid [BMIM][Tf2N] at High Pressure. *Phys. Chem. Chem. Phys.*, 17, 23977–23993.

[49] Mazan, V., Boltoeva, M. 2017. Insight into the Ionic Interactions in Neat Ionic Liquids by Diffusion Ordered Spectroscopy Nuclear Magnetic Resonance. *J. Mol. Liq.*, 240, 74–79.

[50] Tokuda, H., Hayamizu, K., Ishii, K., Susan, M. A. B. H., Watanabe, M. 2004. Physicochemical Properties and Structures of Room Temperature Ionic Liquids. 1. Variation of Anionic Species. *J. Phys. Chem. B*, 108, 16593-16600.

[51] Tokuda, H., Hayamizu, K., Ishii, K., Susan, M. A. B. H., Watanabe, M. 2005. Physicochemical Properties and Structures of Room Temperature Ionic Liquids. 2. Variation of Alkyl Chain Length in Imidazolium Cation. *J. Phys. Chem. B*, 109, 6103-6110.

[52] Tokuda, H., Hayamizu, K., Tsuzuki, S., Susan, M. A. B. H., Watanabe, M. 2006. Physicochemical Properties and Structures of Room Temperature Ionic Liquids. 3. Variation of Cationic Structures. *J. Phys. Chem. B*, 110, 2833-2839.

[53] Ueno, K., Tokuda, H., Watanabe, M. 2010. Ionicity in ionic liquids: correlation with ionic structure and physicochemical properties. *Phys. Chem. Chem. Phys.*, 12, 1649-1658.

[54] Nordness, O., Simoni, L. D., Stadtherr, M. A., Brennecke, J. F. 2019. Characterization of Aqueous 1-Ethyl-3-Methylimidazolium Ionic Liquids for Calculation of Ion Dissociation. *J. Phys. Chem. B*, 123, 1348-1358.

[55] Lin, Y. J., Hossain, N., Chen, C. C. 2021. Modeling dissociation of ionic liquids with electrolyte NRTL model. *J. Mol. Liq.*, 329, 115524.

[56] Abrams, D. S., Prausnitz, J. M. 1975. Statistical thermodynamics of liquid mixtures: A new expression for the excess Gibbs energy of partly or completely miscible systems. *AIChE J.*, 21, 116-128.

[57] Prausnitz, J. M., Lichenthaler, R. N., Azevedo, E. G. 1998. *Molecular Thermodynamic of Fluid-Phase Equilibria*, 3rd ed., Prentice-Hll, Englewood Cliffs, New Jersey.

[58] Sander, B., Fredenslund, A., Rasmussen, P. 1986. Calculation of Vapor-Liquid Equilibria in Mixed Solvent/Salt Systems Using an Extended UNIQUAC Equation. *Chem. Eng. Sci.*, 41, 1171-1183.

[59] Kato, R., Gmehling, J. 2005. Measurement and correlation of vapor-liquid equilibria of binary systems containing the ionic liquids [EMIM][$(CF_3SO_2)_2N$], [BMIM][$(CF_3SO_2)_2N$], [MMIM][$(CH_3)_2PO_4$], and oxygenated organic compounds respectively water. *Fluid Phase Equilibr.*, 231, 38-43.

[60] Chapeaux, A., Simoni, L. D., Ronan, T. S., Stadtherr, M. A., Brennecke, J. F. 2008. Extraction of alcohols from water with 1-hexyl-3-methylimidazolium bis(trifluoromethylsulfonyl)imide. *Green Chem.*, 10, 1301-1306.

[61] Calvar, N., Domínguez, I., Gómez, E., Domínguez, Á. 2011. Separation of binary mixtures aromatic + aliphatic using ionic liquids: Influence of the structure of the ionic liquid, aromatic and aliphatic. *Chem. Eng. J.*, 175, 213-221.

[62] Seoane, R. G., González, E. J., González, B. 2012. 1-Alkyl-3-methylimidazolium bis(trifluoromethylsulfonyl)imide ionic liquids as solvents in the separation of azeotropic mixtures. *J. Chem. Thermodyn.*, 53, 152-157.

[63] Yunus, N. M., Shaharun, M. S., Mutalib, M. I. A., Murugesan, T. 2016. Modeling of CO_2 solubility in pyridinium-based ionic liquid using UNIQUAC. *AIP Conference Proceedings*, 1787.

[64] Santiago, R. S., Santos, G. R., Aznar, M. 2009. UNIQUAC correlation of liquid-liquid equilibrium in systems involving ionic liquids: The DFT-PCM approach. *Fluid Phase Equilibr.*, 278, 54-61.

[65] Santiago, R. S., Aznar, M. 2011. Liquid-liquid equilibrium in ternary ionic liquid systems by UNIFAC: New volume, surface area and interaction parameters. Part II. *Fluid Phase Equilibr.*, 303, 111-114.

[66] Liu, W., Zhang, Z., Ri, Y., Xu, X., Wang, Y. 2016. Liquid-liquid equilibria for ternary mixtures of water + 2-propanol + 1-alkyl-3-methylimidazolium bis(trifluoromethylsulfonyl)imide ionic liquids at 298.15 K. *Fluid Phase Equilibr.*, 412, 205-210.

[67] Pitzer, K. S. 1980. Electrolytes. From Dilute Solutions to Fused Salts. *Am. Chem. Soc.*, 102, 2902-2906.

[68] Pitzer, K. S., Simonson, J. M. 1986. Thermodynamics of Multicomponent, Miscible, Ionic Systems: Theory and Equations. *Am. Chem. Soc.*, 90, 3005-3009.

[69] NIST, National Institute of Standards and Technology (2018). CODATA Internationally recommended 2018 values of the Fundamental Physical Constants. Physics.nist.gov/cuu/Constants/index.html.

[70] Archer, D. G., Wang, P. 1990. The Dielectric Constant of Water and Debye-Hückel Limiting Law Slopes. *J. Phys. Chem. Ref. Data*, 19, 371-411.

[71] USGS, U. S. Geological Survey (2007). Water's density varies with temperature. www.usgs.gov/special-topic/water-science-school/science/water-density?qt-science_center_objects=0#qt-science_center_objects.

[72] Chen, C. C., Evans, L. B. 1986. A Local Composition Model for the Excess Gibbs Energy of Aqueous Electrolyte Systems. *AIChE J.*, 32, 444-454.

[73] Barata, P. A., Serrano, M. L. 1997. Thermodynamic representation of the solubility for potassium dihydrogen phosphate (KDP) + water + alcohols systems. *Fluid Phase Equilibr.*, 247, 247-263.

[74] Achard, C., Dussap, C. G., Gros, J. B. 1994. Representation of vapour-liquid equilibria in water-alcohol-electrolyte 49ixture with a modified UNIFAC group-contribution method. *Fluid Phase Equilibr.*, 98, 71-89.

[75] Jacquemin, J., Ge, R., Nancarrow, P., Rooney, D. W., Gomes, M. F. C., Pádua, A. A. H., Hardcre, C. 2008. Prediction of Ionic Liquidss Properties. I. Volumetric Properties as a Function of Temperature at 0.1 Mpa. *J. Chem. Eng. Data*, 53, 716-726.

[76] Martins, M. A. R., Neves, C. M. S. S., Kurnia, K. A., Carvalho, P. J., Rocha, M. A. A., Santos, L. M. N. B. F., Pinho, S. P., Freire, M. G. 2016. Densities, Viscosities and Derived Thermophysical Properties of Water-Saturated Imidazolium-based Ionic Liquids. *Fluid Phase Equilibr.*, 407, 188-196.

[77] Harris, K. R., Kanakubo, M., Woolf, L. A. 2007. Temperature and Pressure Dependence of the Viscosity of the Ionic Liquids 1-Hexyl-3-methylimidazolium Hexafluorophosphate and 1-Butyl-3-methylimidazolium Bis(trifluoromethylsulfonyl)imide. *J. Chem. Eng. Data*, 52, 1080-1085.

[78] Santos, D., Santos, M., Franceschi, E., Dariva, C., Barison, A., Mattedi, S. 2016. Experimental Density of Ionic Liquids and Thermodynamic Modeling with Group Contribution Equation of State Based on the Lattice Fluid Theory. *J. Chem. Eng. Data*, 61, 348-353.

[79] Oliveira, F. S., Freire, M. G., Carvalho, P. J., Coutinho, J. A. P., Lopes, J. N. C., Rebelo, L. P. N., Marrucho, I. M. 2010. Structural and Positional Isomerism Influence in the Physical Properties of Pyridinium NTf_2-Based Ionic Liquids: Pure and Water-Saturated Mixtures. *J. Chem. Eng. Data*, 55, 4514-4520.

[80] Gardas, R. L., Freire, M. G., Carvalho, P. J., Marrucho, I. M., Fonseca, I. M. A., Ferreira, A. G. M., Coutinho, J. A. P. 2007. High-Pressure, Densities and Derived Thermodynamic Properties of Imidazolium-Based Ionic Liquids. *J. Chem. Eng. Data*, 52, 80-88.

[81] Carissimi, G., Montalbán, M. G., Baños, F. G. D., Víllora, G. 2019. Density, refractive index and volumetric properties of water-ionic liquid binary systems with imidazolium-based cations and tetrafluoroborate, triflate and octylsulphate anions at T=293 to 343 K and p = 0.1 Mpa. *J. Chem. Eng. Data*, 64, 979-994.

[82] Soucková, M., Klomfar, J., Pátek, J. 2016. Surface tension and 0.1 Mpa density of 1-alkyl-3-methylimidazolium tetrafluoroborates in a homologous series perspective. *J. Chem. Thermodynamics*, 100, 79-88.

[83] McLaughlin, E. V. 1958. Self-Difusion in Liquids. *J. Chem. Soc. Faraday Trans.*, 55, 28.

[84] Green, S. M., Ries, M. E., Moffat, J., Budtova, T. 2017. NMR and Rheological Study of Anion Size Influence on the Properties of Two Imidazolium-based Ionic Liquids. *Sci. Rep.*, 8968, 1-12.

[85] Dong, K., Zhang, S., Wang, D., Yao, X. 2006. Hydrogen Bonds in Imidazolium Ionic Liquids. *J. Phys. Chem. A*, 110, 9775-9782.

Appendix A – Selected ionic liquids and properties

I) Structures and IUPAC names of the ionic liquids used in work

- $[C_2mim][NTf_2]$, 1-ethyl-3-methylimidazolium bis(trifluoromethylsulfonyl)imide

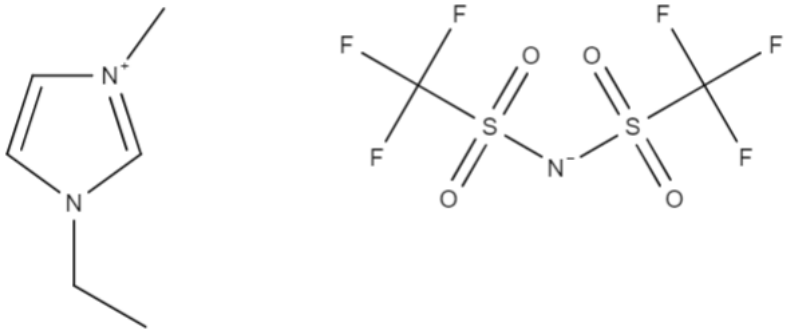


Fig. A.1: 1-ethyl-3-methylimidazolium bis(trifluoromethylsulfonyl)imide.

- $[C_3mim][NTf_2]$, 1-methyl-3-propylimidazolium bis(trifluoromethylsulfonyl)imide

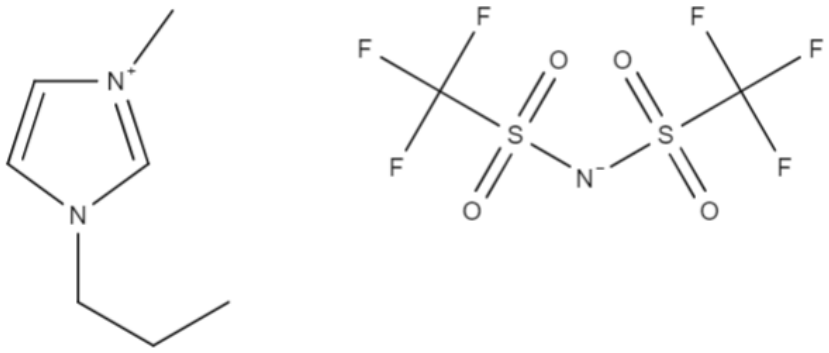


Fig. A.2: 1-methyl-3-propylimidazolium bis(trifluoromethylsulfonyl)imide.

- $[C_4mim][NTf_2]$, 1-butyl-3-methylimidazolium bis(trifluoromethylsulfonyl)imide

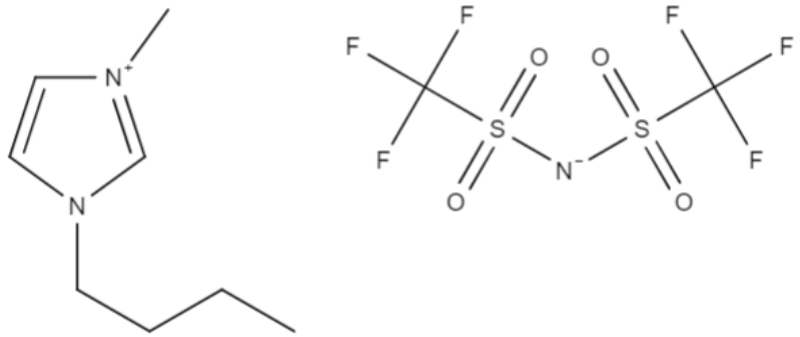


Fig. A.3: 1-butyl-3-methylimidazolium bis(trifluoromethylsulfonyl)imide.

- $[C_5mim][NTf_2]$, 1-pentyl-3-methylimidazolium bis(trifluoromethylsulfonyl)imide

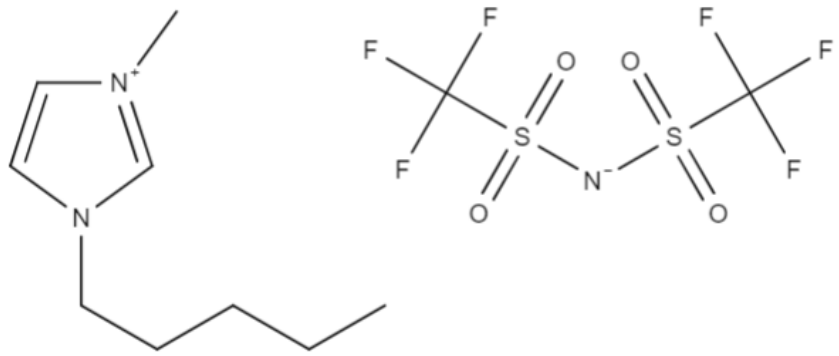


Fig. A.4: 1-pentyl-3-methylimidazolium bis(trifluoromethylsulfonyl)imide.

- $[C_6mim][NTf_2]$, 1-hexyl-3-methylimidazolium bis(trifluoromethylsulfonyl)imide

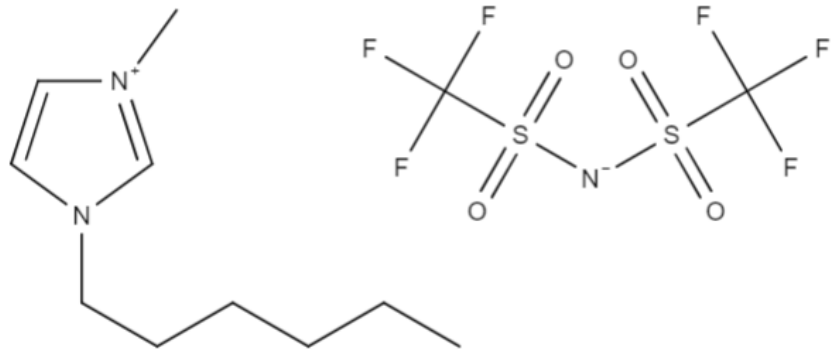


Fig. A.5: 1-hexyl-3-methylimidazolium bis(trifluoromethylsulfonyl)imide.

- $[C_7mim][NTf_2]$, 1-heptyl-3-methylimidazolium bis(trifluoromethylsulfonyl)imide

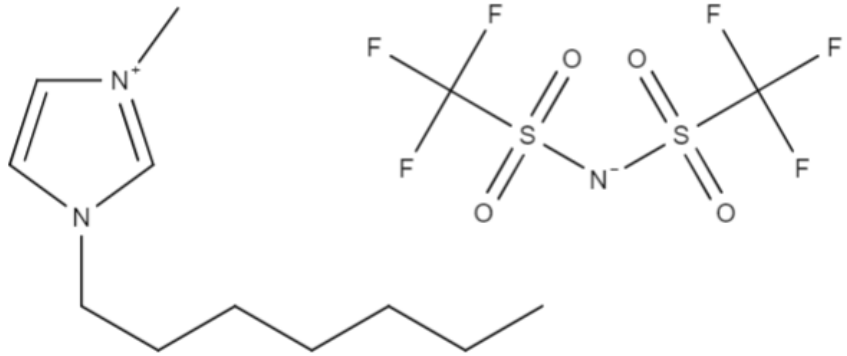


Fig. A.6: 1-heptyl-3-methylimidazolium bis(trifluoromethylsulfonyl)imide.

- $[C_8mim][NTf_2]$, 1-octyl-3-methylimidazolium bis(trifluoromethylsulfonyl)imide

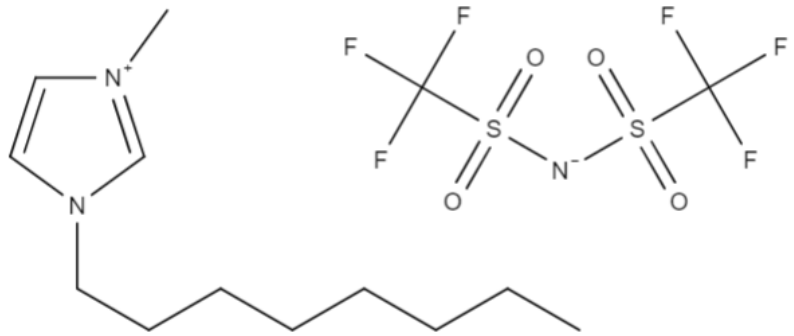


Fig. A.7: 1-octyl-3-methylimidazolium bis(trifluoromethylsulfonyl)imide.

- $[C_4py][NTf_2]$, 1-butylpyridinium bis(trifluoromethylsulfonyl)imide

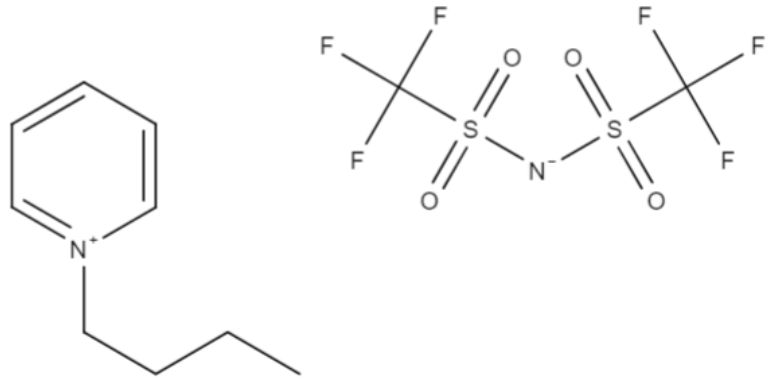


Fig. A.8: 1-butylpyridinium bis(trifluoromethylsulfonyl)imide.

- $[C_4mim][PF_6]$, 1-butyl-3-methylimidazolium hexafluorophosphate

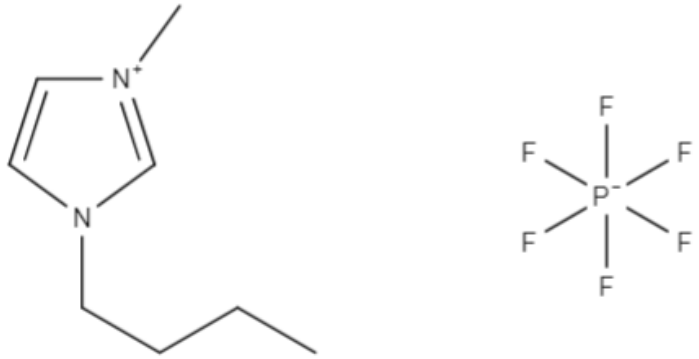


Fig. A.9: 1-butyl-3-methylimidazolium hexafluorophosphate.

- $[C_6mim][PF_6]$, 1-hexyl-3-methylimidazolium hexafluorophosphate

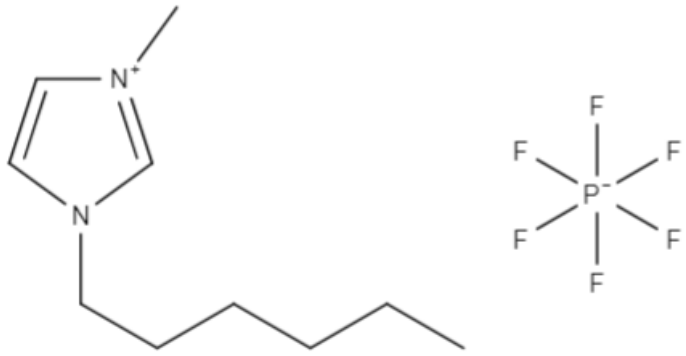


Fig. A.10: 1-hexyl-3-methylimidazolium hexafluorophosphate.

- [C_8mim][PF_6], 1-octyl-3-methylimidazolium hexafluorophosphate

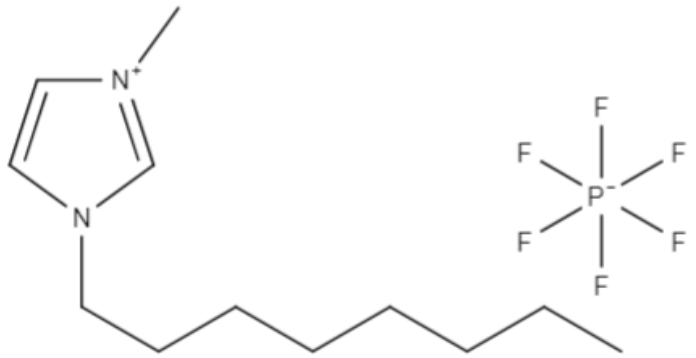


Fig. A.11: 1-octyl-3-methylimidazolium hexafluorophosphate.

- [C_6mim][BF_4], 1-hexyl-3-methylimidazolium tetrafluoroborate

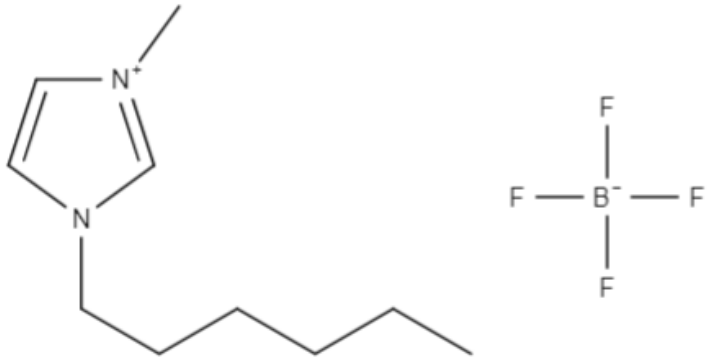


Fig. A.12: 1-hexyl-3-methylimidazolium tetrafluoroborate.

- $[C_8mim][BF_4]$, 1-octyl-3-methylimidazolium tetrafluoroborate

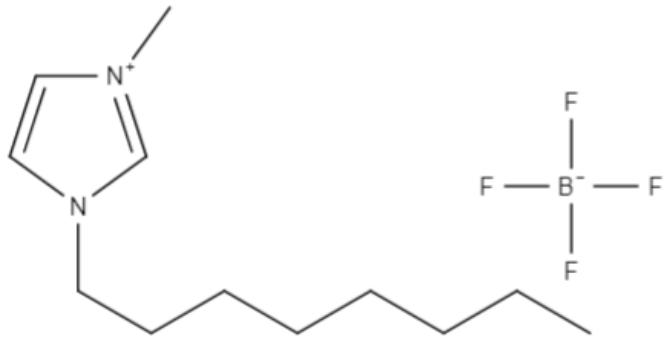


Fig. A.13: 1-octyl-3-methylimidazolium tetrafluoroborate.

- $[C_{10}mim][BF_4]$, 1-decyl-3-methylimidazolium tetrafluoroborate

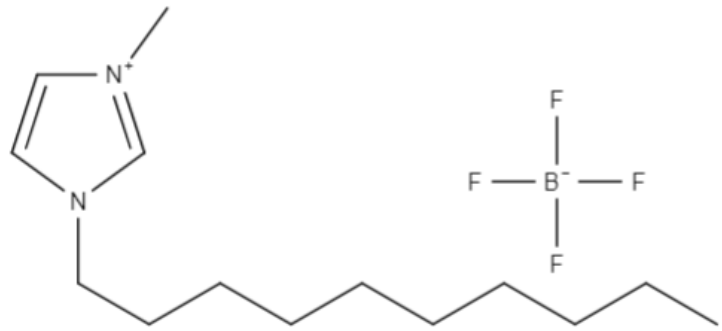


Fig. A.14: 1-decyl-3-methylimidazolium tetrafluoroborate.

II) Properties of the ionic liquids and solvent used in this work

Table A.1: UNIQUAC volume, r_i, and surface area, q_i, structural parameters.

Compound[a]	r_i	q_i	References
$[NTf_2]^-$	5.166	5.116	[59-63]
$[PF_6]^-$	2.427	2.017	[64,65]
$[BF_4]^-$	1.786	1.494	[64,65]
$[C_2mim]^+$	4.728	3.664	[59,64]
$[C_3mim]^+$	5.381	4.228	[63]
$[C_4mim]^+$	6.033	4.791	[59,61,62,64]
$[C_5mim]^+$	6.919	5.298	[63]
$[C_6mim]^+$	7.804	5.804	[60,62,64-66]
$[C_7mim]^+$	8.382	6.415	[63]
$[C_8mim]^+$	8.961	7.025	[62,64-66]
$[C_{10}mim]^+$	9.539	7.636	[66]
$[C_4py]^+$	6.506	4.551	[63]
H_2O	0.920	1.400	[59,60,64,65]

[a] The structural parameters of each ionic liquid molecule were calculated by summing the ones of the ions present.

The density of the solvent, water, was fitted from experimental data[71] following a cubic polynomial, eq.(A.1). Table A.2 presents the values of the fitted parameters. The plot of the experimental points and the fitted curve are present in Figure A.15.

$$\rho_0 = a_0 T^3 + b_0 T^2 + c_0 T + d_0 \quad \text{(A.1)}$$

Table A.2: Fitted parameters for the water density cubic polynomial.

Density Fitted parameters	
a_0 / kg·m^{-3}·K^{-3}	$2.2716 \cdot 10^{-5}$
b_0 / kg·m^{-3}·K^{-2}	-0.0256
c_0 / kg·m^{-3}·K^{-1}	8.9467
d_0 / kg·m^{-3}	1.0789

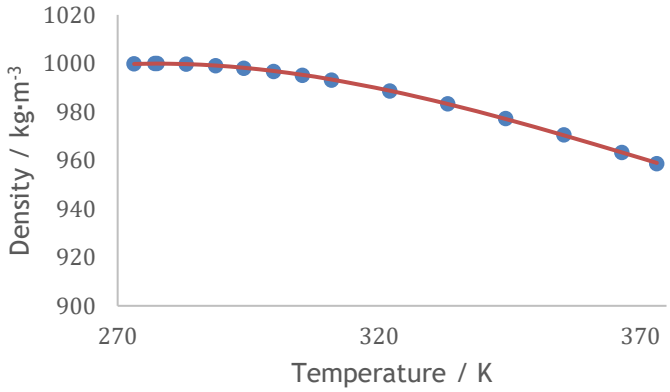


Fig. A.15: Water density as a function of temperature. The blue dots represent the experimental data[71] and the red line corresponds to the eq.(A.1).

Table A.3: Density at 40 °C, molecular mass and calculated radius with the simplified Stokes-Einstein equation for ionic liquids presented in this work.

Ionic liquid	Density kg·m^{-3}	Molecular mass g·mol^{-1}	R_{IL} Å	References
[C_2mim][NTf_2]	1502.9	391.31	3.78	[75]
[C_3mim][NTf_2]	1448.9	405.33	3.87	[76]
[C_4mim][NTf_2]	1423.5	419.36	3.94	[77]
[C_5mim][NTf_2]	1382.0	433.38	4.02	[76]
[C_6mim][NTf_2]	1356.9	447.40	4.09	[75]
[C_7mim][NTf_2]	1323.3	461.42	4.17	[76]
[C_8mim][NTf_2]	1307.0	475.44	4.23	[78]
[C_4py][NTf_2]	1431.2	416.40	3.92	[79]
[C_4mim][PF_6]	1353.3	284.18	3.52	[80]
[C_6mim][PF_6]	1281.17	312.23	3.70	[80]
[C_8mim][PF_6]	1225.3	340.28	3.86	[80]
[C_6mim][BF_4]	1117.9	254.08	3.61	[81]
[C_8mim][BF_4]	1092.9	282.13	3.77	[80]
[C_{10}mim][BF_4]	1061.8	310.18	3.93	[82]

Appendix B – Experimental LLE data for ionic liquid/water systems collected from literature

Table B.1: Experimental mole fractions[12] for the [C_2mim][NTf_2]/water system for the water-rich phase, x_{IL}^{W}, and for the ionic liquid-rich phase, x_{IL}^{IL}.

T / K	$x_{IL}^{W} \cdot 10^3$	x_{IL}^{IL}
288.15	0.766	0.725
293.15	0.803	0.713
298.15	0.838	0.702
303.15	0.875	0.688
308.15	0.933	0.672
313.15	0.985	0.655
318.15	1.050	0.640

Table B.2: Experimental mole fractions[12] for the [C_3mim][NTf_2]/water system for the water-rich phase, x_{IL}^{W}, and for the ionic liquid-rich phase, x_{IL}^{IL}.

T / K	$x_{IL}^{W} \cdot 10^3$	x_{IL}^{IL}
288.15	0.515	0.750
293.15	0.527	0.742
298.15	0.540	0.729
303.15	0.568	0.714
308.15	0.604	0.699
313.15	0.649	0.683
318.15	0.701	0.668

Table B.3: Experimental mole fractions[12] for the $[C_4mim][NTf_2]$/water system for the water-rich phase, ${x_{IL}}^{W}$, and for the ionic liquid-rich phase, ${x_{IL}}^{IL}$.

T / K	${x_{IL}}^{W} \cdot 10^3$	${x_{IL}}^{IL}$
288.15	0.286	0.769
293.15	0.292	0.756
298.15	0.307	0.743
303.15	0.318	0.729
308.15	0.344	0.715
313.15	0.394	0.701

Table B.4: Experimental mole fractions[12] for the $[C_5mim][NTf_2]$/water system for the water-rich phase, ${x_{IL}}^{W}$, and for the ionic liquid-rich phase, ${x_{IL}}^{IL}$.

T / K	${x_{IL}}^{W} \cdot 10^3$	${x_{IL}}^{IL}$
288.15	0.184	0.795
293.15	0.188	0.787
298.15	0.196	0.779
303.15	0.201	0.768
313.15	0.232	0.743
318.15	0.253	0.733

Table B.5: Experimental mole fractions[12] for the $[C_6mim][NTf_2]$/water system for the water-rich phase, ${x_{IL}}^{W}$, and for the ionic liquid-rich phase, ${x_{IL}}^{IL}$.

T / K	${x_{IL}}^{W} \cdot 10^4$	${x_{IL}}^{IL}$
288.15	0.890	0.809
293.15	0.896	0.802
303.15	0.973	0.781
308.15	1.020	0.770
313.15	1.170	0.758
318.15	1.320	0.744

Table B.6: Experimental mole fractions[12] for the $[C_7mim][NTf_2]$/water system for the water-rich phase, ${x_{IL}}^{W}$, and for the ionic liquid-rich phase, ${x_{IL}}^{IL}$.

T / K	${x_{IL}}^{W} \cdot 10^4$	${x_{IL}}^{IL}$
288.15	0.485	0.819
293.15	0.498	0.812
298.15	0.509	0.803
303.15	0.528	0.792
308.15	0.581	0.781
313.15	0.687	0.767

Table B.7: Experimental mole fractions[12] for the $[C_8mim][NTf_2]$/water system for the water-rich phase, ${x_{IL}}^{W}$, and for the ionic liquid-rich phase, ${x_{IL}}^{IL}$.

T / K	${x_{IL}}^{W} \cdot 10^4$	${x_{IL}}^{IL}$
288.15	0.317	0.829
293.15	0.323	0.822
298.15	0.336	0.813
303.15	0.355	0.805
308.15	0.368	0.795
313.15	0.394	0.785
318.15	0.455	0.776

Table B.8: Experimental mole fractions[2] for the $[C_4py][NTf_2]$/water system for the water-rich phase, ${x_{IL}}^{W}$, and for the ionic liquid-rich phase, ${x_{IL}}^{IL}$.

T / K	${x_{IL}}^{W} \cdot 10^3$	${x_{IL}}^{IL}$
293.20	0.398	0.747
298.20	0.399	0.734
303.20	0.409	0.706
308.20	0.440	0.691
313.20	0.508	0.666

Table B.9: Experimental mole fractions[11] for the [C_4mim][PF_6]/water system for the water-rich phase, x_{IL}^{W}, and for the ionic liquid-rich phase, x_{IL}^{IL}.

T / K	$x_{IL}^{W} \cdot 10^2$	x_{IL}^{IL}
288.15	0.101	0.771
293.15	0.110	0.749
298.15	0.121	0.728
303.15	0.129	0.707
313.15	0.158	0.667
318.15	0.176	0.652

Table B.10: Experimental mole fractions[11] for the [C_6mim][PF_6]/water system for the water-rich phase, x_{IL}^{W}, and for the ionic liquid-rich phase, x_{IL}^{IL}.

T / K	$x_{IL}^{W} \cdot 10^3$	x_{IL}^{IL}
288.15	0.354	0.804
293.15	0.392	0.791
298.15	0.434	0.771
303.15	0.468	0.750
308.15	0.504	0.733
313.15	0.559	0.712

Table B.11: Experimental mole fractions[11] for the $[C_8mim][PF_6]$/water system for the water-rich phase, ${x_{IL}}^{W}$, and for the ionic liquid-rich phase, ${x_{IL}}^{IL}$.

T / K	${x_{IL}}^{W} \cdot 10^3$	${x_{IL}}^{IL}$
288.15	0.113	0.828
293.15	0.120	0.815
303.15	0.146	0.783
308.15	0.159	0.771
313.15	0.176	0.750
318.15	0.203	0.743

Table B.12: Experimental mole fractions[1] for the $[C_6mim][BF_4]$/water system for the water-rich phase, ${x_{IL}}^{W}$, and for the ionic liquid-rich phase, ${x_{IL}}^{IL}$.

T / K	${x_{IL}}^{W}$	${x_{IL}}^{IL}$
293.15	0.063	0.849
296.15	0.068	0.837
298.15	0.070	0.830
303.15	0.080	0.816
308.15	0.090	0.802
313.15	0.103	0.787
318.15	0.123	0.771
323.15	0.160	0.755
328.15	0.186	0.731

Table B.13: Experimental mole fractions[1] for the [C_8mim][BF_4]/water system for the water-rich phase, x_{IL}^{W}, and for the ionic liquid-rich phase, x_{IL}^{IL}.

T / K	x_{IL}^{W}	x_{IL}^{IL}
303.15	0.021	0.862
308.15	0.023	0.851
313.15	0.027	0.840
318.15	0.038	0.822
323.15	0.071	0.797
333.15	0.161	0.764
338.15	0.201	0.740
340.15	0.330	0.700

Table B.14: Experimental mole fractions[13] for the [C_{10}mim][BF_4]/water system for the water-rich phase, x_{IL}^{W}, and for the ionic liquid-rich phase, x_{IL}^{IL}.

T / K	x_{IL}^{W}	x_{IL}^{IL}
293.15	0.005	0.819
296.15	0.005	0.812
298.15	0.007	0.808
303.15	0.016	0.799
308.15	0.060	0.780
313.15	0.118	0.765
318.15	0.143	0.726
323.15	0.280	0.679
325.15	0.330	0.520

Appendix C – Modeling results for the UNIQUAC model and the PDH + UNIQUAC model with 6 parameters

The LLE modeling results using the UNIQUAC model and PDH + UNIQUAC model with 6 parameters are displayed throughout this appendix. The aqueous binary systems of ionic liquids already presented in the Results and discussion chapter are also shown with the rest of the ionic liquid/water systems studied in this work.

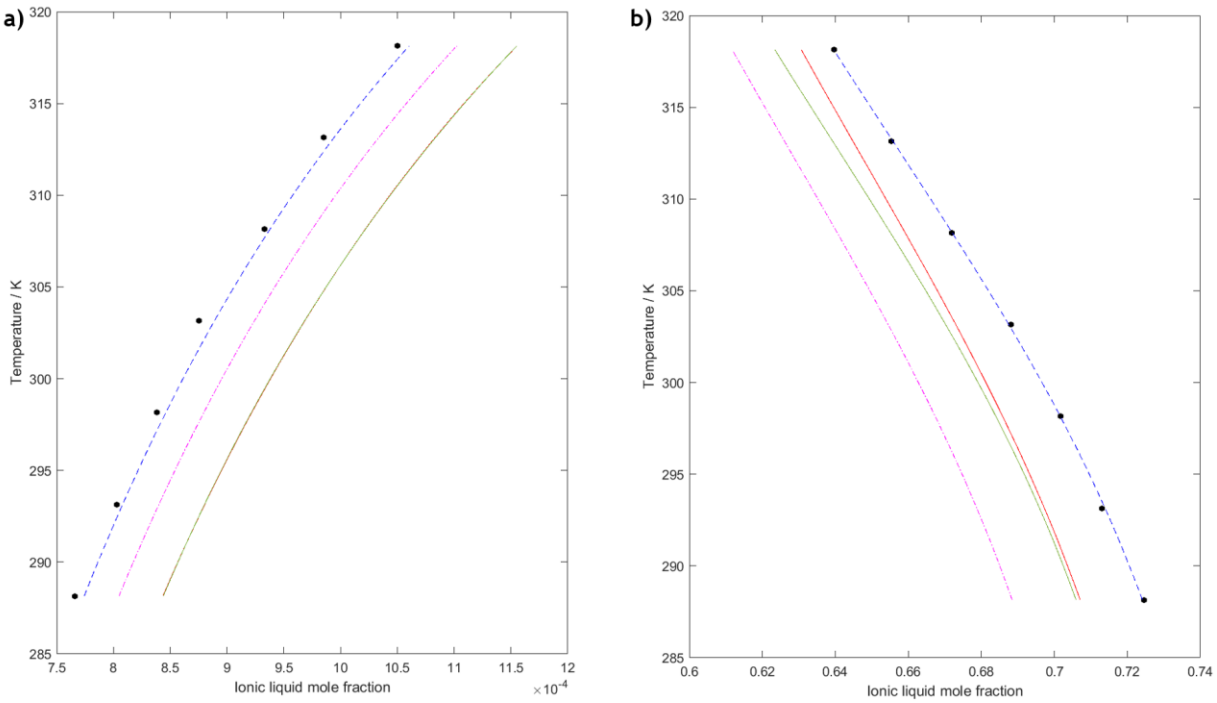


Fig. C.1: Calculated solubility curves for the binary system [C_2mim][NTf_2]/water at atmospheric pressure. a) water-rich phase and b) ionic liquid-rich phase. The black dots represent the experimental points, the red lines correspond to the results from the UNIQUAC model, the green lines are the results from the PDH + UNIQUAC model for a minimum closest approach parameter, the blue lines for a medium closest approach parameter and the pink lines for a maximum closest approach parameter.

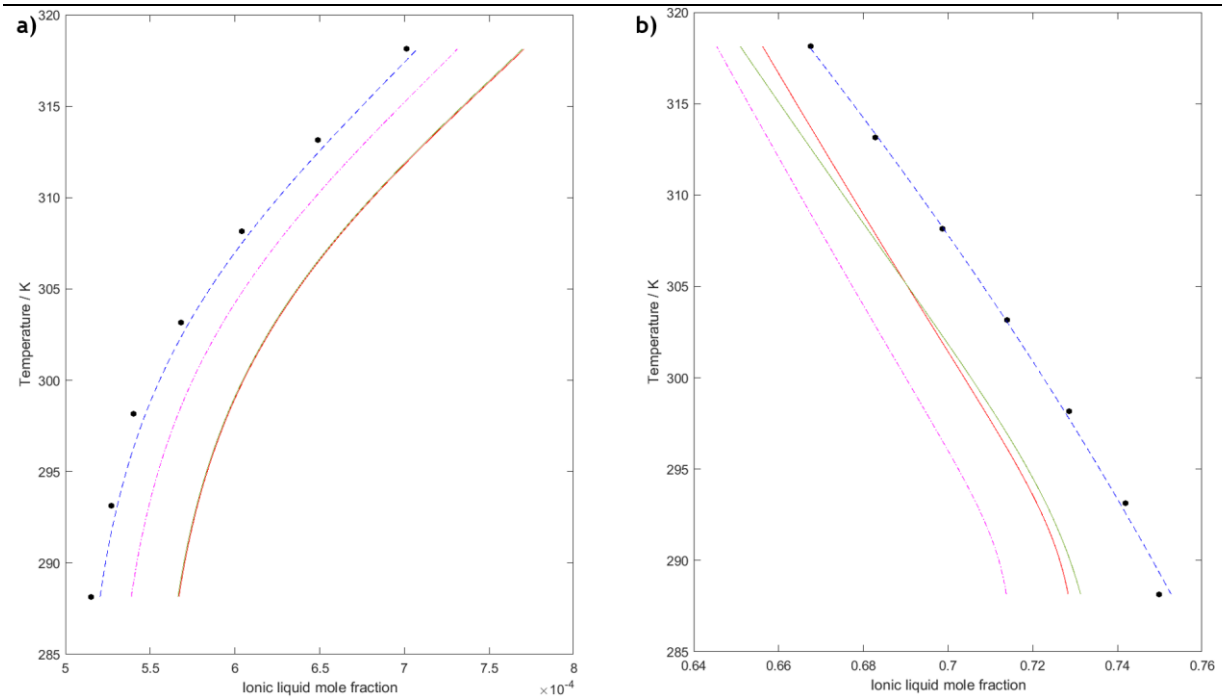


Fig. C.2: Calculated solubility curves for the binary system [C_3mim][NTf_2]/water at atmospheric pressure. a) water-rich phase and b) ionic liquid-rich phase. The black dots represent the experimental points, the red lines correspond to the results from the UNIQUAC model, the green lines are the results from the PDH + UNIQUAC model for a minimum closest approach parameter, the blue lines for a medium closest approach parameter and the pink lines for a maximum closest approach parameter.

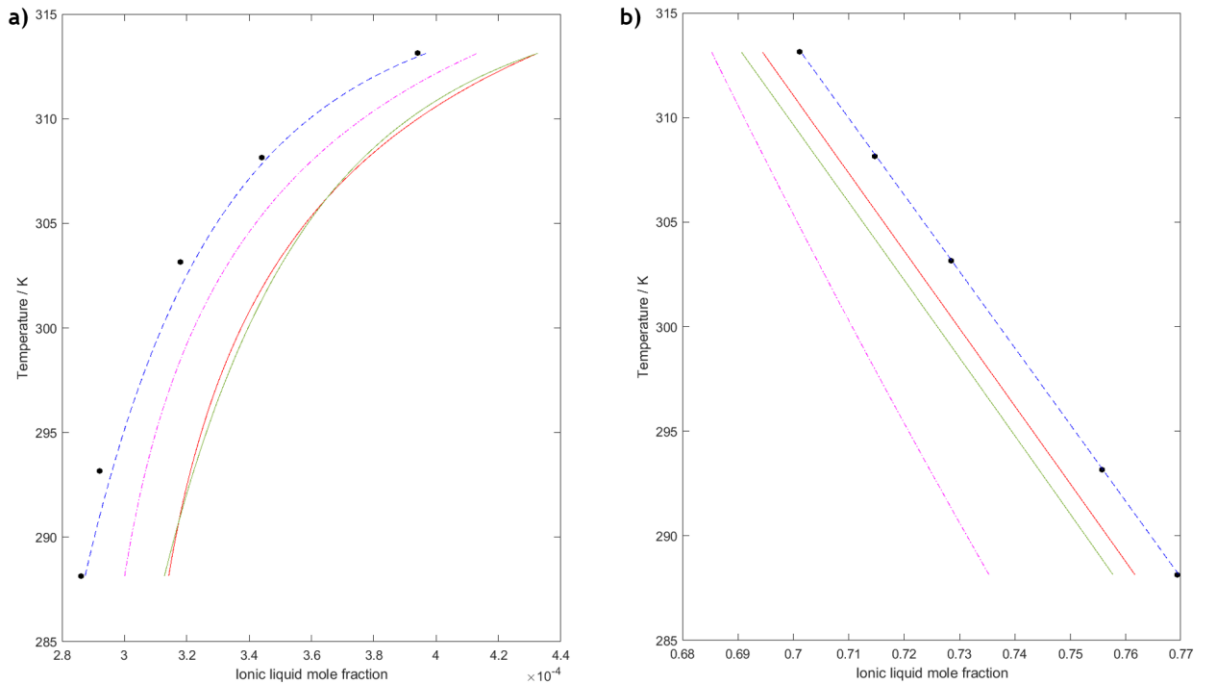


Fig. C.3: Calculated solubility curves for the binary system [C_4mim][NTf_2]/water at atmospheric pressure. a) water-rich phase and b) ionic liquid-rich phase. The black dots represent the experimental points, the red lines correspond to the results from the UNIQUAC model, the green lines are the results from the PDH + UNIQUAC model for a minimum closest approach parameter, the blue lines for a medium closest approach parameter and the pink lines for a maximum closest approach parameter.

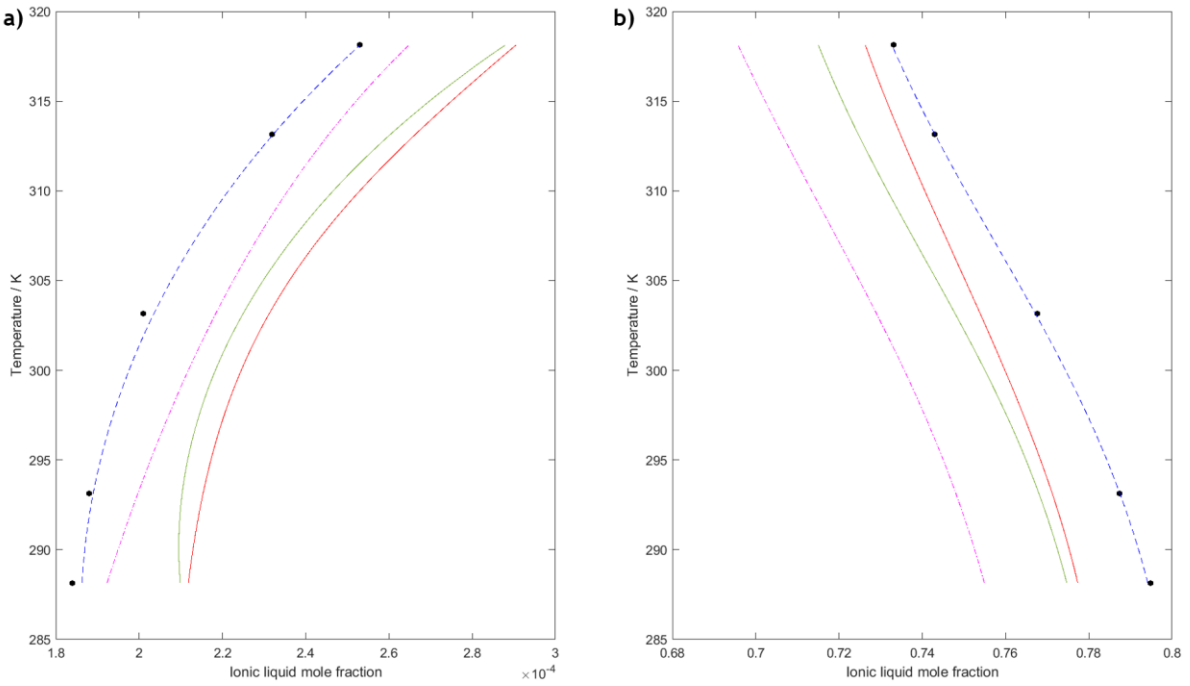


Fig. C.4: Calculated solubility curves for the binary system [C_5mim][NTf_2]/water at atmospheric pressure. a) water-rich phase and b) ionic liquid-rich phase. The black dots represent the experimental points, the red lines correspond to the results from the UNIQUAC model, the green lines are the results from the PDH + UNIQUAC model for a minimum closest approach parameter, the blue lines for a medium closest approach parameter and the pink lines for a maximum closest approach parameter.

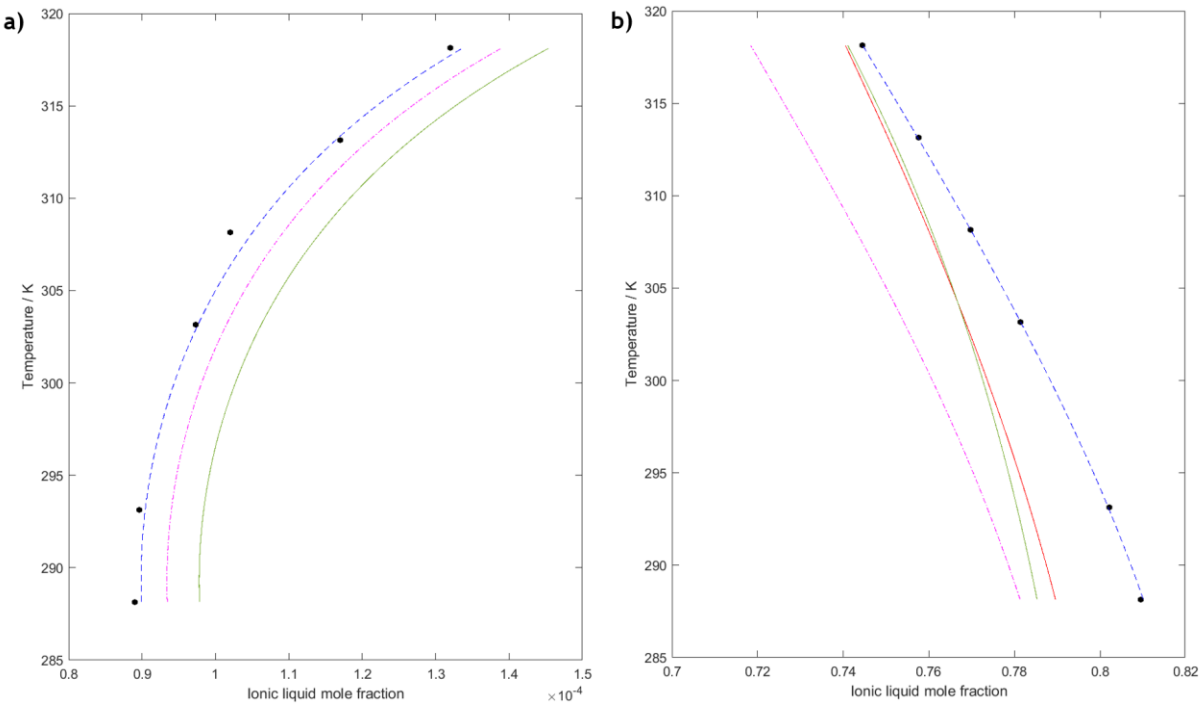


Fig. C.5: Calculated solubility curves for the binary system [C_6mim][NTf_2]/water at atmospheric pressure. a) water-rich phase and b) ionic liquid-rich phase. The black dots represent the experimental points, the red lines correspond to the results from the UNIQUAC model, the green lines are the results from the PDH + UNIQUAC model for a minimum closest approach parameter, the blue lines for a medium closest approach parameter and the pink lines for a maximum closest approach parameter.

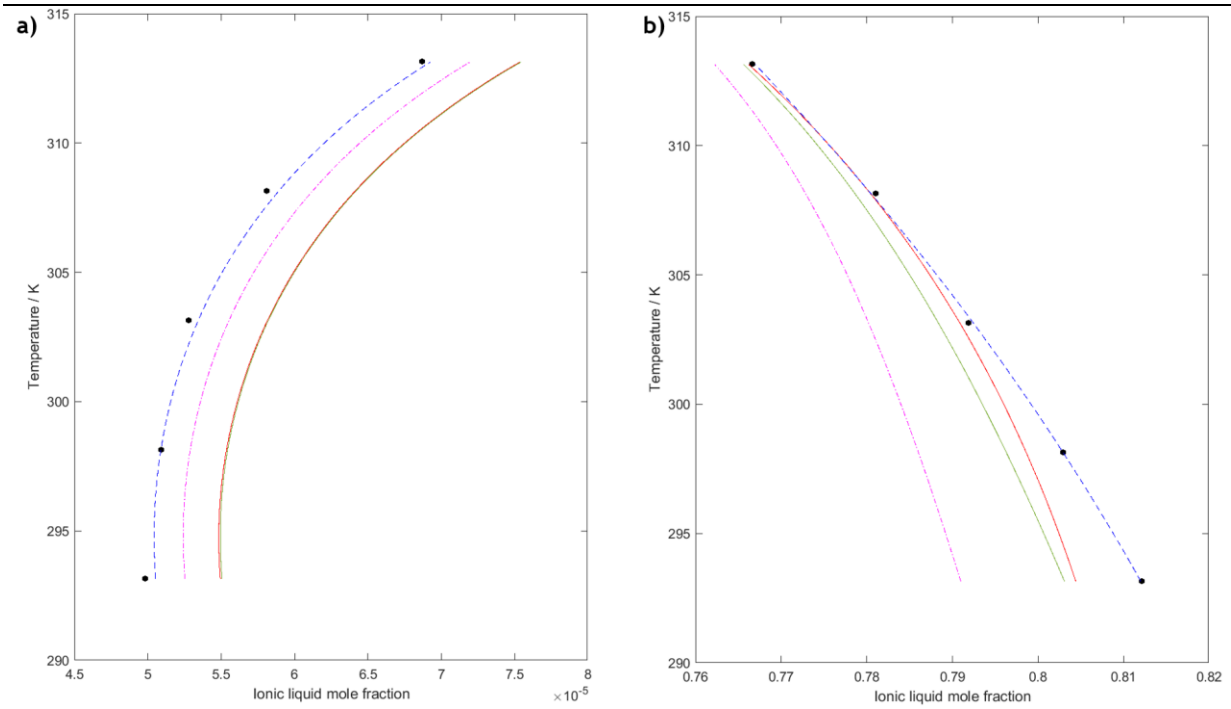


Fig. C.6: Calculated solubility curves for the binary system [C_7mim][NTf_2]/water at atmospheric pressure. a) water-rich phase and b) ionic liquid-rich phase. The black dots represent the experimental points, the red lines correspond to the results from the UNIQUAC model, the green lines are the results from the PDH + UNIQUAC model for a minimum closest approach parameter, the blue lines for a medium closest approach parameter and the pink lines for a maximum closest approach parameter.

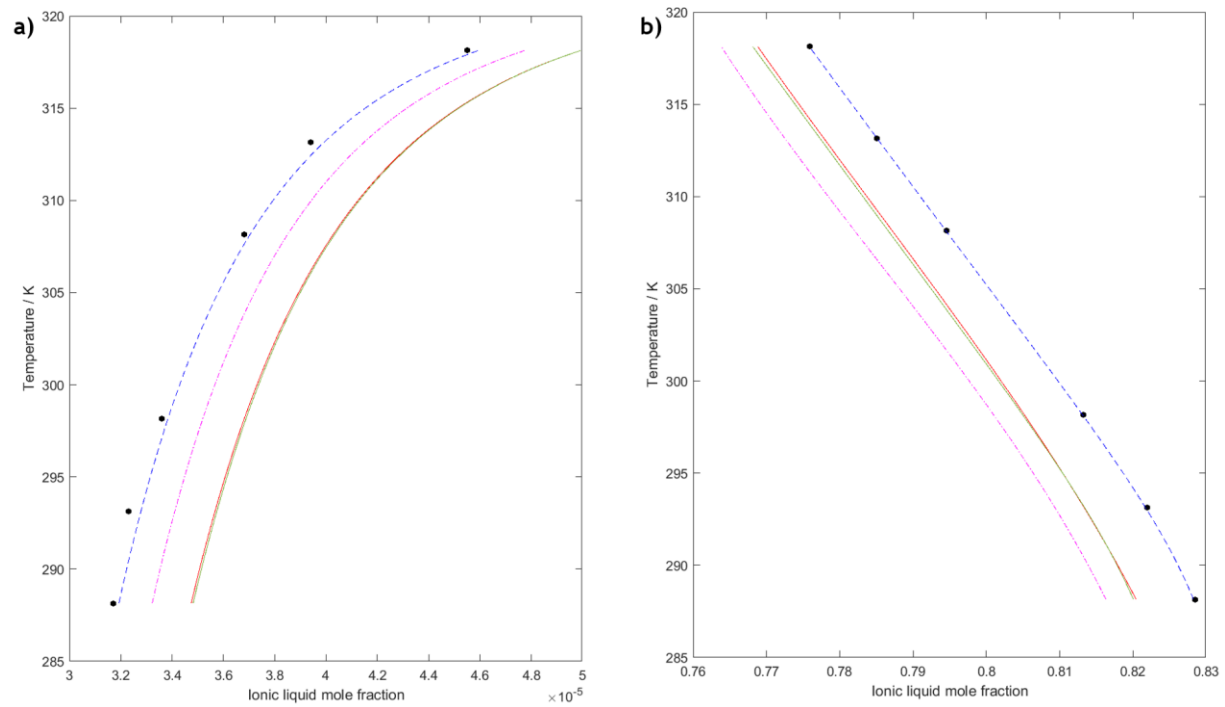


Fig. C.7: Calculated solubility curves for the binary system [C_8mim][NTf_2]/water at atmospheric pressure. a) water-rich phase and b) ionic liquid-rich phase. The black dots represent the experimental points, the red lines correspond to the results from the UNIQUAC model, the green lines are the results from the PDH + UNIQUAC model for a minimum closest approach parameter, the blue lines for a medium closest approach parameter and the pink lines for a maximum closest approach parameter.

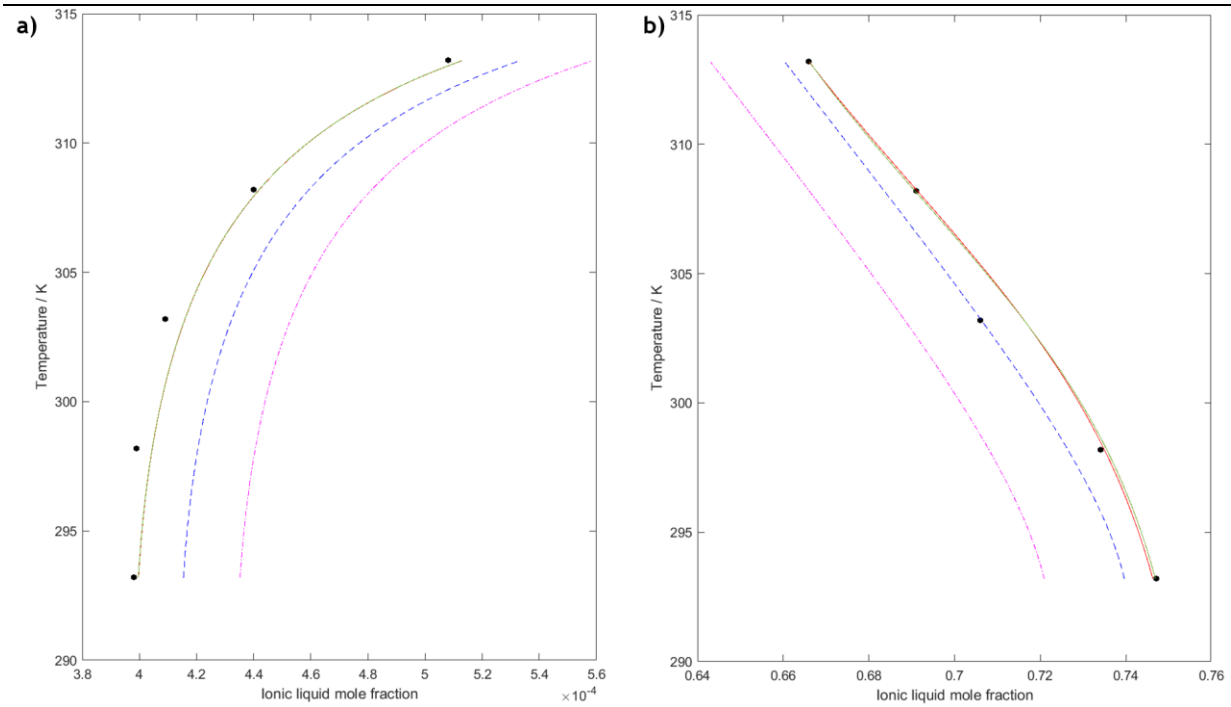


Fig. C.8: Calculated solubility curves for the binary system [C_4py][NTf_2]/water at atmospheric pressure. a) water-rich phase and b) ionic liquid-rich phase. The black dots represent the experimental points, the red lines correspond to the results from the UNIQUAC model, the green lines are the results from the PDH + UNIQUAC model for a minimum closest approach parameter, the blue lines for a medium closest approach parameter and the pink lines for a maximum closest approach parameter.

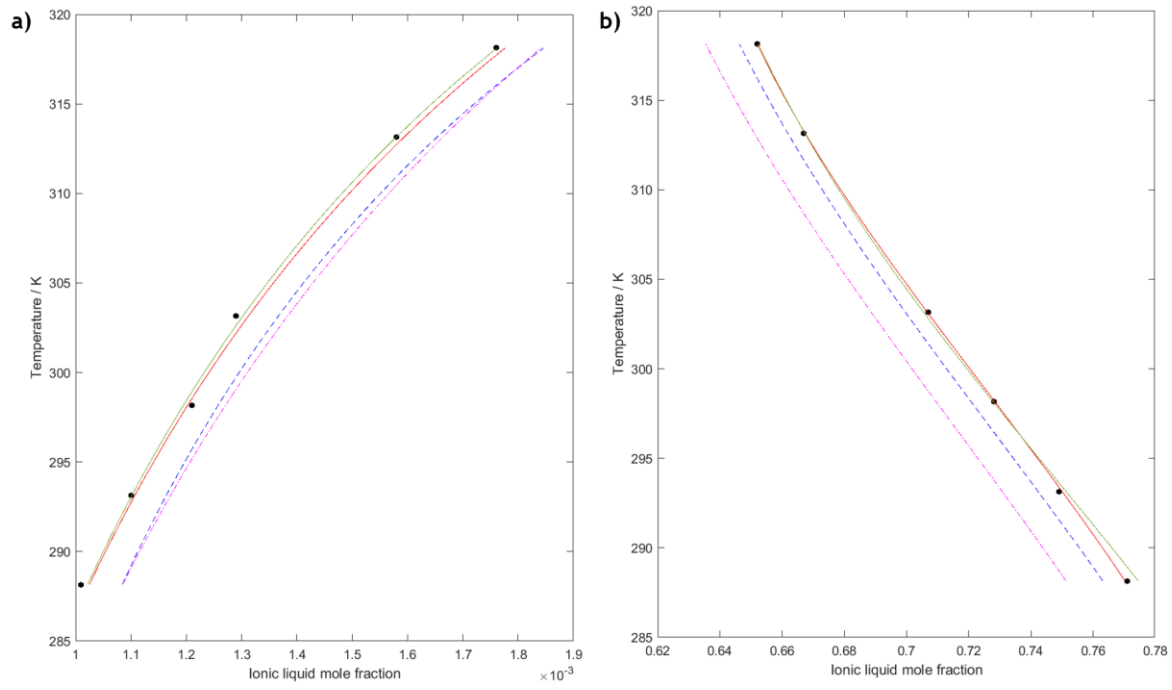


Fig. C.9: Calculated solubility curves for the binary system [C_4mim][PF_6]/water at atmospheric pressure. a) water-rich phase and b) ionic liquid-rich phase. The black dots represent the experimental points, the red lines correspond to the results from the UNIQUAC model, the green lines are the results from the PDH + UNIQUAC model for a minimum closest approach parameter, the blue lines for a medium closest approach parameter and the pink lines for a maximum closest approach parameter.

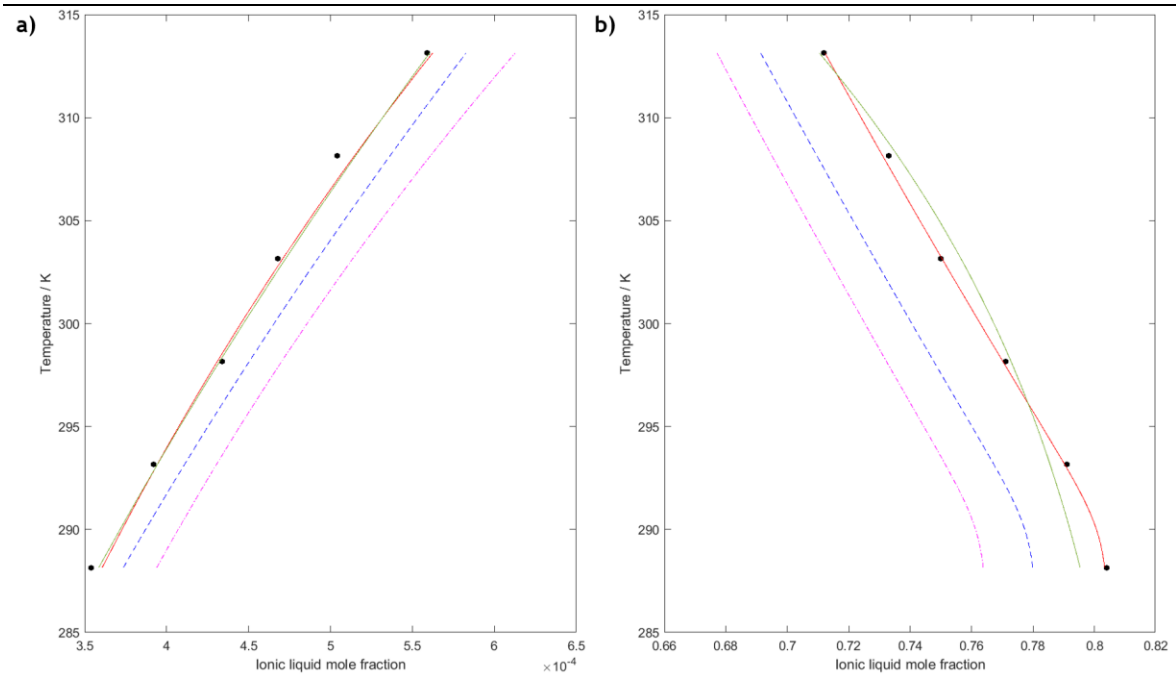


Fig. C.10: Calculated solubility curves for the binary system [C_6mim][PF_6]/water at atmospheric pressure. a) water-rich phase and b) ionic liquid-rich phase. The black dots represent the experimental points, the red lines correspond to the results from the UNIQUAC model, the green lines are the results from the PDH + UNIQUAC model for a minimum closest approach parameter, the blue lines for a medium closest approach parameter and the pink lines for a maximum closest approach parameter.

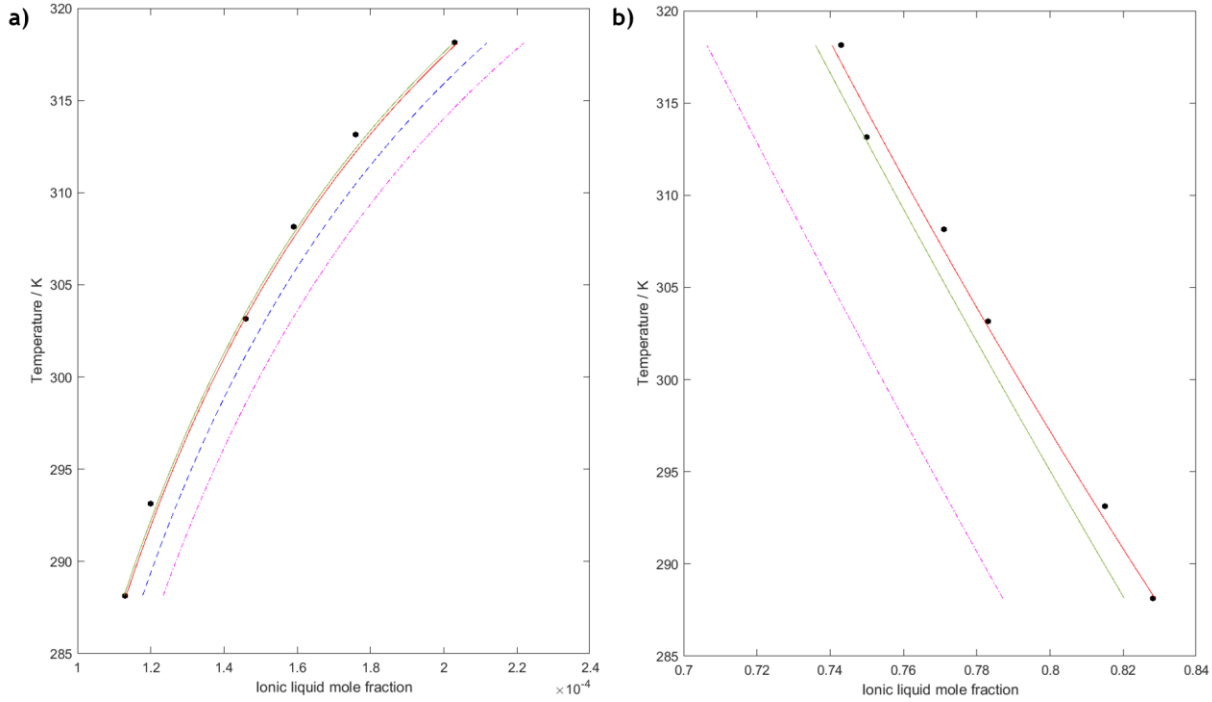


Fig. C.11: Calculated solubility curves for the binary system [C_8mim][PF_6]/water at atmospheric pressure. a) water-rich phase and b) ionic liquid-rich phase. The black dots represent the experimental points, the red lines correspond to the results from the UNIQUAC model, the green lines are the results from the PDH + UNIQUAC model for a minimum closest approach parameter, the blue lines for a medium closest approach parameter and the pink lines for a maximum closest approach parameter.

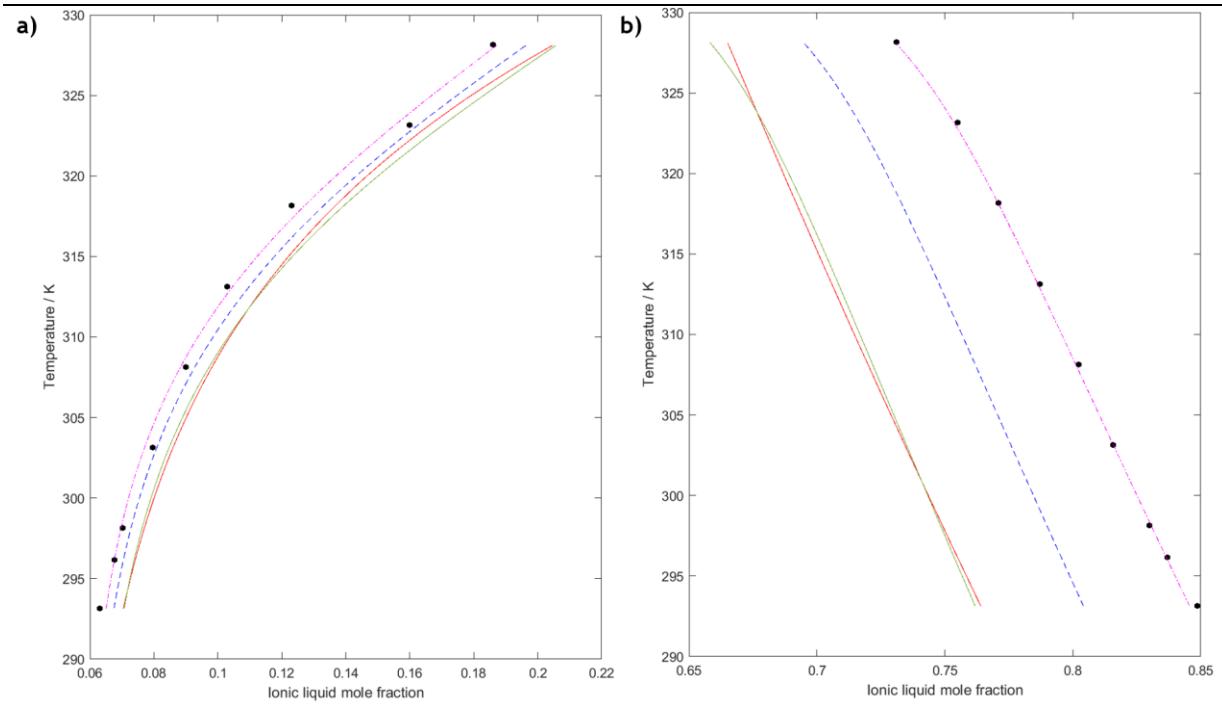


Fig. C.12: Calculated solubility curves for the binary system [C_6mim][BF_4]/water at atmospheric pressure. a) water-rich phase and b) ionic liquid-rich phase. The black dots represent the experimental points, the red lines correspond to the results from the UNIQUAC model, the green lines are the results from the PDH + UNIQUAC model for a minimum closest approach parameter, the blue lines for a medium closest approach parameter and the pink lines for a maximum closest approach parameter.

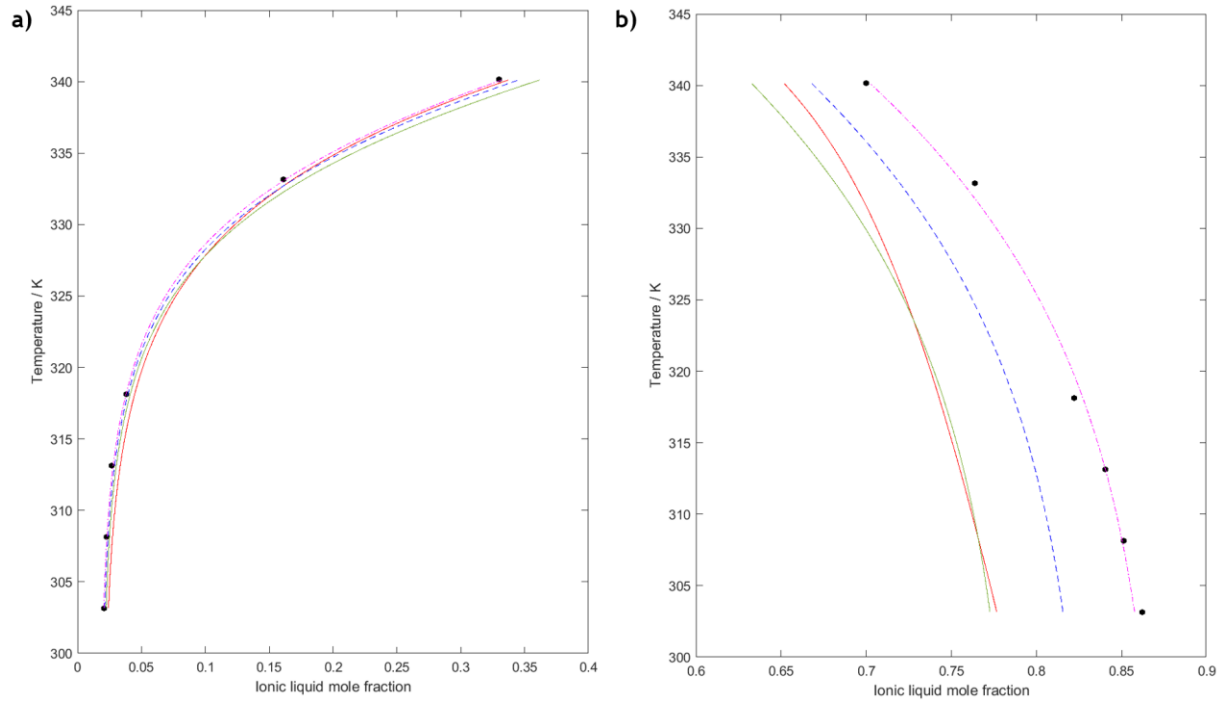


Fig. C.13: Calculated solubility curves for the binary system [C_8mim][BF_4]/water at atmospheric pressure. a) water-rich phase and b) ionic liquid-rich phase. The black dots represent the experimental points, the red lines correspond to the results from the UNIQUAC model, the green lines are the results from the PDH + UNIQUAC model for a minimum closest approach parameter, the blue lines for a medium closest approach parameter and the pink lines for a maximum closest approach parameter.

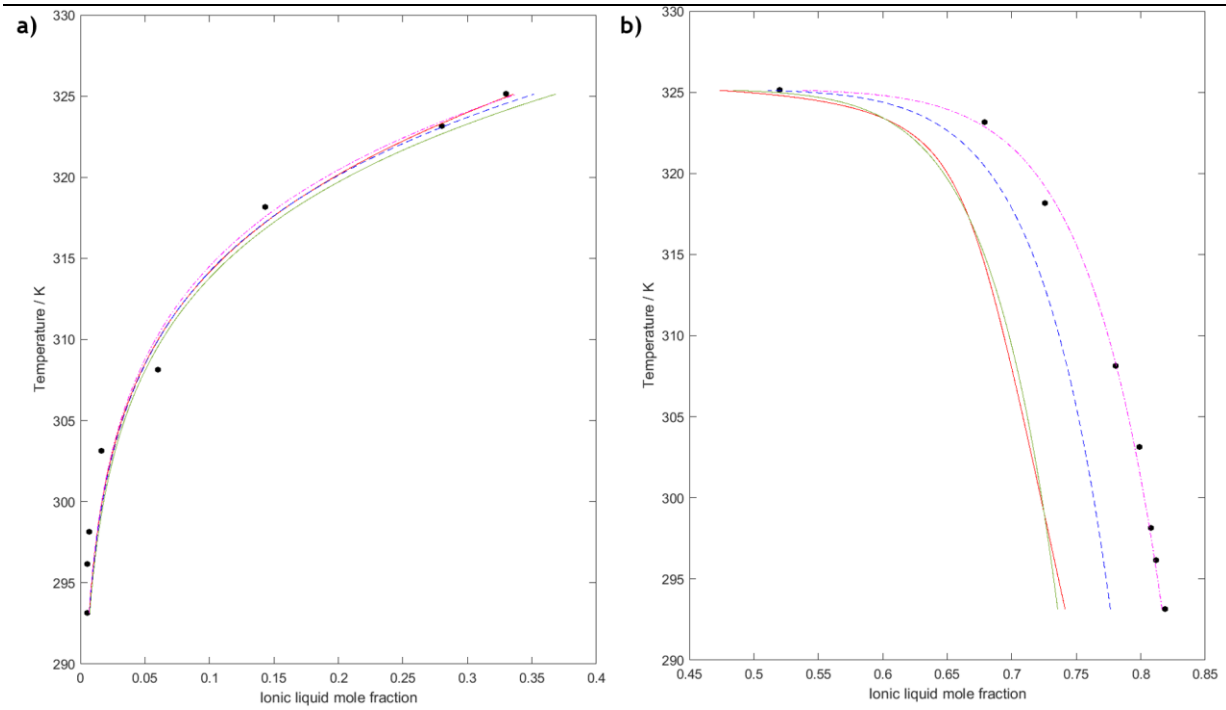


Fig. C.14: Calculated solubility curves for the binary system $[C_{10}mim][BF_4]$/water at atmospheric pressure. a) water-rich phase and b) ionic liquid-rich phase. The black dots represent the experimental points, the red lines correspond to the results from the UNIQUAC model, the green lines are the results from the PDH + UNIQUAC model for a minimum closest approach parameter, the blue lines for a medium closest approach parameter and the pink lines for a maximum closest approach parameter.

Appendix D – Calculated ionic liquid mole fractions for the ionic liquid/water mixtures and deviations of compositions

Table D.1: Calculated solubility points for the [C_2mim][NTf_2]/water system for the water-rich phase, x_{IL}^{W}, and for the ionic liquid-rich phase, x_{IL}^{IL}, for the UNIQUAC model and for the PDH + UNIQUAC model with 6 parameters for the three closest approach parameters (ρ_{min}, ρ_{med}, ρ_{max}).

	UNIQUAC		PDH + UNIQUAC ρ_{min}		PDH + UNIQUAC ρ_{med}		PDH + UNIQUAC ρ_{max}	
T / K	$x_{IL}^{W} \cdot 10^3$	x_{IL}^{IL}	$x_{IL}^{W} \cdot 10^3$	x_{IL}^{IL}	$x_{IL}^{W} \cdot 10^3$	x_{IL}^{IL}	$x_{IL}^{W} \cdot 10^3$	x_{IL}^{IL}
288.15	0.843	0.707	0.842	0.706	0.773	0.725	0.804	0.689
293.15	0.883	0.697	0.883	0.695	0.811	0.713	0.843	0.678
298.15	0.922	0.686	0.921	0.684	0.846	0.702	0.880	0.668
303.15	0.962	0.679	0.962	0.671	0.883	0.688	0.918	0.655
308.15	1.026	0.659	1.026	0.655	0.942	0.672	0.979	0.640
313.15	1.083	0.645	1.083	0.639	0.994	0.655	1.034	0.626
318.15	1.155	0.631	1.154	0.624	1.060	0.640	1.102	0.612

Table D.2: Calculated solubility points for the [C_3mim][NTf_2]/water system for the water-rich phase, x_{IL}^{W}, and for the ionic liquid-rich phase, x_{IL}^{IL}, for the UNIQUAC model and for the PDH + UNIQUAC model with 6 parameters for the three closest approach parameters (ρ_{min}, ρ_{med}, ρ_{max}).

	UNIQUAC		PDH + UNIQUAC ρ_{min}		PDH + UNIQUAC ρ_{med}		PDH + UNIQUAC ρ_{max}	
T / K	$x_{IL}^{W} \cdot 10^3$	x_{IL}^{IL}	$x_{IL}^{W} \cdot 10^3$	x_{IL}^{IL}	$x_{IL}^{W} \cdot 10^3$	x_{IL}^{IL}	$x_{IL}^{W} \cdot 10^3$	x_{IL}^{IL}
288.15	0.566	0.728	0.556	0.731	0.520	0.754	0.538	0.714
293.15	0.580	0.721	0.579	0.723	0.532	0.739	0.551	0.707
298.15	0.594	0.709	0.593	0.710	0.545	0.726	0.564	0.695
303.15	0.625	0.695	0.624	0.696	0.574	0.715	0.594	0.682
308.15	0.664	0.682	0.664	0.681	0.610	0.700	0.631	0.670
313.15	0.714	0.669	0.713	0.666	0.655	0.683	0.678	0.657
318.15	0.771	0.656	0.770	0.651	0.708	0.667	0.732	0.646

Table D.3: Calculated solubility points for the [C_4mim][NTf_2]/water system for the water-rich phase, $x_{IL}{}^{W}$, and for the ionic liquid-rich phase, $x_{IL}{}^{IL}$, for the UNIQUAC model and for the PDH + UNIQUAC model with 6 parameters for the three closest approach parameters (ρ_{min}, ρ_{med}, ρ_{max}).

	UNIQUAC		PDH + UNIQUAC ρ_{min}		PDH + UNIQUAC ρ_{med}		PDH + UNIQUAC ρ_{max}	
T / K	$x_{IL}{}^{W} \cdot 10^3$	$x_{IL}{}^{IL}$	$x_{IL}{}^{W} \cdot 10^3$	$x_{IL}{}^{IL}$	$x_{IL}{}^{W} \cdot 10^3$	$x_{IL}{}^{IL}$	$x_{IL}{}^{W} \cdot 10^3$	$x_{IL}{}^{IL}$
288.15	0.314	0.762	0.315	0.758	0.289	0.770	0.300	0.735
293.15	0.321	0.748	0.321	0.744	0.295	0.756	0.307	0.725
303.15	0.349	0.721	0.350	0.718	0.321	0.729	0.334	0.704
308.15	0.378	0.708	0.378	0.704	0.347	0.715	0.361	0.695
313.15	0.433	0.694	0.433	0.691	0.398	0.701	0.414	0.685

Table D.4: Calculated solubility points for the [C_5mim][NTf_2]/water system for the water-rich phase, $x_{IL}{}^{W}$, and for the ionic liquid-rich phase, $x_{IL}{}^{IL}$, for the UNIQUAC model and for the PDH + UNIQUAC model with 6 parameters for the three closest approach parameters (ρ_{min}, ρ_{med}, ρ_{max}).

	UNIQUAC		PDH + UNIQUAC ρ_{min}		PDH + UNIQUAC ρ_{med}		PDH + UNIQUAC ρ_{max}	
T / K	$x_{IL}{}^{W} \cdot 10^3$	$x_{IL}{}^{IL}$	$x_{IL}{}^{W} \cdot 10^3$	$x_{IL}{}^{IL}$	$x_{IL}{}^{W} \cdot 10^3$	$x_{IL}{}^{IL}$	$x_{IL}{}^{W} \cdot 10^3$	$x_{IL}{}^{IL}$
288.15	0.211	0.778	0.210	0.775	0.186	0.794	0.193	0.755
293.15	0.216	0.771	0.211	0.768	0.190	0.787	0.197	0.748
303.15	0.231	0.754	0.225	0.748	0.203	0.768	0.221	0.729
313.15	0.266	0.734	0.260	0.724	0.232	0.743	0.244	0.706
318.15	0.291	0.726	0.288	0.715	0.253	0.733	0.266	0.696

Table D.5: Calculated solubility points for the [C_6mim][NTf_2]/water system for the water-rich phase, $x_{IL}{}^{W}$, and for the ionic liquid-rich phase, $x_{IL}{}^{IL}$, for the UNIQUAC model and for the PDH + UNIQUAC model with 6 parameters for the three closest approach parameters (ρ_{min}, ρ_{med}, ρ_{max}).

	UNIQUAC		PDH + UNIQUAC ρ_{min}		PDH + UNIQUAC ρ_{med}		PDH + UNIQUAC ρ_{max}	
T / K	$x_{IL}{}^{W} \cdot 10^4$	$x_{IL}{}^{IL}$	$x_{IL}{}^{W} \cdot 10^4$	$x_{IL}{}^{IL}$	$x_{IL}{}^{W} \cdot 10^4$	$x_{IL}{}^{IL}$	$x_{IL}{}^{W} \cdot 10^4$	$x_{IL}{}^{IL}$
288.15	0.978	0.789	0.979	0.785	0.899	0.810	0.934	0.781
293.15	0.985	0.784	0.986	0.781	0.905	0.802	0.941	0.774
303.15	1.069	0.768	1.070	0.768	0.983	0.781	1.022	0.754
308.15	1.121	0.760	1.122	0.760	1.030	0.770	1.071	0.743
313.15	1.286	0.751	1.287	0.752	1.182	0.758	1.228	0.731
318.15	1.450	0.740	1.452	0.741	1.333	0.744	1.386	0.718

Table D.6: Calculated solubility points for the [C_7mim][NTf_2]/water system for the water-rich phase, $x_{IL}{}^{W}$, and for the ionic liquid-rich phase, $x_{IL}{}^{IL}$, for the UNIQUAC model and for the PDH + UNIQUAC model with 6 parameters for the three closest approach parameters (ρ_{min}, ρ_{med}, ρ_{max}).

	UNIQUAC		PDH + UNIQUAC ρ_{min}		PDH + UNIQUAC ρ_{med}		PDH + UNIQUAC ρ_{max}	
T / K	$x_{IL}{}^{W} \cdot 10^4$	$x_{IL}{}^{IL}$	$x_{IL}{}^{W} \cdot 10^4$	$x_{IL}{}^{IL}$	$x_{IL}{}^{W} \cdot 10^4$	$x_{IL}{}^{IL}$	$x_{IL}{}^{W} \cdot 10^4$	$x_{IL}{}^{IL}$
293.15	0.547	0.804	0.548	0.803	0.503	0.812	0.523	0.791
298.15	0.559	0.799	0.560	0.797	0.514	0.803	0.534	0.786
303.15	0.580	0.791	0.581	0.788	0.533	0.792	0.554	0.780
308.15	0.639	0.780	0.639	0.779	0.587	0.781	0.610	0.773
313.15	0.755	0.766	0.756	0.766	0.694	0.767	0.721	0.762

Table D.7: Calculated solubility points for the [C_8mim][NTf_2]/water system for the water-rich phase, $x_{IL}{}^{W}$, and for the ionic liquid-rich phase, $x_{IL}{}^{IL}$, for the UNIQUAC model and for the PDH + UNIQUAC model with 6 parameters for the three closest approach parameters (ρ_{min}, ρ_{med}, ρ_{max}).

	UNIQUAC		PDH + UNIQUAC ρ_{min}		PDH + UNIQUAC ρ_{med}		PDH + UNIQUAC ρ_{max}	
T / K	$x_{IL}{}^{W} \cdot 10^4$	$x_{IL}{}^{IL}$	$x_{IL}{}^{W} \cdot 10^4$	$x_{IL}{}^{IL}$	$x_{IL}{}^{W} \cdot 10^4$	$x_{IL}{}^{IL}$	$x_{IL}{}^{W} \cdot 10^4$	$x_{IL}{}^{IL}$
288.15	0.348	0.820	0.349	0.820	0.320	0.828	0.333	0.816
293.15	0.355	0.814	0.355	0.813	0.326	0.822	0.339	0.809
298.15	0.369	0.805	0.370	0.805	0.339	0.813	0.353	0.801
308.15	0.404	0.787	0.405	0.787	0.372	0.795	0.386	0.782
313.15	0.433	0.778	0.433	0.777	0.398	0.785	0.414	0.773
318.15	0.500	0.769	0.500	0.768	0.460	0.776	0.478	0.764

Table D.8: Calculated solubility points for the [C_4py][NTf_2]/water system for the water-rich phase, $x_{IL}{}^{W}$, and for the ionic liquid-rich phase, $x_{IL}{}^{IL}$, for the UNIQUAC model and for the PDH + UNIQUAC model with 6 parameters for the three closest approach parameters (ρ_{min}, ρ_{med}, ρ_{max}).

	UNIQUAC		PDH + UNIQUAC ρ_{min}		PDH + UNIQUAC ρ_{med}		PDH + UNIQUAC ρ_{max}	
T / K	$x_{IL}{}^{W} \cdot 10^3$	$x_{IL}{}^{IL}$	$x_{IL}{}^{W} \cdot 10^3$	$x_{IL}{}^{IL}$	$x_{IL}{}^{W} \cdot 10^3$	$x_{IL}{}^{IL}$	$x_{IL}{}^{W} \cdot 10^3$	$x_{IL}{}^{IL}$
293.20	0.402	0.746	0.402	0.747	0.418	0.740	0.438	0.721
298.20	0.403	0.734	0.403	0.735	0.419	0.727	0.439	0.708
303.20	0.413	0.717	0.413	0.717	0.429	0.705	0.450	0.688
308.20	0.444	0.691	0.444	0.690	0.462	0.684	0.484	0.667
313.20	0.513	0.666	0.513	0.666	0.533	0.660	0.559	0.643

Table D.9: Calculated solubility points for the [C_4mim][PF_6]/water system for the water-rich phase, $x_{IL}{}^{W}$, and for the ionic liquid-rich phase, $x_{IL}{}^{IL}$, for the UNIQUAC model and for the PDH + UNIQUAC model with 6 parameters for the three closest approach parameters (ρ_{min}, ρ_{med}, ρ_{max}).

	UNIQUAC		PDH + UNIQUAC ρ_{min}		PDH + UNIQUAC ρ_{med}		PDH + UNIQUAC ρ_{max}	
T / K	$x_{IL}{}^{W} \cdot 10^2$	$x_{IL}{}^{IL}$	$x_{IL}{}^{W} \cdot 10^2$	$x_{IL}{}^{IL}$	$x_{IL}{}^{W} \cdot 10^2$	$x_{IL}{}^{IL}$	$x_{IL}{}^{W} \cdot 10^2$	$x_{IL}{}^{IL}$
288.15	0.102	0.770	0.101	0.774	0.108	0.763	0.108	0.752
293.15	0.111	0.750	0.110	0.752	0.117	0.742	0.117	0.730
298.15	0.121	0.728	0.121	0.727	0.125	0.721	0.129	0.710
303.15	0.130	0.707	0.129	0.706	0.137	0.700	0.137	0.689
313.15	0.160	0.667	0.158	0.667	0.166	0.661	0.166	0.650
318.15	0.178	0.652	0.176	0.652	0.184	0.647	0.184	0.636

Table D.10: Calculated solubility points for the [C_6mim][PF_6]/water system for the water-rich phase, $x_{IL}{}^{W}$, and for the ionic liquid-rich phase, $x_{IL}{}^{IL}$, for the UNIQUAC model and for the PDH + UNIQUAC model with 6 parameters for the three closest approach parameters (ρ_{min}, ρ_{med}, ρ_{max}).

	UNIQUAC		PDH + UNIQUAC ρ_{min}		PDH + UNIQUAC ρ_{med}		PDH + UNIQUAC ρ_{max}	
T / K	$x_{IL}{}^{W} \cdot 10^3$	$x_{IL}{}^{IL}$	$x_{IL}{}^{W} \cdot 10^3$	$x_{IL}{}^{IL}$	$x_{IL}{}^{W} \cdot 10^3$	$x_{IL}{}^{IL}$	$x_{IL}{}^{W} \cdot 10^3$	$x_{IL}{}^{IL}$
288.15	0.358	0.803	0.354	0.797	0.372	0.780	0.389	0.764
293.15	0.396	0.790	0.392	0.785	0.412	0.767	0.431	0.751
298.15	0.434	0.770	0.434	0.766	0.456	0.748	0.477	0.732
303.15	0.473	0.749	0.468	0.749	0.491	0.728	0.515	0.713
308.15	0.509	0.732	0.504	0.731	0.529	0.711	0.554	0.696
313.15	0.565	0.712	0.560	0.711	0.587	0.691	0.615	0.676

Table D.11: Calculated solubility points for the [C_8mim][PF_6]/water system for the water-rich phase, $x_{IL}{}^{W}$, and for the ionic liquid-rich phase, $x_{IL}{}^{IL}$, for the UNIQUAC model and for the PDH + UNIQUAC model with 6 parameters for the three closest approach parameters (ρ_{min}, ρ_{med}, ρ_{max}).

	UNIQUAC		PDH + UNIQUAC ρ_{min}		PDH + UNIQUAC ρ_{med}		PDH + UNIQUAC ρ_{max}	
T / K	$x_{IL}{}^{W} \cdot 10^3$	$x_{IL}{}^{IL}$	$x_{IL}{}^{W} \cdot 10^3$	$x_{IL}{}^{IL}$	$x_{IL}{}^{W} \cdot 10^3$	$x_{IL}{}^{IL}$	$x_{IL}{}^{W} \cdot 10^3$	$x_{IL}{}^{IL}$
288.15	0.114	0.827	0.114	0.820	0.119	0.820	0.124	0.787
293.15	0.121	0.814	0.121	0.807	0.126	0.807	0.132	0.774
303.15	0.147	0.782	0.147	0.775	0.153	0.775	0.161	0.744
308.15	0.161	0.770	0.160	0.763	0.167	0.763	0.175	0.733
313.15	0.178	0.749	0.177	0.750	0.185	0.746	0.194	0.720
318.15	0.205	0.742	0.204	0.736	0.213	0.736	0.223	0.706

Table D.12: Calculated solubility points for the [C_6mim][BF_4]/water system for the water-rich phase, $x_{IL}{}^{W}$, and for the ionic liquid-rich phase, $x_{IL}{}^{IL}$, for the UNIQUAC model and for the PDH + UNIQUAC model with 6 parameters for the three closest approach parameters (ρ_{min}, ρ_{med}, ρ_{max}).

	UNIQUAC		PDH + UNIQUAC ρ_{min}		PDH + UNIQUAC ρ_{med}		PDH + UNIQUAC ρ_{max}	
T / K	$x_{IL}{}^{W}$	$x_{IL}{}^{IL}$	$x_{IL}{}^{W}$	$x_{IL}{}^{IL}$	$x_{IL}{}^{W}$	$x_{IL}{}^{IL}$	$x_{IL}{}^{W}$	$x_{IL}{}^{IL}$
293.15	0.069	0.764	0.069	0.764	0.066	0.806	0.063	0.848
296.15	0.074	0.753	0.074	0.753	0.071	0.795	0.068	0.836
298.15	0.077	0.747	0.077	0.747	0.073	0.788	0.070	0.829
303.15	0.088	0.734	0.087	0.734	0.083	0.775	0.080	0.815
308.15	0.099	0.722	0.099	0.722	0.094	0.762	0.090	0.802
313.15	0.113	0.709	0.113	0.708	0.108	0.748	0.103	0.786
318.15	0.135	0.694	0.135	0.694	0.129	0.732	0.123	0.770
323.15	0.168	0.680	0.176	0.680	0.168	0.717	0.160	0.754
328.15	0.204	0.659	0.204	0.658	0.195	0.694	0.186	0.730

Table D.13: Calculated solubility points for the [C_8mim][BF_4]/water system for the water-rich phase, $x_{IL}{}^{W}$, and for the ionic liquid-rich phase, $x_{IL}{}^{IL}$, for the UNIQUAC model and for the PDH + UNIQUAC model with 6 parameters for the three closest approach parameters (ρ_{min}, ρ_{med}, ρ_{max}).

	UNIQUAC		PDH + UNIQUAC ρ_{min}		PDH + UNIQUAC ρ_{med}		PDH + UNIQUAC ρ_{max}	
T / K	$x_{IL}{}^{W}$	$x_{IL}{}^{IL}$	$x_{IL}{}^{W}$	$x_{IL}{}^{IL}$	$x_{IL}{}^{W}$	$x_{IL}{}^{IL}$	$x_{IL}{}^{W}$	$x_{IL}{}^{IL}$
303.15	0.025	0.776	0.023	0.776	0.022	0.819	0.021	0.861
308.15	0.027	0.767	0.025	0.766	0.024	0.809	0.023	0.850
313.15	0.032	0.757	0.029	0.756	0.028	0.798	0.027	0.839
318.15	0.046	0.741	0.042	0.740	0.040	0.781	0.038	0.821
333.15	0.169	0.693	0.177	0.688	0.169	0.726	0.163	0.763
340.15	0.339	0.652	0.363	0.630	0.346	0.665	0.333	0.699

Table D.14: Calculated solubility points for the [C_{10}mim][BF_4]/water system for the water-rich phase, $x_{IL}{}^{W}$, and for the ionic liquid-rich phase, $x_{IL}{}^{IL}$, for the UNIQUAC model and for the PDH + UNIQUAC model with 6 parameters for the three closest approach parameters (ρ_{min}, ρ_{med}, ρ_{max}).

	UNIQUAC		PDH + UNIQUAC ρ_{min}		PDH + UNIQUAC ρ_{med}		PDH + UNIQUAC ρ_{max}	
T / K	$x_{IL}{}^{W}$	$x_{IL}{}^{IL}$	$x_{IL}{}^{W}$	$x_{IL}{}^{IL}$	$x_{IL}{}^{W}$	$x_{IL}{}^{IL}$	$x_{IL}{}^{W}$	$x_{IL}{}^{IL}$
293.15	0.006	0.752	0.006	0.737	0.005	0.778	0.005	0.818
296.15	0.006	0.747	0.006	0.731	0.006	0.771	0.005	0.811
298.15	0.008	0.742	0.007	0.727	0.007	0.768	0.007	0.807
303.15	0.020	0.717	0.018	0.719	0.017	0.759	0.017	0.798
308.15	0.063	0.702	0.066	0.702	0.063	0.741	0.061	0.780
318.15	0.149	0.653	0.158	0.653	0.151	0.689	0.145	0.725
323.15	0.285	0.610	0.308	0.611	0.294	0.645	0.283	0.678
325.15	0.333	0.467	0.363	0.468	0.346	0.494	0.333	0.519

Table D.15: UNIQUAC and PDH + UNIQUAC with 6 parameter deviations of composition, σ^a, obtained from LLE modeling.

Ionic liquid	UNIQUAC	PDH + UNIQUAC	PDH + UNIQUAC	PDH + UNIQUAC
	$\sigma_{\mathrm{UNIQUAC}}$ %	$\sigma_{\rho_{\min}}$ %	$\sigma_{\rho_{\mathrm{med}}}$%	$\sigma_{\rho_{\max}}$ %
$[C_2mim][NTf_2]$	5.9946	6.2260	0.4815	4.8427
$[C_3mim][NTf_2]$	6.2162	6.1881	0.6059	4.3744
$[C_4mim][NTf_2]$	5.4392	5.7512	0.5102	4.1768
$[C_5mim][NTf_2]$	8.2476	7.6478	0.3350	5.5062
$[C_6mim][NTf_2]$	5.7185	5.8140	0.5064	4.2526
$[C_7mim][NTf_2]$	5.1296	5.2811	0.5035	3.2803
$[C_8mim][NTf_2]$	5.4288	5.5062	0.5077	3.2914
$[C_4py][NTf_2]$	0.6655	0.6674	2.8841	6.6611
$[C_4mim][PF_6]$	0.4419	0.1775	3.1798	4.2668
$[C_6mim][PF_6]$	0.4620	0.3018	3.9989	7.4989
$[C_8mim][PF_6]$	0.5481	0.6623	2.9563	4.4090
$[C_6mim][BF_4]$	9.6865	9.8251	4.8264	0.0565
$[C_8mim][BF_4]$	11.9157	9.9915	4.9920	0.5053
$[C_{10}mim][BF_4]$	10.3807	9.9973	4.9974	0.5377

[a] $\sigma = \frac{1}{2n}\sum_{i=1}^{n}\left[\frac{|x_{\mathrm{exp}}{}^{\mathrm{IL}} - x_{\mathrm{calc}}{}^{\mathrm{IL}}|}{x_{\mathrm{exp}}{}^{\mathrm{IL}}} + \frac{|x_{\mathrm{exp}}{}^{\mathrm{W}} - x_{\mathrm{calc}}{}^{\mathrm{W}}|}{x_{\mathrm{exp}}{}^{\mathrm{W}}}\right] \times 100$

Appendix E – UNIQUAC interaction parameters based on the UNIQUAC model and the PDH + UNIQUAC model with 6 parameters

I) UNIQUAC modeling results

Table E.1: UNIQUAC interaction parameters for the ionic liquid, IL, and water, W, obtained from LLE modeling with the UNIQUAC model for ionic liquid/water systems.

Ionic liquid	$a_{\mathrm{IL-W}}$ / K	$b_{\mathrm{IL-W}}$	$a_{\mathrm{W-IL}}$ / K	$b_{\mathrm{W-IL}}$
$[C_2mim][NTf_2]$	-99.993	-9.234	-97.751	-4.192
$[C_3mim][NTf_2]$	-99.975	-10.738	-94.798	-4.482
$[C_4mim][NTf_2]$	-99.986	-11.558	-96.884	-4.529
$[C_5mim][NTf_2]$	-99.956	-11.987	-96.221	-4.687
$[C_6mim][NTf_2]$	-99.998	-12.223	-2.021	-5.293
$[C_7mim][NTf_2]$	-99.951	-12.949	-62.064	-5.319
$[C_8mim][NTf_2]$	-99.952	-13.441	-79.604	-5.531
$[C_4py][NTf_2]$	-99.990	-11.199	-98.480	-4.498
$[C_4mim][PF_6]$	-49.994	-9.129	-49.958	-4.200
$[C_6mim][PF_6]$	-49.945	-9.520	-40.128	-4.956
$[C_8mim][PF_6]$	-49.989	-10.138	-49.741	-5.099
$[C_6mim][BF_4]$	-99.991	-6.169	-99.732	-4.399
$[C_8mim][BF_4]$	-99.978	-7.577	-97.259	-4.691
$[C_{10}mim][BF_4]$	-99.986	-8.422	-61.479	-5.680

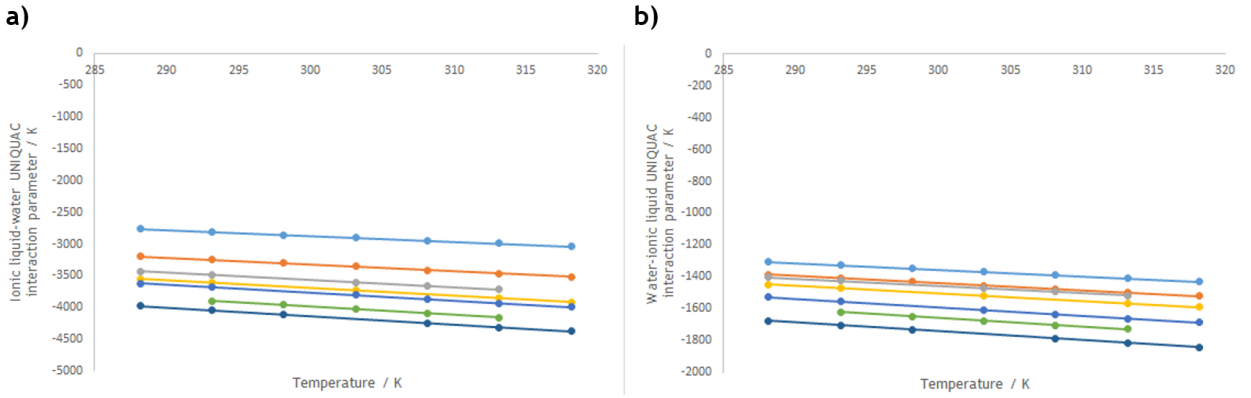


Fig. E.1: Influence of alkyl chain length a) in the ionic liquid-water interactions and b) in the water-ionic liquid interactions in $[NTf_2]^-$-based ionic liquid/water systems. The light blue line is the $[C_2mim][NTf_2]$/water, the orange line corresponds to the $[C_3mim][NTf_2]$/water, the grey line represents the $[C_4mim][NTf_2]$/water, the yellow line refers to the $[C_5mim][NTf_2]$/water, the blue line displays the $[C_6mim][NTf_2]$/water, the green line presents the $[C_7mim][NTf_2]$/water and the dark blue line shows the $[C_8mim][NTf_2]$ /water.

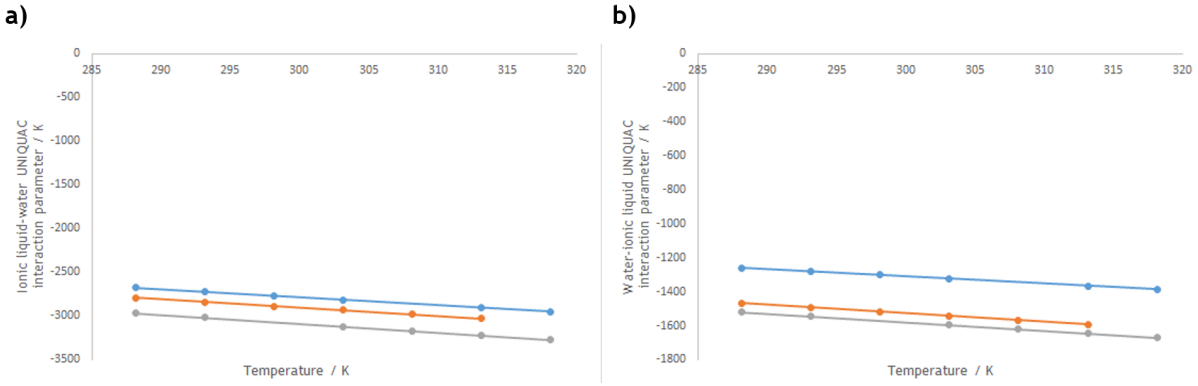


Fig. E.2: Influence of alkyl chain length a) in the ionic liquid-water interactions and b) in the water-ionic liquid interactions in $[PF_6]^-$-based ionic liquid/water systems. The light blue line is the $[C_4mim][PF_6]$/water, the orange line corresponds to the $[C_6mim][PF_6]$ and the grey line represents the $[C_8mim][PF_6]$/water.

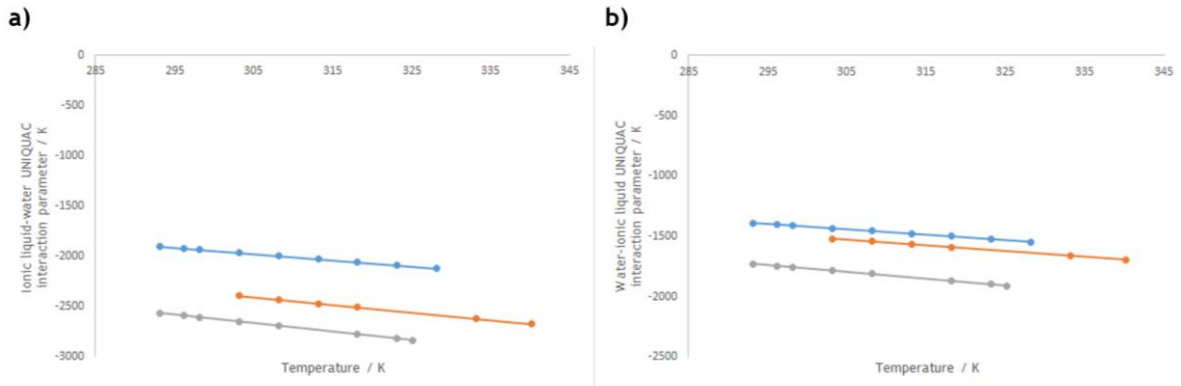


Fig. E.3: Influence of alkyl chain length a) in the ionic liquid-water interactions and b) in the water-ionic liquid interactions in $[BF_4]^-$-based ionic liquid/water systems. The light blue line is the $[C_6mim][BF_4]$/water, the orange line corresponds to the $[C_8mim][BF_4]$ and the grey line represents the $[C_{10}mim][BF_4]$/water.

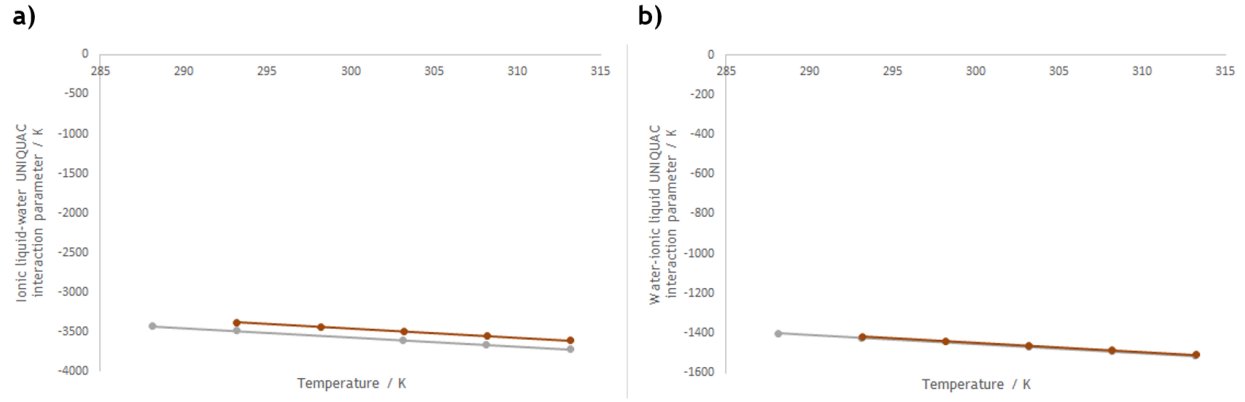


Fig. E.4: Influence of cation a) in the ionic liquid-water interactions and b) in the water-ionic liquid interactions in $[NTf_2]^-$-based ionic liquid/water systems. The brown line is the $[C_4py][NTf_2]$/water and the grey line represents the $[C_4mim][NTf_2]$/water.

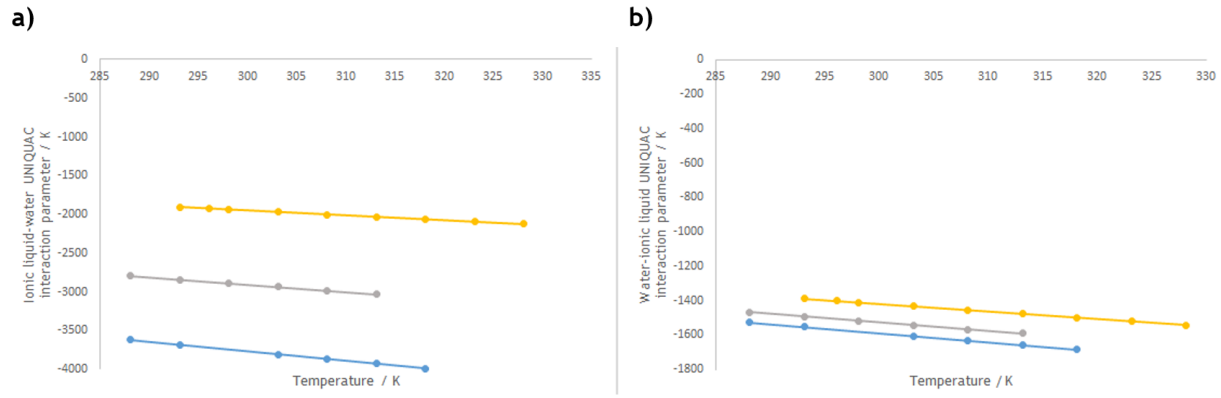


Fig. E.5: Influence of anion a) in the ionic liquid-water interactions and b) in the water-ionic liquid interactions in $[C_6mim]^+$-based ionic liquid/water systems. The yellow line is the $[C_6mim][BF_4]$/water, the grey line represents $[C_6mim][PF_6]$/water and the light blue line displays the $[C_6mim][NTf_2]$/water.

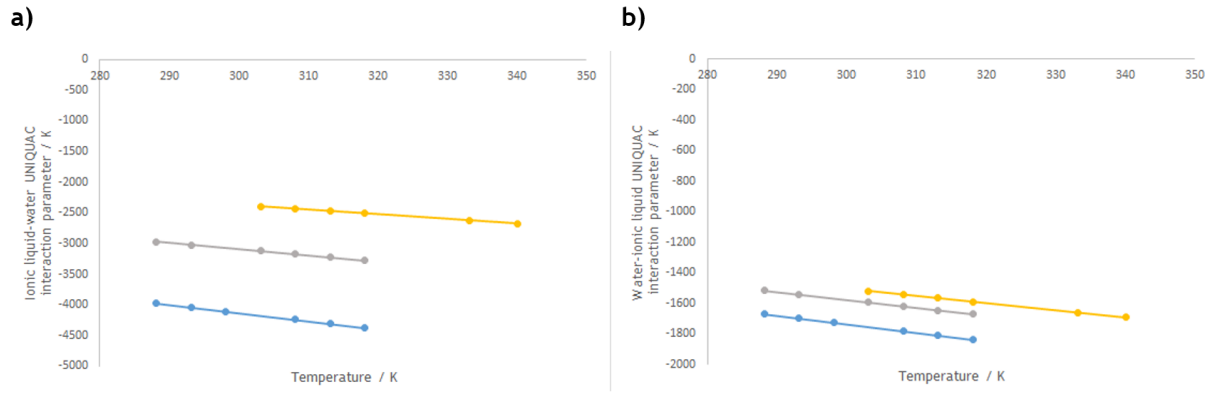


Fig. E.6: Influence of anion a) in the ionic liquid-water interactions and b) in the water-ionic liquid interactions in $[C_8mim]^+$-based ionic liquid/water systems. The yellow line is the $[C_8mim][BF_4]$/water, the grey line represents $[C_8mim][PF_6]$/water and the light blue line displays the $[C_8mim][NTf_2]$/water.

II) PDH + UNIQUAC with 6 parameters modeling results

Table E.2: UNIQUAC interaction parameters for the cation, C, the anion, A, and water, W, obtained from LLE modeling with the PDH + UNIQUAC model with 6 parameters for ionic liquid/water systems.

Ionic liquid	a_{C-A} / K	b_{C-A}	a_{C-W} / K	b_{C-W}	a_{A-C} / K	b_{A-C}
$[C_2mim][NTf_2]$	0.690	3.490	-99.983	-10.999	0.690	3.490
$[C_3mim][NTf_2]$	0.994	3.093	-99.991	-10.589	0.985	2.996
$[C_4mim][NTf_2]$	0.995	2.690	-99.996	-9.950	0.987	2.690
$[C_5mim][NTf_2]$	0.992	2.300	-99.999	-9.490	0.992	2.345
$[C_6mim][NTf_2]$	0.999	1.502	-99.997	-9.090	0.999	1.759
$[C_7mim][NTf_2]$	0.998	1.251	-99.999	-8.488	1.061	1.351
$[C_8mim][NTf_2]$	0.995	0.873	-99.999	-7.998	0.931	0.972
$[C_4py][NTf_2]$	0.948	2.952	-99.954	-10.450	0.941	2.739
$[C_4mim][PF_6]$	0.751	1.445	0.817	-9.990	0.736	1.344
$[C_6mim][PF_6]$	0.319	1.150	-99.999	-9.082	0.889	0.805
$[C_8mim][PF_6]$	0.924	0.657	-99.997	-8.103	0.982	0.525
$[C_6mim][BF_4]$	-9.990	0.652	8.575	-9.050	-9.774	0.442
$[C_8mim][BF_4]$	-9.996	0.352	-9.968	-8.022	-9.998	0.315
$[C_{10}mim][BF_4]$	-0.993	$2.519 \cdot 10^{-4}$	-99.998	-7.400	-0.993	$2.431 \cdot 10^{-4}$

Table E.3: UNIQUAC interaction parameters for the cation, C, the anion, A, and water, W, obtained from LLE modeling with the PDH + UNIQUAC model with 6 parameters for ionic liquid/water systems.

Ionic liquid	a_{A-W} / K	b_{A-W}	a_{W-C} / K	b_{W-C}	a_{W-A} / K	b_{W-A}
$[C_2mim][NTf_2]$	-99.338	-7.658	0.690	-13.450	0.690	-11.650
$[C_3mim][NTf_2]$	-5.639	-7.598	0.923	-11.962	0.994	-11.599
$[C_4mim][NTf_2]$	-99.958	-7.647	0.965	-10.690	0.995	-11.600
$[C_5mim][NTf_2]$	-99.992	-7.650	0.967	-9.945	0.992	-11.599
$[C_6mim][NTf_2]$	-24.283	-7.694	0.999	-8.652	0.999	-11.657
$[C_7mim][NTf_2]$	-99.997	-7.648	0.998	-7.648	0.998	-11.651
$[C_8mim][NTf_2]$	-99.999	-7.654	0.570	-6.740	0.996	-11.647
$[C_4py][NTf_2]$	-99.444	-7.648	0.864	-11.251	0.948	-11.555
$[C_4mim][PF_6]$	0.992	-5.108	0.864	-10.644	0.939	-6.458
$[C_6mim][PF_6]$	-10.173	-5.100	1.109	-8.625	-99.987	-6.509
$[C_8mim][PF_6]$	-0.723	-5.100	1.018	-6.180	-0.526	-6.600
$[C_6mim][BF_4]$	-9.884	-3.050	9.479	-8.601	-9.998	-4.005
$[C_8mim][BF_4]$	-8.595	-3.099	9.998	-6.713	-9.999	-4.026
$[C_{10}mim][BF_4]$	-16.929	-3.099	-99.945	-3.524	-99.998	-4.051

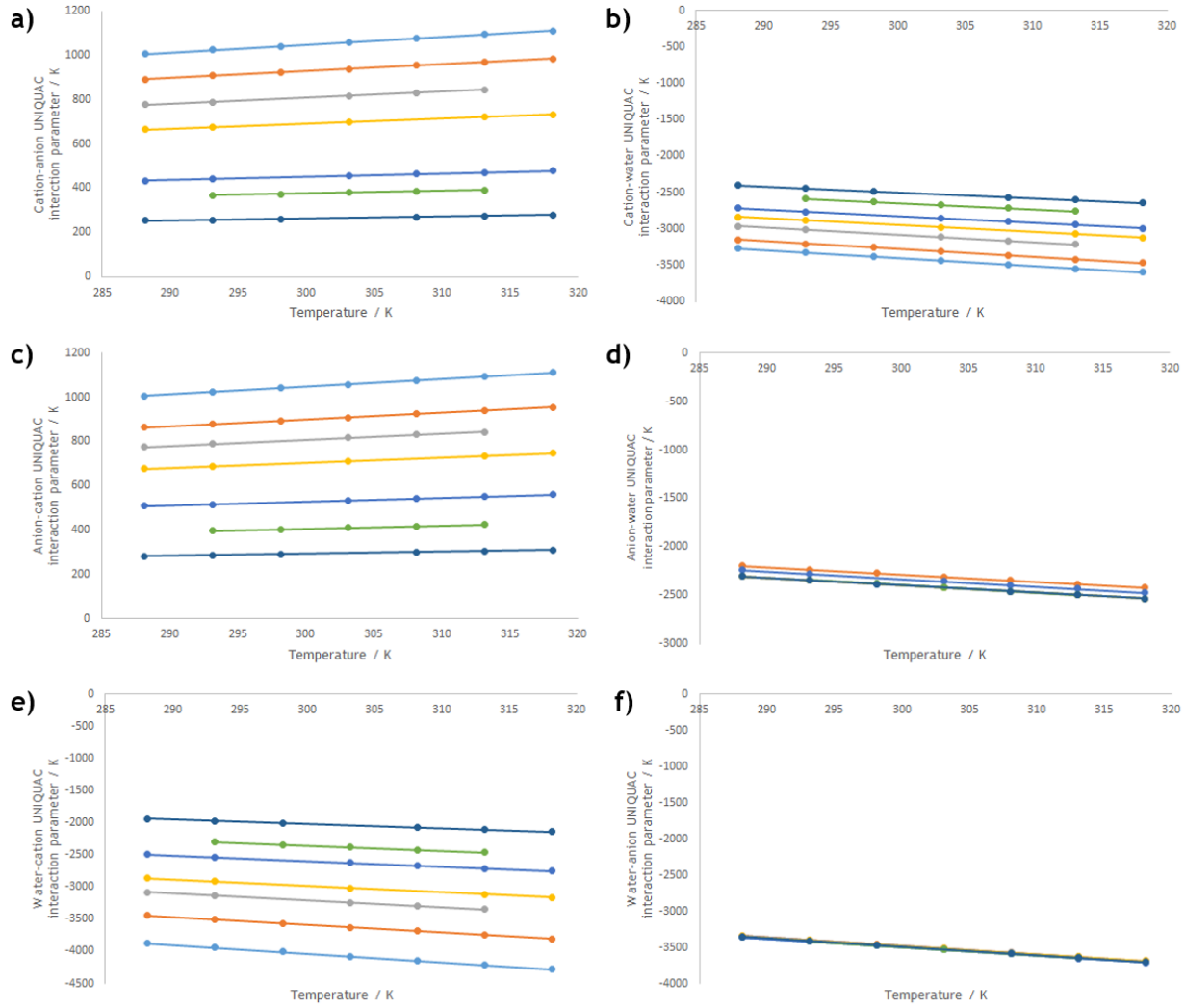


Fig. E.7: Influence of the alkyl chain length on the UNIQUAC interaction parameters for the PDH + UNIQUAC model with 6 parameters of $[NTf_2]^-$-based ionic liquids in water systems. a) cation-anion interactions, b) cation-water interactions, c) anion-cation interactions, d) anion-water interactions, e) water-cation interactions and f) water-anion interactions. The light blue line is the $[C_2mim][NTf_2]$/water, the orange line represents the $[C_3mim][NTf_2]$/water, the grey line displays the $[C_4mim][NTf_2]$/water, the yellow line portrays the $[C_5mim][NTf_2]$/water, the blue line shows the $[C_6mim][NTf_2]$/water, the green line presents the $[C_7mim][NTf_2]$/water and the dark blue line denotes the $[C_8mim][NTf_2]$/water.

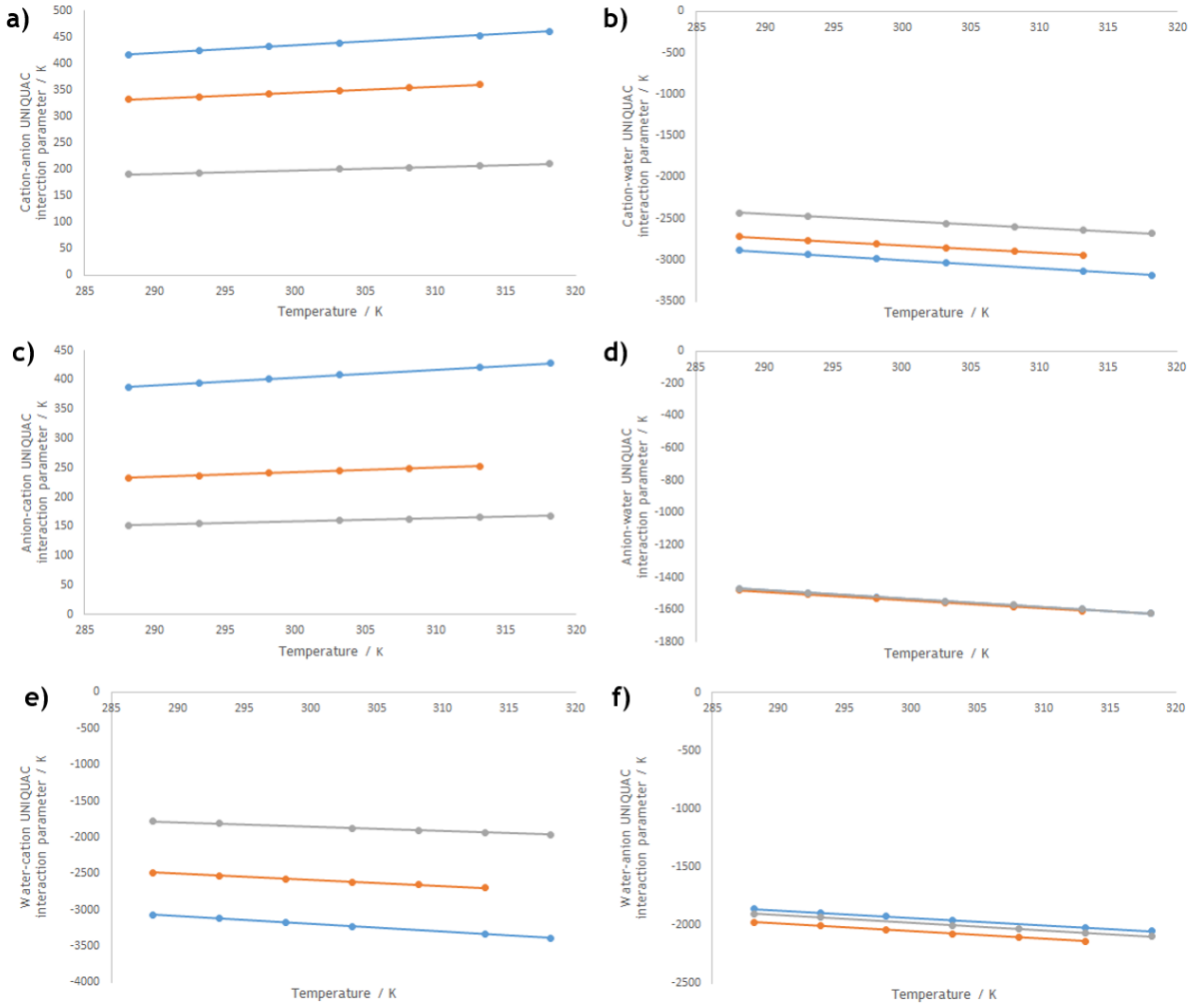


Fig. E.8: Influence of the alkyl chain length on the UNIQUAC interaction parameters for the PDH + UNIQUAC model with 6 parameters of $[PF_6]^-$-based ionic liquids in water systems. a) cation-anion interactions, b) cation-water interactions, c) anion-cation interactions, d) anion-water interactions, e) water-cation interactions and f) water-anion interactions. The light blue line is the $[C_4mim][PF_6]$/water, the orange line corresponds to the $[C_6mim][PF_6]$ and the grey line represents the $[C_8mim][PF_6]$/water.

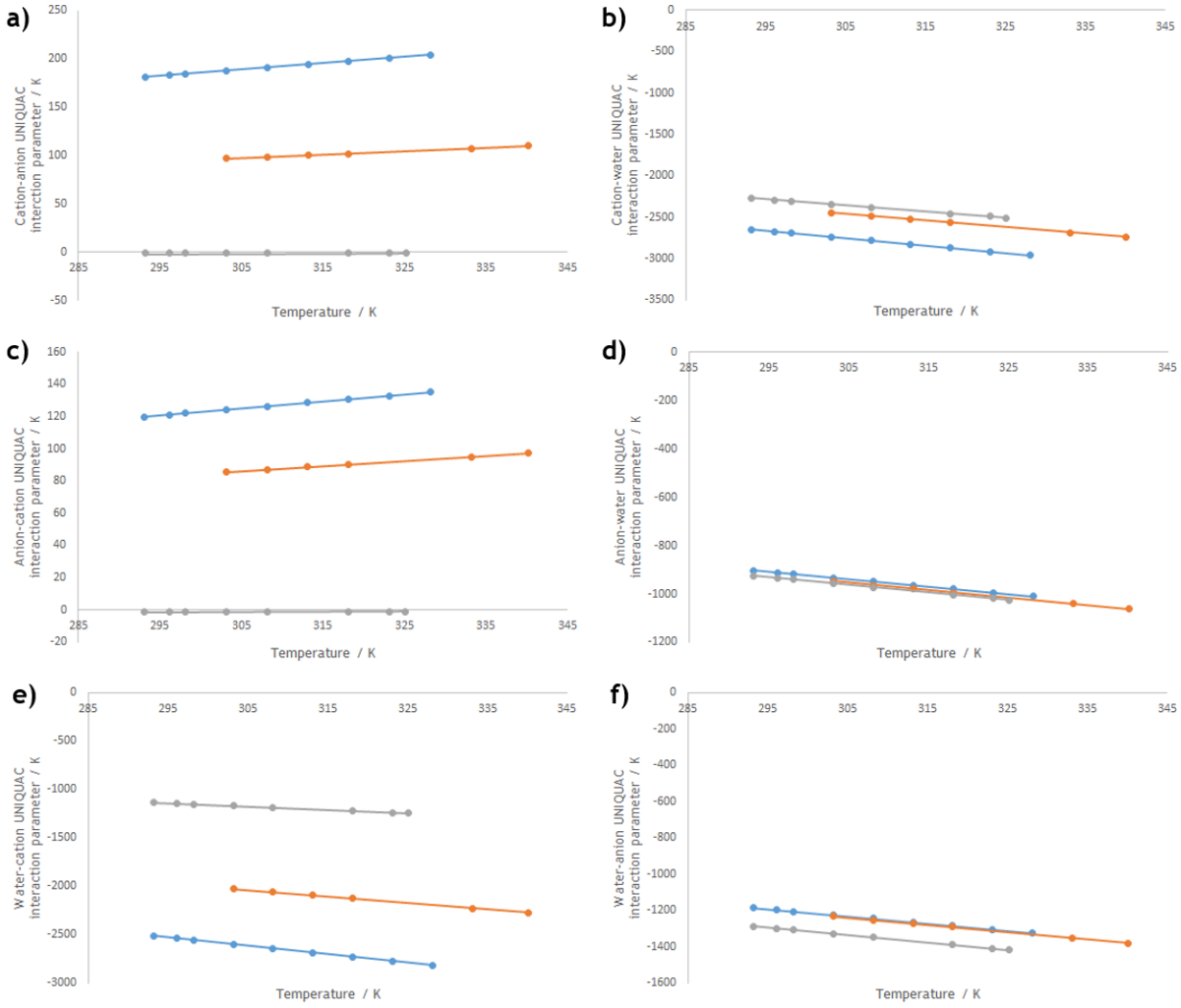


Fig. E.9: Influence of the alkyl chain length on the UNIQUAC interaction parameters for the PDH + UNIQUAC model with 6 parameters of $[BF_4]^-$-based ionic liquids in water systems. a) cation-anion interactions, b) cation-water interactions, c) anion-cation interactions, d) anion-water interactions, e) water-cation interactions and f) water-anion interactions. The light blue line is the $[C_6mim][BF_4]$/water, the orange line corresponds to the $[C_8mim][BF_4]$ and the grey line represents the $[C_{10}mim][BF_4]$/water.

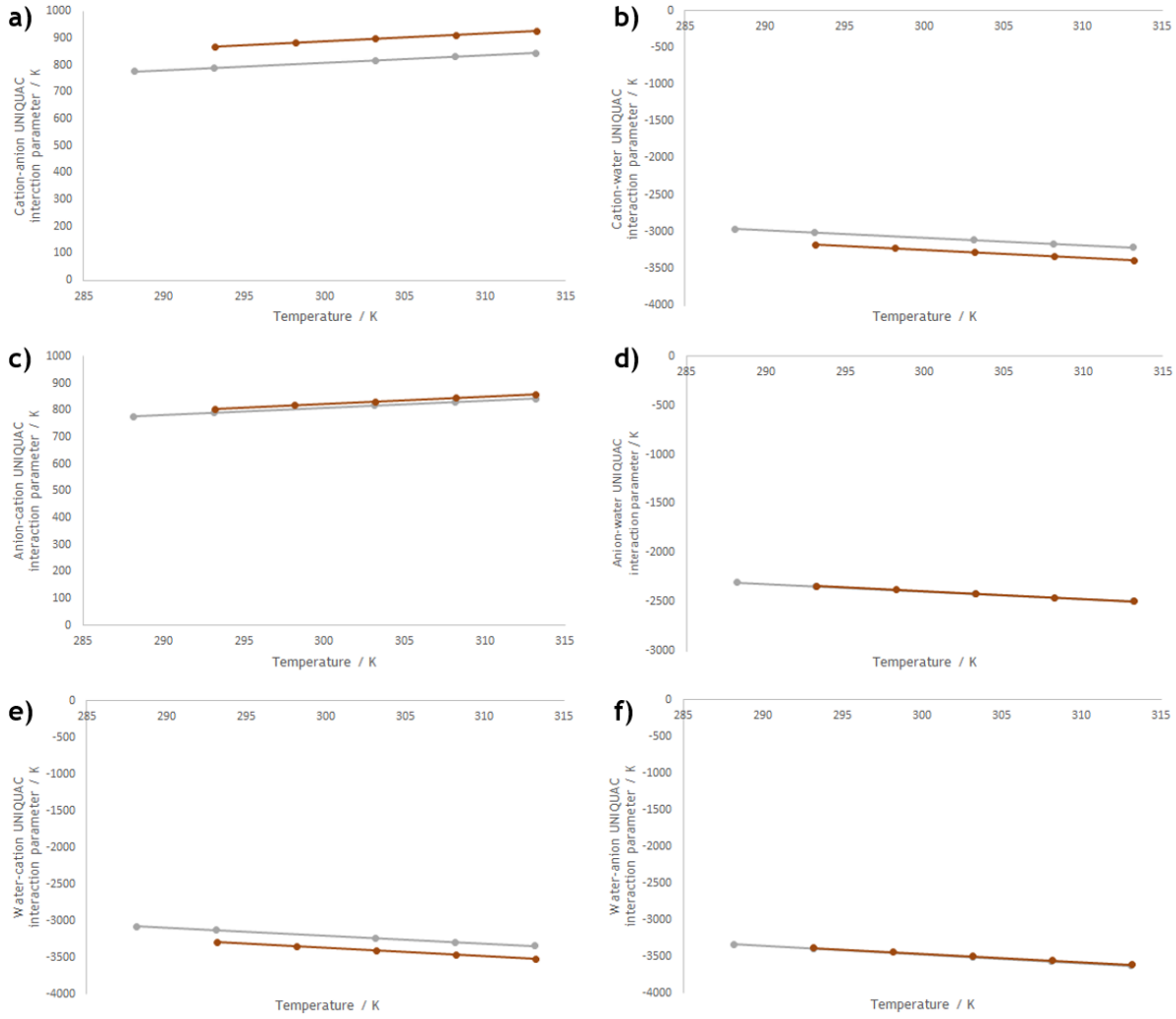


Fig. E.10: Influence of the cation on the UNIQUAC interaction parameters for the PDH + UNIQUAC model with 6 parameters of $[NTf_2]^-$-based ionic liquids in water systems. a) cation-anion interactions, b) cation-water interactions, c) anion-cation interactions, d) anion-water interactions, e) water-cation interactions and f) water-anion interactions. The brown line is the $[C_4py][NTf_2]$/water and the grey line represents the $[C_4mim][NTf_2]$/water.

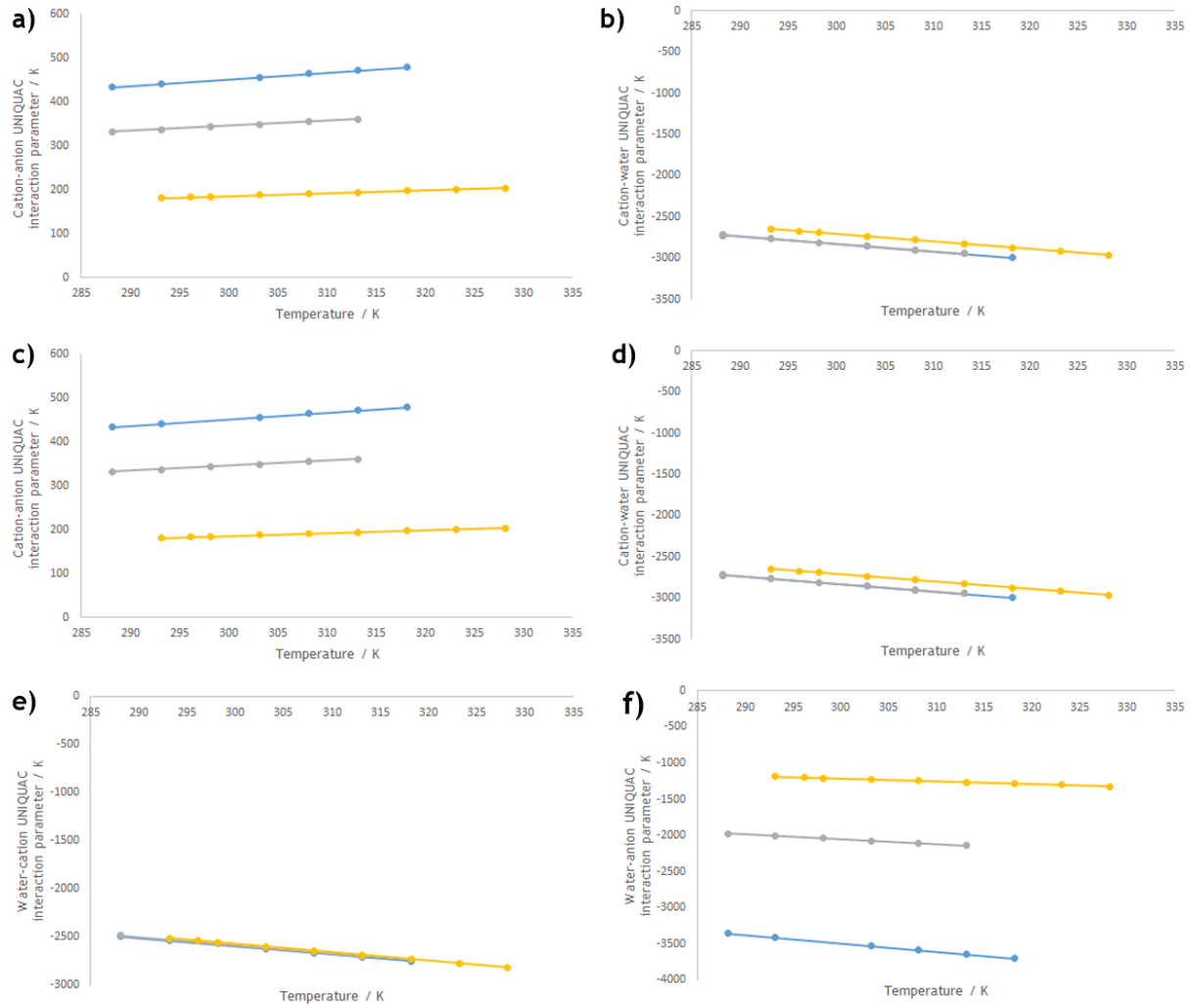


Fig. E.11: Influence of the anion on the UNIQUAC interaction parameters for the PDH + UNIQUAC model with 6 parameters of $[C_6mim]^+$-based ionic liquids in water systems. a) cation-anion interactions, b) cation-water interactions, c) anion-cation interactions, d) anion-water interactions, e) water-cation interactions and f) water-anion interactions. The yellow line is the $[C_6mim][BF_4]$/water, the grey line represents $[C_6mim][PF_6]$/water and the light blue line displays the $[C_6mim][NTf_2]$/water.

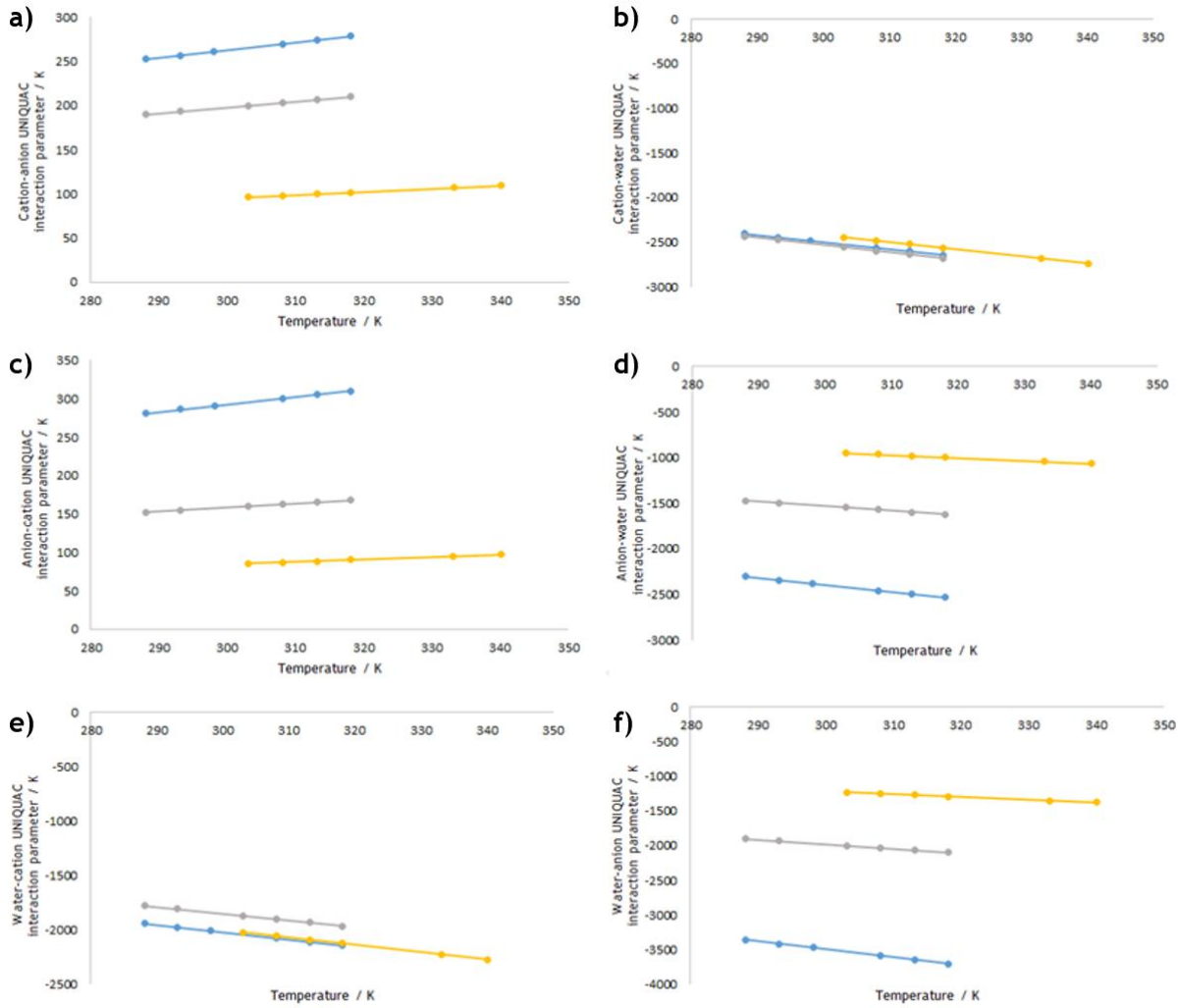


Fig. E.12: Influence of the anion on the UNIQUAC interaction parameters for the PDH + UNIQUAC model with 6 parameters of $[C_8mim]^+$-based ionic liquids in water systems. a) cation-anion interactions, b) cation-water interactions, c) anion-cation interactions, d) anion-water interactions, e) water-cation interactions and f) water-anion interactions. The yellow line is the $[C_8mim][BF_4]$/water, the grey line represents $[C_8mim][PF_6]$/water and the light blue line displays the $[C_8mim][NTf_2]$/water.

Appendix F - Modeling results for PDH + UNIQUAC model with 4 parameters

The LLE modeling results using the UNIQUAC model and the PDH + UNIQUAC model with 4 parameters are displayed throughout this appendix. The aqueous binary systems of ionic liquids already presented in the Results and discussion chapter are also shown with the rest of the ionic liquid/water systems studied in this work.

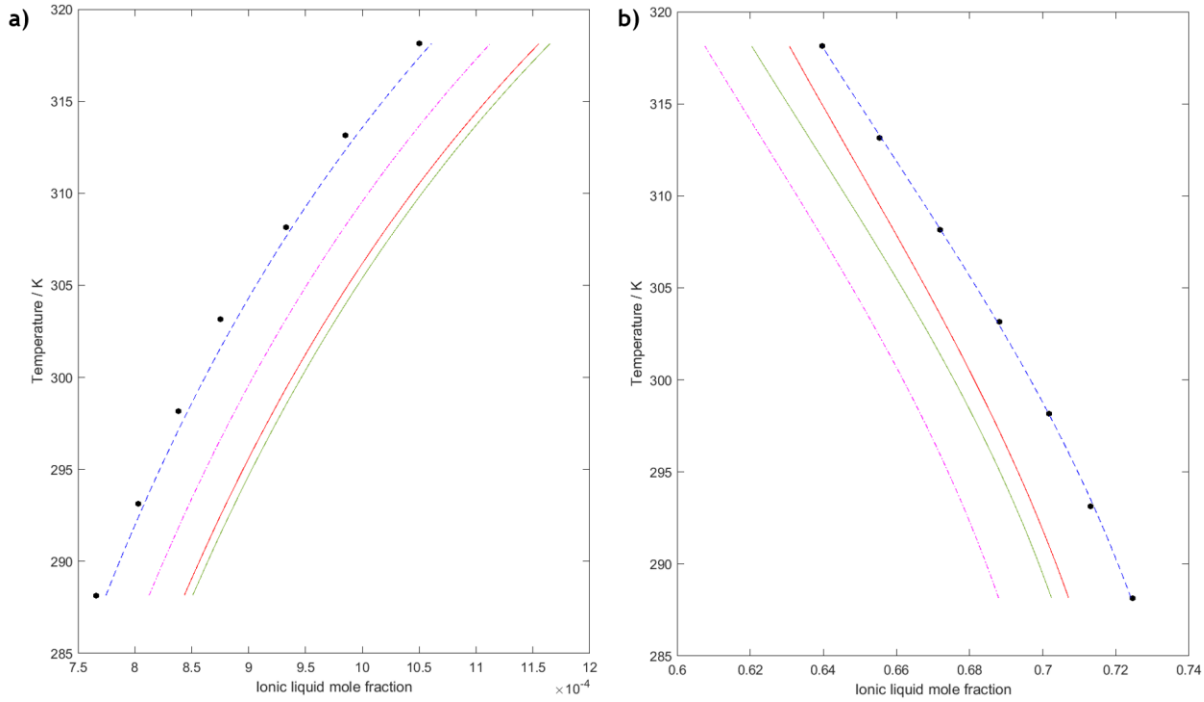


Fig. F.1: Calculated solubility curves for the binary system [C_2mim][NTf_2]/water at atmospheric pressure, concerning the PDH + UNIQUAC model with 4 parameters. a) water-rich phase and b) ionic liquid-rich phase. The black dots represent the experimental points, the red lines correspond to the results from the UNIQUAC model, the green lines are the results from the PDH + UNIQUAC model for a minimum closest approach parameter, the blue lines for a medium closest approach parameter and the pink lines for a maximum closest approach parameter.

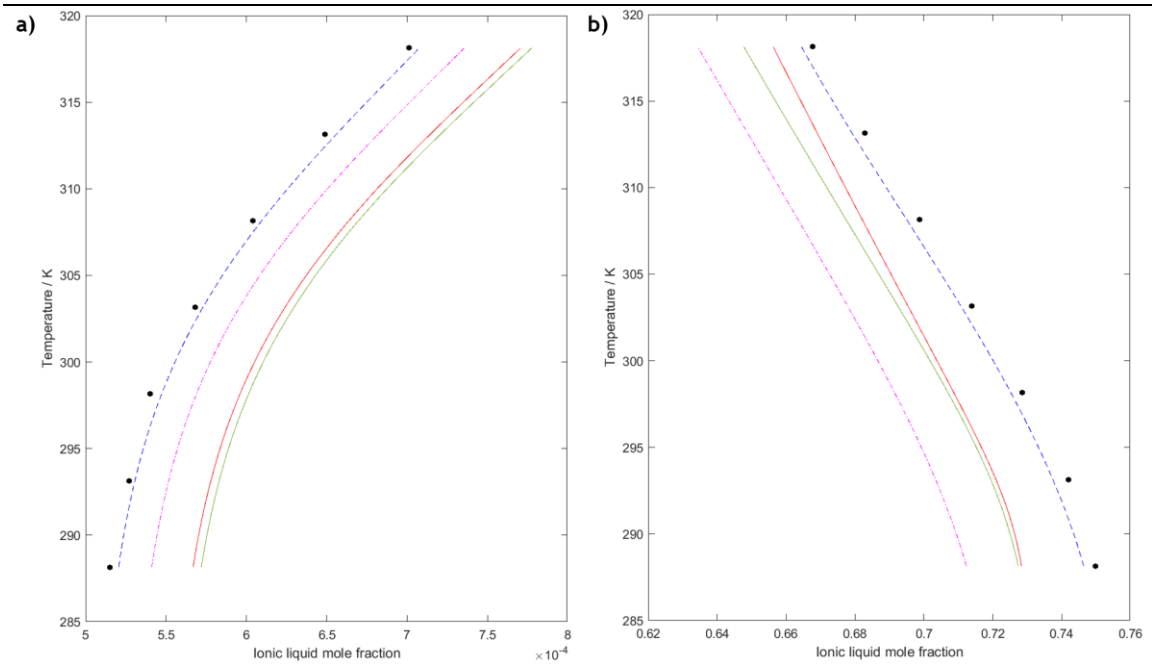


Fig. F.2: Calculated solubility curves for the binary system [C_3mim][NTf_2]/water at atmospheric pressure, concerning the PDH + UNIQUAC model with 4 parameters. a) water-rich phase and b) ionic liquid-rich phase. The black dots represent the experimental points, the red lines correspond to the results from the UNIQUAC model, the green lines are the results from the PDH + UNIQUAC model for a minimum closest approach parameter, the blue lines for a medium closest approach parameter and the pink lines for a maximum closest approach parameter.

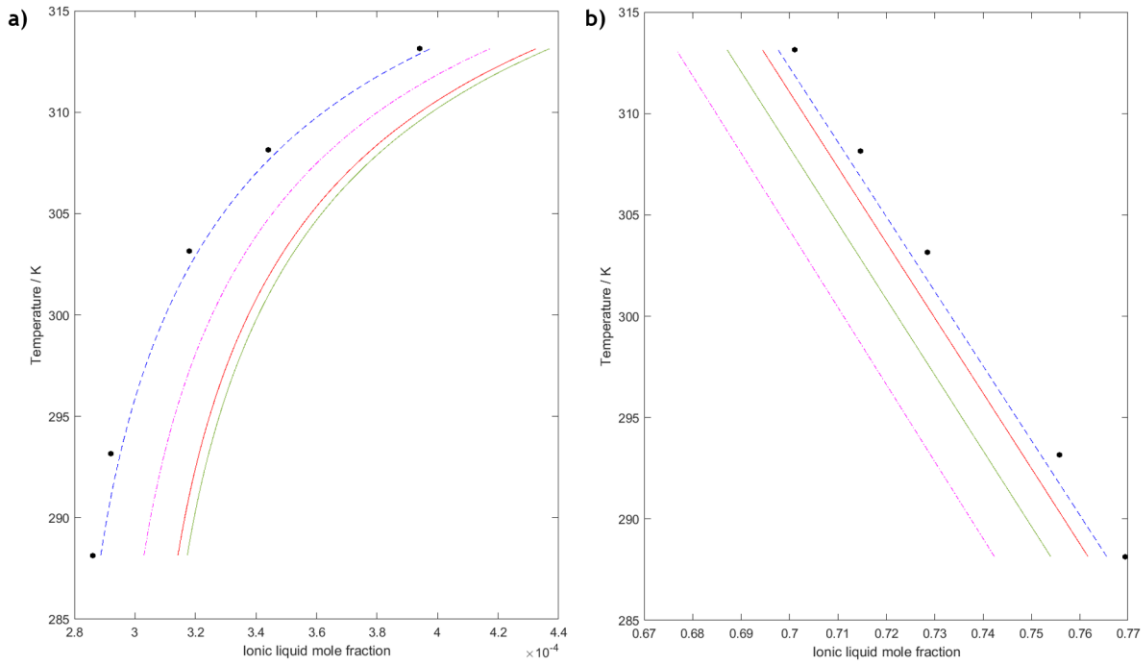


Fig. F.3: Calculated solubility curves for the binary system [C_4mim][NTf_2]/water at atmospheric pressure, concerning the PDH + UNIQUAC model with 4 parameters. a) water-rich phase and b) ionic liquid-rich phase. The black dots represent the experimental points, the red lines correspond to the results from the UNIQUAC model, the green lines are the results from the PDH + UNIQUAC model for a minimum closest approach parameter, the blue lines for a medium closest approach parameter and the pink lines for a maximum closest approach parameter.

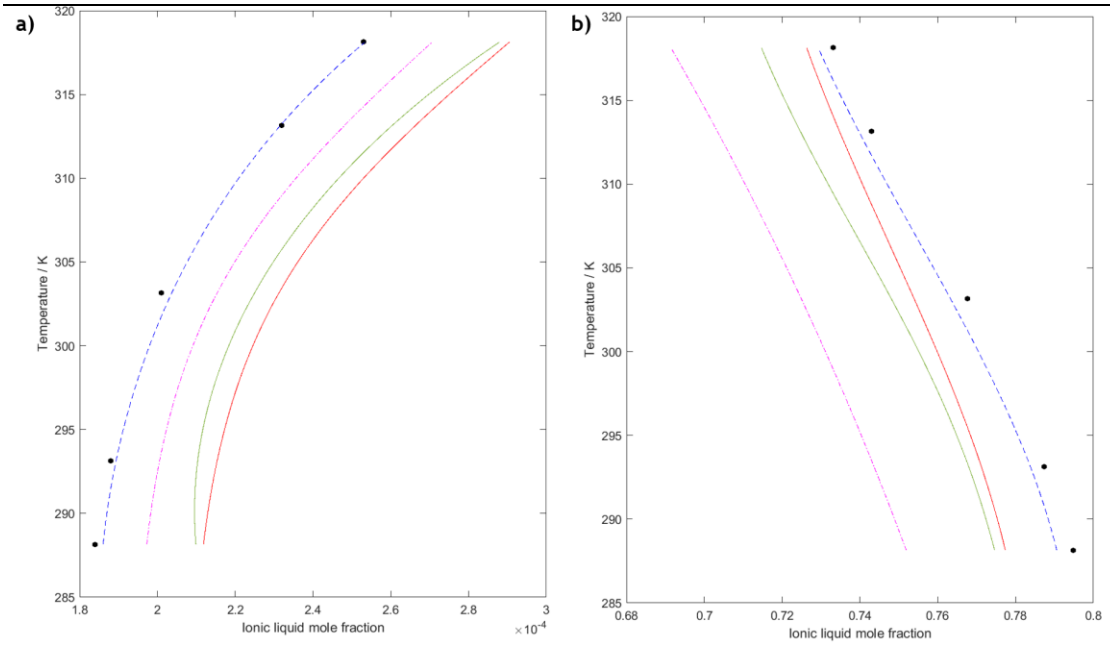


Fig. F.4: Calculated solubility curves for the binary system [C_5mim][NTf_2]/water at atmospheric pressure, concerning the PDH + UNIQUAC model with 4 parameters. a) water-rich phase and b) ionic liquid-rich phase. The black dots represent the experimental points, the red lines correspond to the results from the UNIQUAC model, the green lines are the results from the PDH + UNIQUAC model for a minimum closest approach parameter, the blue lines for a medium closest approach parameter and the pink lines for a maximum closest approach parameter.

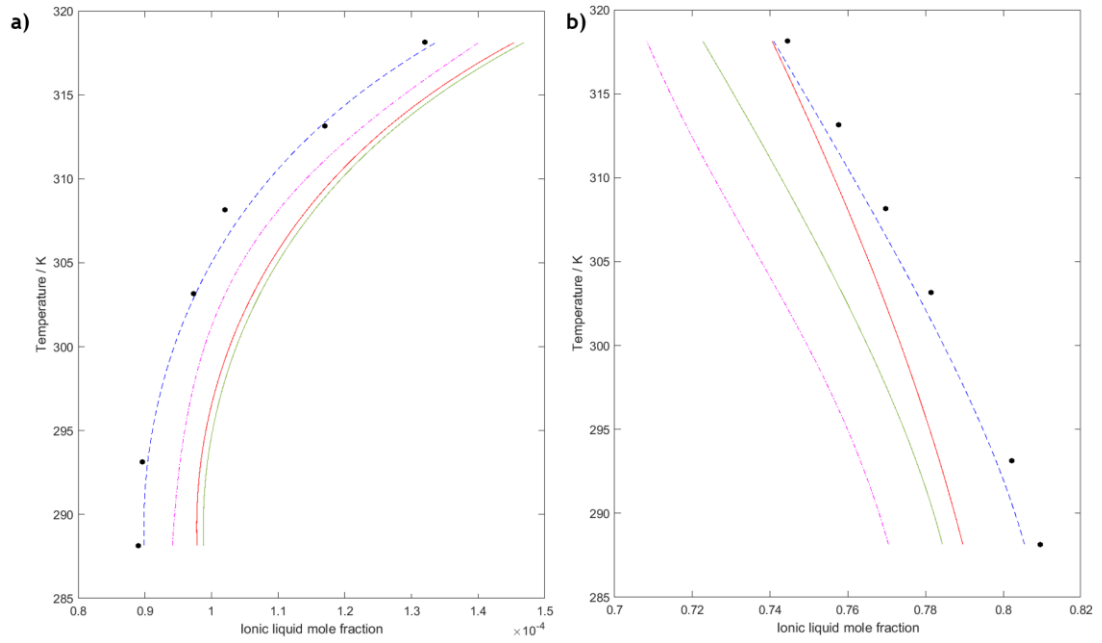


Fig. F.5: Calculated solubility curves for the binary system [C_6mim][NTf_2]/water at atmospheric pressure, concerning the PDH + UNIQUAC model with 4 parameters. a) water-rich phase and b) ionic liquid-rich phase. The black dots represent the experimental points, the red lines correspond to the results from the UNIQUAC model, the green lines are the results from the PDH + UNIQUAC model for a minimum closest approach parameter, the blue lines for a medium closest approach parameter and the pink lines for a maximum closest approach parameter.

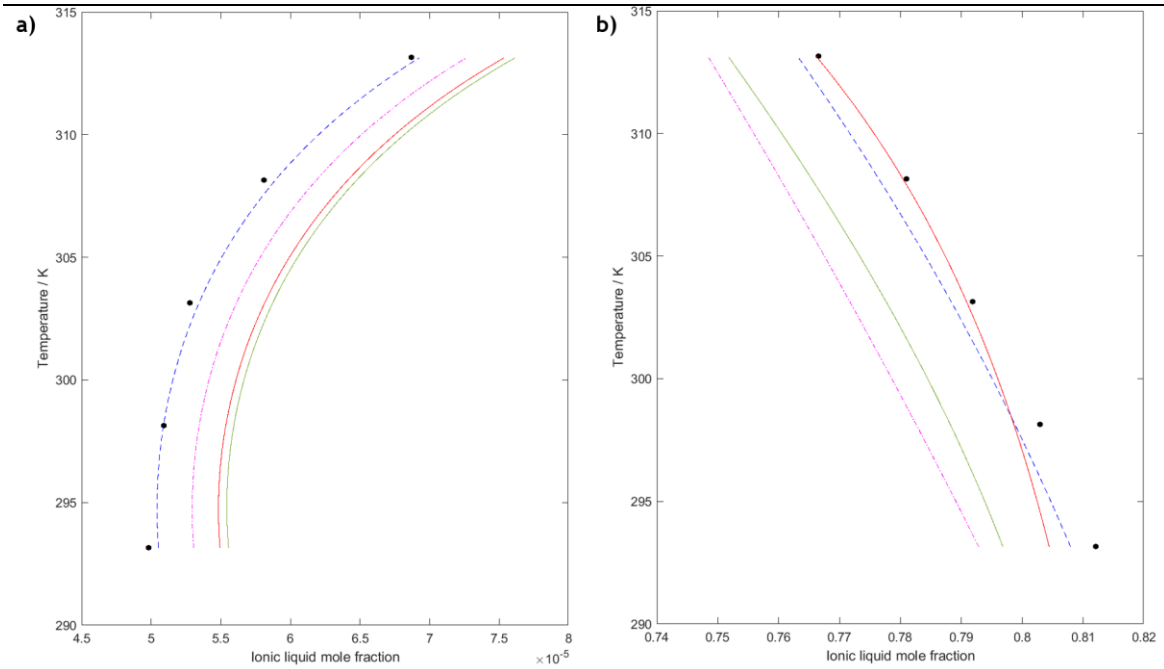


Fig. F.6: Calculated solubility curves for the binary system [C_7mim][NTf_2]/water at atmospheric pressure, concerning the PDH + UNIQUAC model with 4 parameters. a) water-rich phase and b) ionic liquid-rich phase. The black dots represent the experimental points, the red lines correspond to the results from the UNIQUAC model, the green lines are the results from the PDH + UNIQUAC model for a minimum closest approach parameter, the blue lines for a medium closest approach parameter and the pink lines for a maximum closest approach parameter.

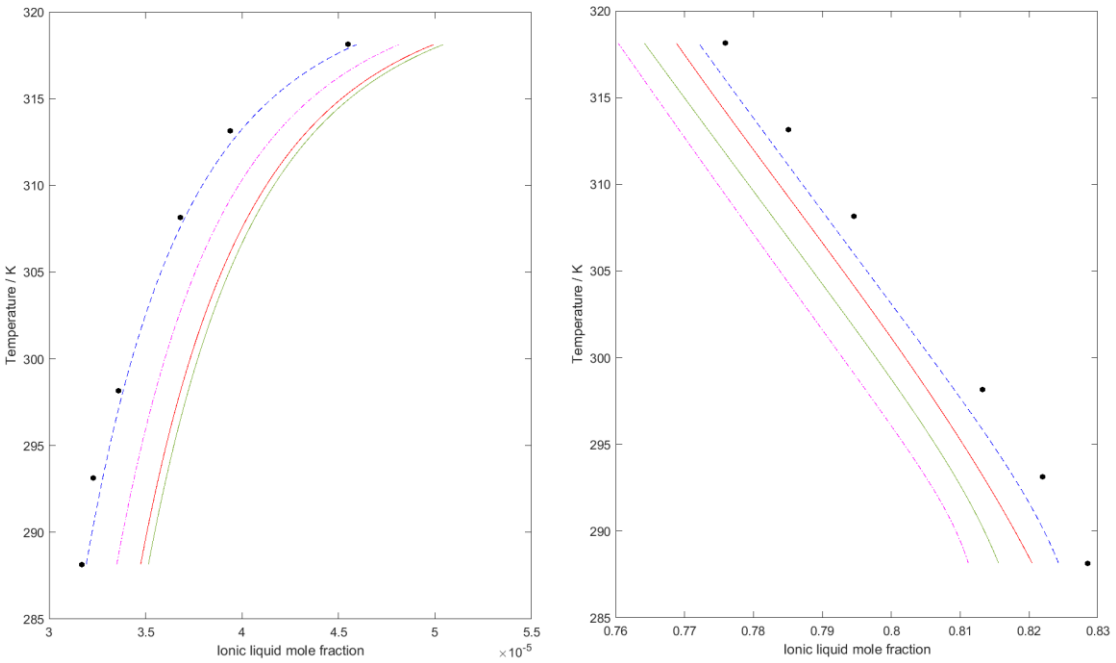


Fig. F.7: Calculated solubility curves for the binary system [C_8mim][NTf_2]/water at atmospheric pressure, concerning the PDH + UNIQUAC model with 4 parameters. a) water-rich phase and b) ionic liquid-rich phase. The black dots represent the experimental points, the red lines correspond to the results from the UNIQUAC model, the green lines are the results from the PDH + UNIQUAC model for a minimum closest approach parameter, the blue lines for a medium closest approach parameter and the pink lines for a maximum closest approach parameter.

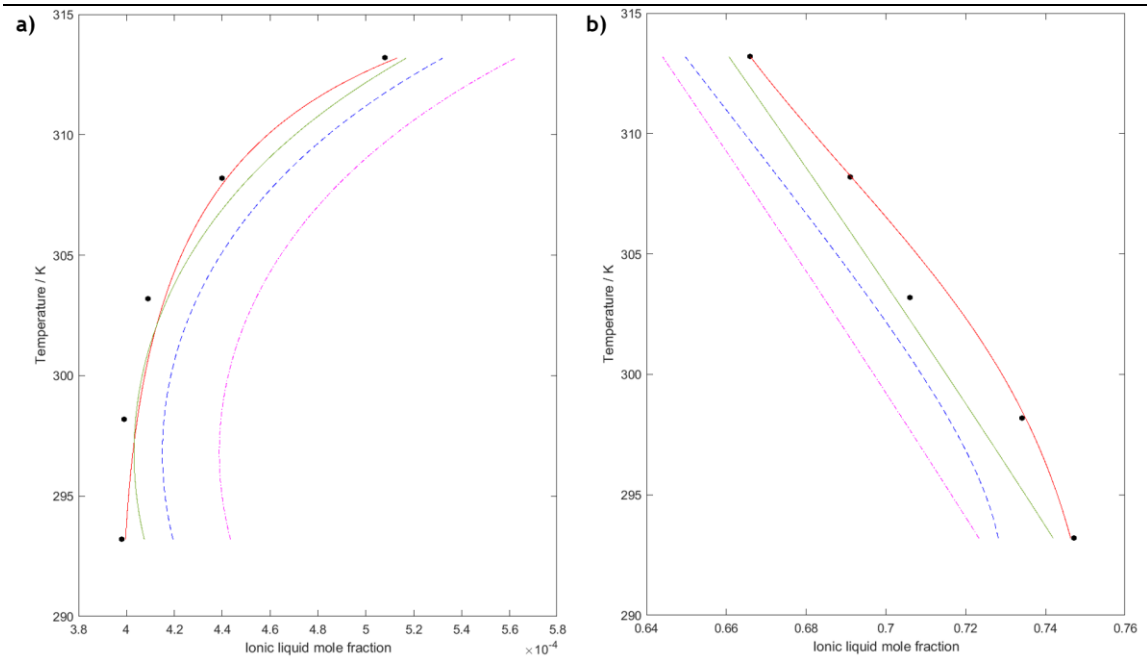


Fig. F.8: Calculated solubility curves for the binary system [C_4py][NTf_2]/water at atmospheric pressure, concerning the PDH + UNIQUAC model with 4 parameters. a) water-rich phase and b) ionic liquid-rich phase. The black dots represent the experimental points, the red lines correspond to the results from the UNIQUAC model, the green lines are the results from the PDH + UNIQUAC model for a minimum closest approach parameter, the blue lines for a medium closest approach parameter and the pink lines for a maximum closest approach parameter.

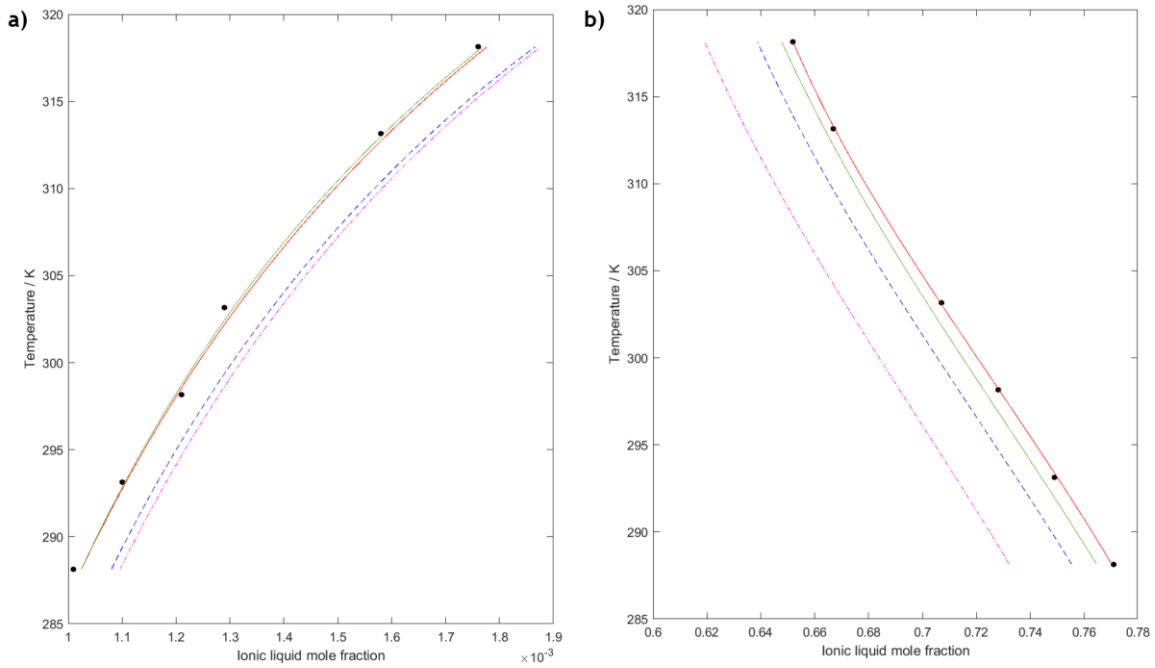


Fig. F.9: Calculated solubility curves for the binary system [C_4mim][PF_6]/water at atmospheric pressure, concerning the PDH + UNIQUAC model with 4 parameters. a) water-rich phase and b) ionic liquid-rich phase. The black dots represent the experimental points, the red lines correspond to the results from the UNIQUAC model, the green lines are the results from the PDH + UNIQUAC model for a minimum closest approach parameter, the blue lines for a medium closest approach parameter and the pink lines for a maximum closest approach parameter.

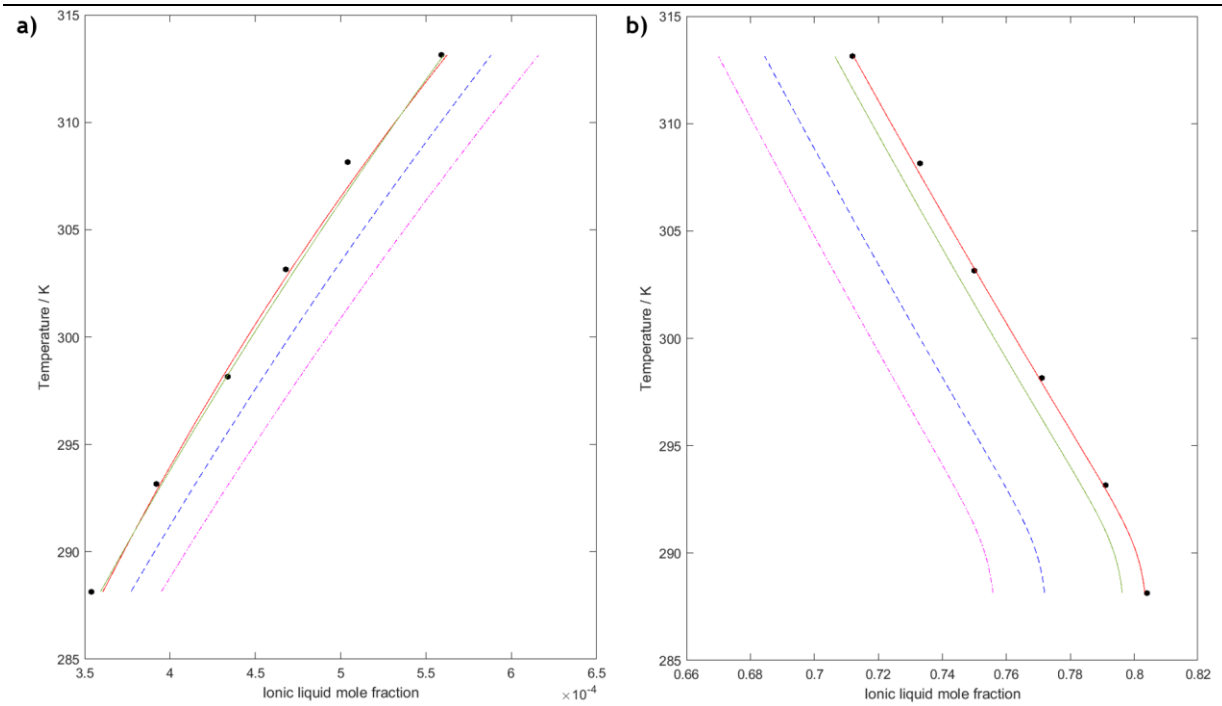


Fig. F.10: Calculated solubility curves for the binary system [C_6mim][PF_6]/water at atmospheric pressure, concerning the PDH + UNIQUAC model with 4 parameters. a) water-rich phase and b) ionic liquid-rich phase. The black dots represent the experimental points, the red lines correspond to the results from the UNIQUAC model, the green lines are the results from the PDH + UNIQUAC model for a minimum closest approach parameter, the blue lines for a medium closest approach parameter and the pink lines for a maximum closest approach parameter.

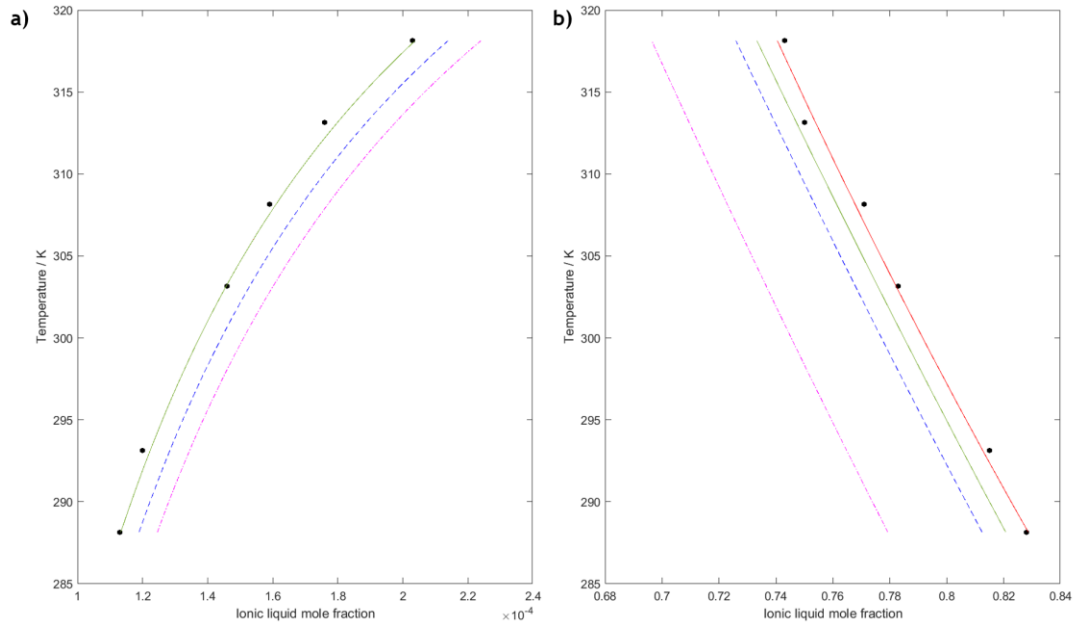


Fig. F.11: Calculated solubility curves for the binary system [C_8mim][PF_6]/water at atmospheric pressure, concerning the PDH + UNIQUAC model with 4 parameters. a) water-rich phase and b) ionic liquid-rich phase. The black dots represent the experimental points, the red lines correspond to the results from the UNIQUAC model, the green lines are the results from the PDH + UNIQUAC model for a minimum closest approach parameter, the blue lines for a medium closest approach parameter and the pink lines for a maximum closest approach parameter.

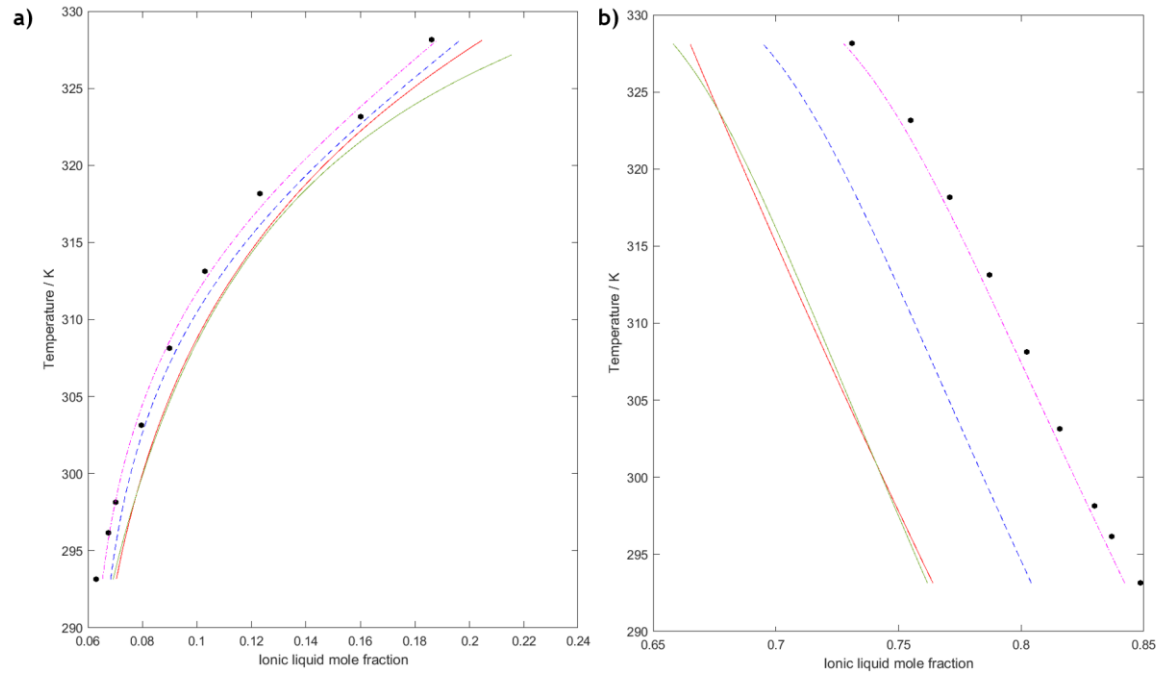


Fig. F.12: Calculated solubility curves for the binary system [C_6mim][BF_4]/water at atmospheric pressure, concerning the PDH + UNIQUAC model with 4 parameters. a) water-rich phase and b) ionic liquid-rich phase. The black dots represent the experimental points, the red lines correspond to the results from the UNIQUAC model, the green lines are the results from the PDH + UNIQUAC model for a minimum closest approach parameter, the blue lines for a medium closest approach parameter and the pink lines for a maximum closest approach parameter.

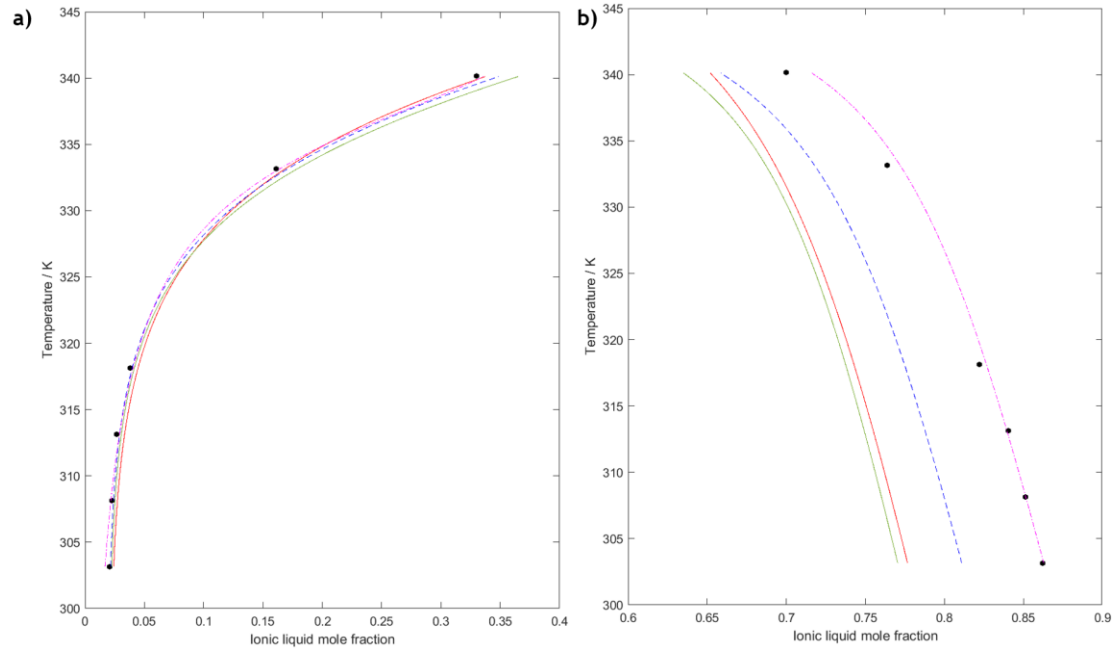


Fig. F.13: Calculated solubility curves for the binary system [C_8mim][BF_4]/water at atmospheric pressure, concerning the PDH + UNIQUAC model with 4 parameters. a) water-rich phase and b) ionic liquid-rich phase. The black dots represent the experimental points, the red lines correspond to the results from the UNIQUAC model, the green lines are the results from the PDH + UNIQUAC model for a minimum closest approach parameter, the blue lines for a medium closest approach parameter and the pink lines for a maximum closest approach parameter.

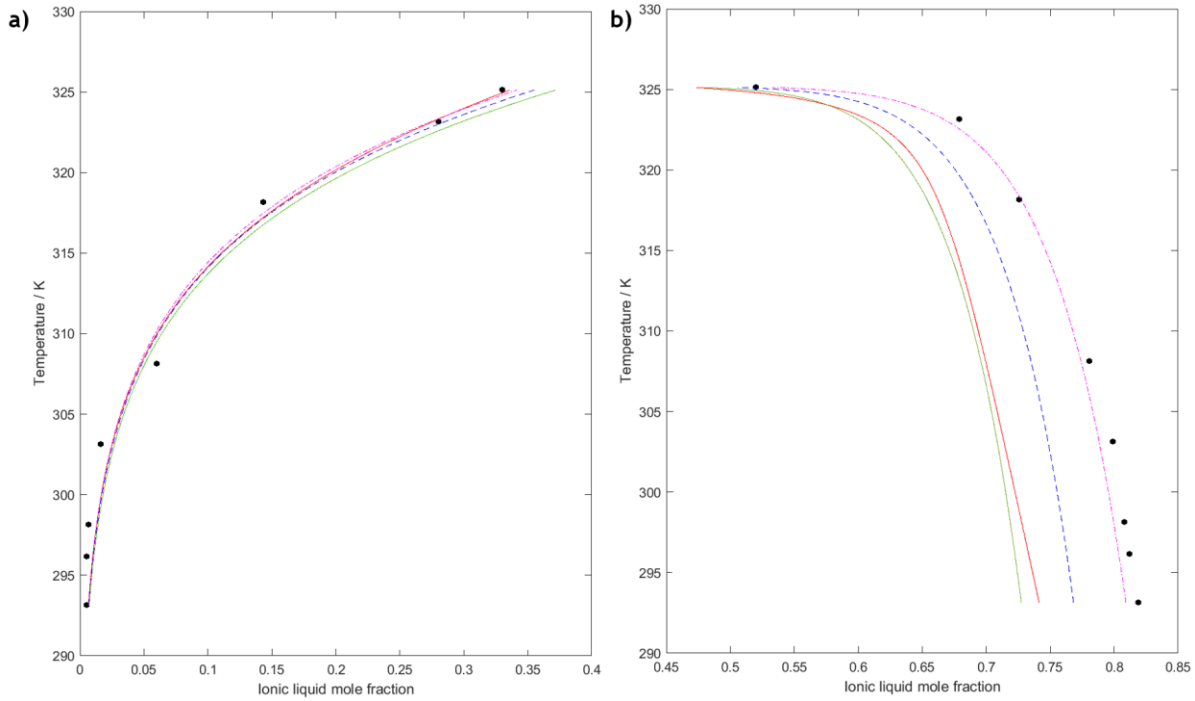


Fig. F.14: Calculated solubility curves for the binary system [C_{10}mim][BF_4]/water at atmospheric pressure, concerning the PDH + UNIQUAC model with 4 parameters. a) water-rich phase and b) ionic liquid-rich phase. The black dots represent the experimental points, the red lines correspond to the results from the UNIQUAC model, the green lines are the results from the PDH + UNIQUAC model for a minimum closest approach parameter, the blue lines for a medium closest approach parameter and the pink lines for a maximum closest approach parameter.

Appendix G – Calculated ionic liquid mole fractions for the ionic liquid/water mixtures and deviations of composition for the PDH + UNIQUAC model with 4 parameters

Table G.1: Calculated solubility points for the [C_2mim][NTf_2]/water system for the water-rich phase, x_{IL}^{W}, and for the ionic liquid-rich phase, x_{IL}^{IL}, for the UNIQUAC model and PDH + UNIQUAC model with 4 parameters for the three closest approach parameters (ρ_{min}, ρ_{med}, ρ_{max}).

	UNIQUAC		PDH + UNIQUAC ρ_{min}		PDH + UNIQUAC ρ_{med}		PDH + UNIQUAC ρ_{max}	
T / K	$x_{IL}^{W} \cdot 10^3$	x_{IL}^{IL}	$x_{IL}^{W} \cdot 10^3$	x_{IL}^{IL}	$x_{IL}^{W} \cdot 10^3$	x_{IL}^{IL}	$x_{IL}^{W} \cdot 10^3$	x_{IL}^{IL}
288.15	0.843	0.707	0.850	0.703	0.774	0.725	0.812	0.688
293.15	0.883	0.697	0.891	0.692	0.811	0.713	0.851	0.677
298.15	0.922	0.686	0.930	0.681	0.846	0.702	0.888	0.667
303.15	0.962	0.679	0.971	0.667	0.884	0.688	0.927	0.654
308.15	1.026	0.659	1.035	0.652	0.942	0.672	0.988	0.638
313.15	1.083	0.645	1.093	0.636	0.995	0.655	1.044	0.623
318.15	1.155	0.631	1.165	0.621	1.060	0.640	1.112	0.608

Table G.2: Calculated solubility points for the [C_3mim][NTf_2]/water system for the water-rich phase, x_{IL}^{W}, and for the ionic liquid-rich phase, x_{IL}^{IL}, for the UNIQUAC model and PDH + UNIQUAC model with 4 parameters for the three closest approach parameters (ρ_{min}, ρ_{med}, ρ_{max}).

	UNIQUAC		PDH + UNIQUAC ρ_{min}		PDH + UNIQUAC ρ_{med}		PDH + UNIQUAC ρ_{max}	
T / K	$x_{IL}^{W} \cdot 10^3$	x_{IL}^{IL}	$x_{IL}^{W} \cdot 10^3$	x_{IL}^{IL}	$x_{IL}^{W} \cdot 10^3$	x_{IL}^{IL}	$x_{IL}^{W} \cdot 10^3$	x_{IL}^{IL}
288.15	0.566	0.728	0.572	0.727	0.520	0.746	0.541	0.712
293.15	0.580	0.721	0.585	0.720	0.532	0.738	0.553	0.703
298.15	0.594	0.709	0.599	0.707	0.545	0.725	0.567	0.692
303.15	0.625	0.695	0.630	0.692	0.574	0.710	0.596	0.678
308.15	0.664	0.682	0.670	0.678	0.610	0.695	0.634	0.664
313.15	0.714	0.669	0.720	0.662	0.655	0.679	0.681	0.648
318.15	0.771	0.656	0.778	0.648	0.708	0.664	0.736	0.635

Table G.3: Calculated solubility points for the [C_4mim][NTf_2]/water system for the water-rich phase, $x_{IL}{}^{W}$, and for the ionic liquid-rich phase, $x_{IL}{}^{IL}$, for the UNIQUAC model and PDH + UNIQUAC model with 4 parameters for the three closest approach parameters (ρ_{min}, ρ_{med}, ρ_{max}).

	UNIQUAC		PDH + UNIQUAC ρ_{min}		PDH + UNIQUAC ρ_{med}		PDH + UNIQUAC ρ_{max}	
T / K	$x_{IL}{}^{W} \cdot 10^3$	$x_{IL}{}^{IL}$	$x_{IL}{}^{W} \cdot 10^3$	$x_{IL}{}^{IL}$	$x_{IL}{}^{W} \cdot 10^3$	$x_{IL}{}^{IL}$	$x_{IL}{}^{W} \cdot 10^3$	$x_{IL}{}^{IL}$
288.15	0.314	0.762	0.317	0.754	0.289	0.765	0.303	0.742
293.15	0.321	0.748	0.324	0.741	0.295	0.752	0.310	0.729
303.15	0.349	0.721	0.353	0.714	0.321	0.725	0.337	0.703
308.15	0.378	0.708	0.382	0.700	0.347	0.711	0.365	0.690
313.15	0.433	0.694	0.437	0.687	0.398	0.698	0.418	0.677

Table G.4: Calculated solubility points for the [C_5mim][NTf_2]/water system for the water-rich phase, $x_{IL}{}^{W}$, and for the ionic liquid-rich phase, $x_{IL}{}^{IL}$, for the UNIQUAC model and PDH + UNIQUAC model with 4 parameters for the three closest approach parameters (ρ_{min}, ρ_{med}, ρ_{max}).

	UNIQUAC		PDH + UNIQUAC ρ_{min}		PDH + UNIQUAC ρ_{med}		PDH + UNIQUAC ρ_{max}	
T / K	$x_{IL}{}^{W} \cdot 10^3$	$x_{IL}{}^{IL}$	$x_{IL}{}^{W} \cdot 10^3$	$x_{IL}{}^{IL}$	$x_{IL}{}^{W} \cdot 10^3$	$x_{IL}{}^{IL}$	$x_{IL}{}^{W} \cdot 10^3$	$x_{IL}{}^{IL}$
288.15	0.211	0.778	0.210	0.775	0.186	0.791	0.197	0.755
293.15	0.216	0.771	0.211	0.768	0.190	0.783	0.201	0.739
303.15	0.231	0.754	0.225	0.748	0.203	0.764	0.215	0.727
313.15	0.266	0.734	0.260	0.724	0.232	0.739	0.248	0.704
318.15	0.291	0.726	0.288	0.715	0.253	0.729	0.271	0.691

Table G.5: Calculated solubility points for the [C_6mim][NTf_2]/water system for the water-rich phase, $x_{IL}{}^{W}$, and for the ionic liquid-rich phase, $x_{IL}{}^{IL}$, for the UNIQUAC model and PDH + UNIQUAC model with 4 parameters for the three closest approach parameters (ρ_{min}, ρ_{med}, ρ_{max}).

	UNIQUAC		PDH + UNIQUAC ρ_{min}		PDH + UNIQUAC ρ_{med}		PDH + UNIQUAC ρ_{max}	
T / K	$x_{IL}{}^{W} \cdot 10^4$	$x_{IL}{}^{IL}$	$x_{IL}{}^{W} \cdot 10^4$	$x_{IL}{}^{IL}$	$x_{IL}{}^{W} \cdot 10^4$	$x_{IL}{}^{IL}$	$x_{IL}{}^{W} \cdot 10^4$	$x_{IL}{}^{IL}$
288.15	0.978	0.789	0.988	0.784	0.899	0.805	0.943	0.770
293.15	0.985	0.784	0.995	0.778	0.905	0.798	0.950	0.763
303.15	1.069	0.768	1.080	0.758	0.983	0.777	1.031	0.742
308.15	1.121	0.760	1.132	0.747	1.030	0.766	1.081	0.730
313.15	1.286	0.751	1.299	0.735	1.182	0.754	1.240	0.718
318.15	1.450	0.740	1.465	0.723	1.333	0.741	1.399	0.708

Table G.6: Calculated solubility points for the [C_7mim][NTf_2]/water system for the water-rich phase, $x_{IL}{}^{W}$, and for the ionic liquid-rich phase, $x_{IL}{}^{IL}$, for the UNIQUAC model and PDH + UNIQUAC model with 4 parameters for the three closest approach parameters (ρ_{min}, ρ_{med}, ρ_{max}).

	UNIQUAC		PDH + UNIQUAC ρ_{min}		PDH + UNIQUAC ρ_{med}		PDH + UNIQUAC ρ_{max}	
T / K	$x_{IL}{}^{W} \cdot 10^4$	$x_{IL}{}^{IL}$	$x_{IL}{}^{W} \cdot 10^4$	$x_{IL}{}^{IL}$	$x_{IL}{}^{W} \cdot 10^4$	$x_{IL}{}^{IL}$	$x_{IL}{}^{W} \cdot 10^4$	$x_{IL}{}^{IL}$
293.15	0.547	0.804	0.533	0.797	0.503	0.808	0.528	0.793
298.15	0.559	0.799	0.565	0.788	0.514	0.799	0.540	0.783
303.15	0.580	0.791	0.586	0.777	0.533	0.788	0.560	0.771
308.15	0.639	0.780	0.645	0.766	0.587	0.777	0.616	0.761
313.15	0.755	0.766	0.763	0.751	0.694	0.763	0.728	0.748

Table G.7: Calculated solubility points for the [C_8mim][NTf_2]/water system for the water-rich phase, $x_{IL}{}^{W}$, and for the ionic liquid-rich phase, $x_{IL}{}^{IL}$, for the UNIQUAC model and PDH + UNIQUAC model with 4 parameters for the three closest approach parameters (ρ_{min}, ρ_{med}, ρ_{max}).

	UNIQUAC		PDH + UNIQUAC ρ_{min}		PDH + UNIQUAC ρ_{med}		PDH + UNIQUAC ρ_{max}	
T / K	$x_{IL}{}^{W} \cdot 10^4$	$x_{IL}{}^{IL}$	$x_{IL}{}^{W} \cdot 10^4$	$x_{IL}{}^{IL}$	$x_{IL}{}^{W} \cdot 10^4$	$x_{IL}{}^{IL}$	$x_{IL}{}^{W} \cdot 10^4$	$x_{IL}{}^{IL}$
288.15	0.348	0.820	0.352	0.815	0.320	0.824	0.336	0.811
293.15	0.355	0.814	0.359	0.809	0.326	0.818	0.342	0.805
298.15	0.369	0.805	0.373	0.801	0.339	0.809	0.356	0.796
308.15	0.404	0.787	0.408	0.783	0.372	0.791	0.390	0.778
313.15	0.433	0.778	0.437	0.773	0.398	0.781	0.418	0.769
318.15	0.500	0.769	0.505	0.764	0.460	0.772	0.482	0.760

Table G.8: Calculated solubility points for the [C_4py][NTf_2]/water system for the water-rich phase, $x_{IL}{}^{W}$, and for the ionic liquid-rich phase, $x_{IL}{}^{IL}$, for the UNIQUAC model and PDH + UNIQUAC model with 4 parameters for the three closest approach parameters (ρ_{min}, ρ_{med}, ρ_{max}).

	UNIQUAC		PDH + UNIQUAC ρ_{min}		PDH + UNIQUAC ρ_{med}		PDH + UNIQUAC ρ_{max}	
T / K	$x_{IL}{}^{W} \cdot 10^3$	$x_{IL}{}^{IL}$	$x_{IL}{}^{W} \cdot 10^3$	$x_{IL}{}^{IL}$	$x_{IL}{}^{W} \cdot 10^3$	$x_{IL}{}^{IL}$	$x_{IL}{}^{W} \cdot 10^3$	$x_{IL}{}^{IL}$
293.20	0.402	0.746	0.406	0.740	0.418	0.728	0.442	0.721
298.20	0.403	0.734	0.407	0.727	0.419	0.716	0.443	0.708
303.20	0.413	0.717	0.417	0.699	0.429	0.695	0.454	0.681
308.20	0.444	0.691	0.449	0.684	0.462	0.674	0.488	0.667
313.20	0.513	0.666	0.518	0.659	0.533	0.659	0.564	0.643

Table G.9: Calculated solubility points for the [C_4mim][PF_6]/water system for the water-rich phase, x_{IL}^{W}, and for the ionic liquid-rich phase, x_{IL}^{IL}, for the UNIQUAC model and PDH + UNIQUAC model with 4 parameters for the three closest approach parameters (ρ_{min}, ρ_{med}, ρ_{max}).

	UNIQUAC		PDH + UNIQUAC ρ_{min}		PDH + UNIQUAC ρ_{med}		PDH + UNIQUAC ρ_{max}	
T / K	$x_{IL}^{W} \cdot 10^2$	x_{IL}^{IL}	$x_{IL}^{W} \cdot 10^2$	x_{IL}^{IL}	$x_{IL}^{W} \cdot 10^2$	x_{IL}^{IL}	$x_{IL}^{W} \cdot 10^2$	x_{IL}^{IL}
288.15	0.102	0.770	0.102	0.765	0.107	0.756	0.109	0.732
293.15	0.111	0.750	0.111	0.743	0.117	0.734	0.118	0.712
298.15	0.121	0.728	0.122	0.723	0.128	0.713	0.130	0.692
303.15	0.130	0.707	0.130	0.702	0.137	0.693	0.138	0.672
313.15	0.160	0.667	0.159	0.663	0.167	0.654	0.169	0.634
318.15	0.178	0.652	0.177	0.648	0.187	0.639	0.188	0.619

Table G.10: Calculated solubility points for the [C_6mim][PF_6]/water system for the water-rich phase, x_{IL}^{W}, and for the ionic liquid-rich phase, x_{IL}^{IL}, for the UNIQUAC model and PDH + UNIQUAC model with 4 parameters for the three closest approach parameters (ρ_{min}, ρ_{med}, ρ_{max}).

	UNIQUAC		PDH + UNIQUAC ρ_{min}		PDH + UNIQUAC ρ_{med}		PDH + UNIQUAC ρ_{max}	
T / K	$x_{IL}^{W} \cdot 10^3$	x_{IL}^{IL}	$x_{IL}^{W} \cdot 10^3$	x_{IL}^{IL}	$x_{IL}^{W} \cdot 10^3$	x_{IL}^{IL}	$x_{IL}^{W} \cdot 10^3$	x_{IL}^{IL}
288.15	0.358	0.803	0.357	0.796	0.375	0.772	0.393	0.756
293.15	0.396	0.790	0.396	0.783	0.416	0.759	0.435	0.744
298.15	0.434	0.770	0.438	0.764	0.460	0.740	0.482	0.725
303.15	0.473	0.749	0.473	0.743	0.496	0.720	0.519	0.705
308.15	0.509	0.732	0.509	0.726	0.534	0.704	0.559	0.689
313.15	0.565	0.712	0.564	0.706	0.593	0.684	0.620	0.669

Table G.11: Calculated solubility points for the [C_8mim][PF_6]/water system for the water-rich phase, $x_{IL}{}^{W}$, and for the ionic liquid-rich phase, $x_{IL}{}^{IL}$, for the UNIQUAC model and PDH + UNIQUAC model with 4 parameters for the three closest approach parameters (ρ_{min}, ρ_{med}, ρ_{max}).

	UNIQUAC		PDH + UNIQUAC ρ_{min}		PDH + UNIQUAC ρ_{med}		PDH + UNIQUAC ρ_{max}	
T / K	$x_{IL}{}^{W} \cdot 10^3$	$x_{IL}{}^{IL}$	$x_{IL}{}^{W} \cdot 10^3$	$x_{IL}{}^{IL}$	$x_{IL}{}^{W} \cdot 10^3$	$x_{IL}{}^{IL}$	$x_{IL}{}^{W} \cdot 10^3$	$x_{IL}{}^{IL}$
288.15	0.114	0.827	0.114	0.820	0.120	0.811	0.125	0.778
293.15	0.121	0.814	0.121	0.807	0.127	0.799	0.133	0.766
303.15	0.147	0.782	0.147	0.775	0.155	0.767	0.162	0.736
308.15	0.161	0.770	0.161	0.763	0.169	0.756	0.176	0.725
313.15	0.178	0.749	0.178	0.743	0.187	0.735	0.195	0.705
318.15	0.205	0.742	0.205	0.736	0.215	0.728	0.225	0.699

Table G.12: Calculated solubility points for the [C_6mim][BF_4]/water system for the water-rich phase, $x_{IL}{}^{W}$, and for the ionic liquid-rich phase, $x_{IL}{}^{IL}$, for the UNIQUAC model and PDH + UNIQUAC model with 4 parameters for the three closest approach parameters (ρ_{min}, ρ_{med}, ρ_{max}).

	UNIQUAC		PDH + UNIQUAC ρ_{min}		PDH + UNIQUAC ρ_{med}		PDH + UNIQUAC ρ_{max}	
T / K	$x_{IL}{}^{W}$	$x_{IL}{}^{IL}$	$x_{IL}{}^{W}$	$x_{IL}{}^{IL}$	$x_{IL}{}^{W}$	$x_{IL}{}^{IL}$	$x_{IL}{}^{W}$	$x_{IL}{}^{IL}$
293.15	0.069	0.764	0.069	0.764	0.066	0.806	0.063	0.844
296.15	0.074	0.753	0.074	0.753	0.071	0.795	0.068	0.833
298.15	0.077	0.747	0.077	0.747	0.074	0.788	0.071	0.826
303.15	0.088	0.734	0.088	0.734	0.084	0.775	0.080	0.812
308.15	0.099	0.722	0.099	0.722	0.094	0.762	0.090	0.798
313.15	0.113	0.709	0.113	0.708	0.108	0.748	0.103	0.783
318.15	0.135	0.694	0.135	0.694	0.129	0.732	0.124	0.767
323.15	0.168	0.680	0.176	0.680	0.168	0.717	0.161	0.751
328.15	0.204	0.659	0.205	0.658	0.195	0.694	0.187	0.727

Table G.13: Calculated solubility points for the [C_8mim][BF_4]/water system for the water-rich phase, $x_{IL}{}^{W}$, and for the ionic liquid-rich phase, $x_{IL}{}^{IL}$, for the UNIQUAC model and PDH + UNIQUAC model with 4 parameters for the three closest approach parameters (ρ_{min}, ρ_{med}, ρ_{max}).

	UNIQUAC		PDH + UNIQUAC ρ_{min}		PDH + UNIQUAC ρ_{med}		PDH + UNIQUAC ρ_{max}	
T / K	$x_{IL}{}^{W}$	$x_{IL}{}^{IL}$	$x_{IL}{}^{W}$	$x_{IL}{}^{IL}$	$x_{IL}{}^{W}$	$x_{IL}{}^{IL}$	$x_{IL}{}^{W}$	$x_{IL}{}^{IL}$
303.15	0.025	0.776	0.023	0.767	0.022	0.810	0.021	0.858
308.15	0.027	0.767	0.025	0.758	0.024	0.800	0.023	0.847
313.15	0.032	0.757	0.030	0.748	0.028	0.790	0.027	0.836
318.15	0.046	0.741	0.042	0.732	0.040	0.773	0.039	0.818
333.15	0.169	0.693	0.179	0.680	0.171	0.718	0.164	0.760
340.15	0.339	0.652	0.366	0.623	0.350	0.658	0.337	0.697

Table G.14: Calculated solubility points for the [C_{10}mim][BF_4]/water system for the water-rich phase, $x_{IL}{}^{W}$, and for the ionic liquid-rich phase, $x_{IL}{}^{IL}$, for the UNIQUAC model and PDH + UNIQUAC model with 4 parameters for the three closest approach parameters (ρ_{min}, ρ_{med}, ρ_{max}).

	UNIQUAC		PDH + UNIQUAC ρ_{min}		PDH + UNIQUAC ρ_{med}		PDH + UNIQUAC ρ_{max}	
T / K	$x_{IL}{}^{W}$	$x_{IL}{}^{IL}$	$x_{IL}{}^{W}$	$x_{IL}{}^{IL}$	$x_{IL}{}^{W}$	$x_{IL}{}^{IL}$	$x_{IL}{}^{W}$	$x_{IL}{}^{IL}$
293.15	0.006	0.752	0.006	0.729	0.006	0.770	0.005	0.811
296.15	0.006	0.747	0.006	0.723	0.006	0.763	0.005	0.804
298.15	0.008	0.742	0.007	0.719	0.007	0.760	0.007	0.800
303.15	0.020	0.717	0.018	0.711	0.017	0.751	0.017	0.791
308.15	0.063	0.702	0.067	0.694	0.064	0.733	0.061	0.773
318.15	0.149	0.653	0.159	0.646	0.152	0.682	0.146	0.718
323.15	0.285	0.610	0.311	0.604	0.297	0.638	0.286	0.672
325.15	0.333	0.467	0.366	0.463	0.350	0.489	0.337	0.515

Table G.15: UNIQUAC and PDH + UNIQUAC with 4 parameter deviations of composition, σ^a, obtained from LLE modeling.

Ionic liquid	$\sigma_{\mathrm{UNIQUAC}}$ %	$\sigma_{\rho_{\mathrm{min}}}$ %	$\sigma_{\rho_{\mathrm{med}}}$ %	$\sigma_{\rho_{\mathrm{max}}}$ %
$[C_2mim][NTf_2]$	5.9946	6.9698	0.5003	5.4730
$[C_3mim][NTf_2]$	6.2162	6.9875	0.7474	5.0229
$[C_4mim][NTf_2]$	5.4392	6.4979	0.7497	4.7500
$[C_5mim][NTf_2]$	8.2476	7.6524	0.5703	6.2535
$[C_6mim][NTf_2]$	5.7185	6.9909	0.7495	5.4889
$[C_7mim][NTf_2]$	5.1296	6.4461	0.7497	4.2493
$[C_8mim][NTf_2]$	5.4288	6.2583	0.7526	4.0283
$[C_4py][NTf_2]$	0.6655	1.4990	3.6565	7.2514
$[C_4mim][PF_6]$	0.4419	0.5952	3.9920	6.0763
$[C_6mim][PF_6]$	0.4620	0.9578	4.9884	8.4973
$[C_8mim][PF_6]$	0.5481	0.9952	3.9947	8.4923
$[C_6mim][BF_4]$	9.6865	9.9941	4.9940	0.4737
$[C_8mim][BF_4]$	11.9157	10.9915	5.9919	1.2422
$[C_{10}mim][BF_4]$	10.3807	10.9893	5.9898	1.4903

[a] $\sigma = \frac{1}{2n}\sum_{i=1}^{n}\left[\frac{|x_{\mathrm{exp}}{}^{\mathrm{IL}} - x_{\mathrm{calc}}{}^{\mathrm{IL}}|}{x_{\mathrm{exp}}{}^{\mathrm{IL}}} + \frac{|x_{\mathrm{exp}}{}^{\mathrm{W}} - x_{\mathrm{calc}}{}^{\mathrm{W}}|}{x_{\mathrm{exp}}{}^{\mathrm{W}}}\right] \times 100$

Appendix H – UNIQUAC interaction parameters based on the PDH + UNIQUAC model with 4 parameters

Table H.1: UNIQUAC interaction parameters for the cation, C, the anion, A, and water, W, obtained from LLE modeling with the PDH + UNIQUAC model with 4 parameters for ionic liquid/water systems.

Ionic liquid	a_{C-A} / K	b_{C-A}	a_{C-W} / K	b_{C-W}	a_{A-C} / K	b_{A-C}
$[C_2mim][NTf_2]$	0.998	3.499	-99.997	-11.000	0.998	3.499
$[C_3mim][NTf_2]$	0.971	3.100	-99.998	-10.600	0.961	3.001
$[C_4mim][NTf_2]$	0.977	2.650	-100.000	-9.997	0.971	2.690
$[C_5mim][NTf_2]$	0.997	2.299	-99.999	-9.489	0.997	2.199
$[C_6mim][NTf_2]$	0.999	1.572	-99.999	-9.089	0.999	1.752
$[C_7mim][NTf_2]$	0.999	1.377	-99.995	-8.488	0.999	1.377
$[C_8mim][NTf_2]$	0.996	0.876	-99.999	-7.999	0.939	1.144
$[C_4py][NTf_2]$	0.984	2.960	-99.997	-10.500	0.977	2.753
$[C_4mim][PF_6]$	0.854	1.410	-99.996	-9.999	0.901	1.305
$[C_6mim][PF_6]$	0.972	1.113	-99.998	-9.090	0.996	0.807
$[C_8mim][PF_6]$	0.980	0.654	-99.999	-8.100	0.979	0.404
$[C_6mim][BF_4]$	-99.997	0.655	-2.311	-9.098	-99.991	0.448
$[C_8mim][BF_4]$	-79.997	0.350	-99.959	-8.100	-79.998	0.310
$[C_{10}mim][BF_4]$	-0.998	$6.692 \cdot 10^{-6}$	-99.993	-7.101	-0.999	$5.067 \cdot 10^{-6}$

Table H.2: UNIQUAC interaction parameters for the cation, C, the anion, A, and water, W, obtained from LLE modeling with the PDH + UNIQUAC model with 4 parameters for ionic liquid/water systems.

Ionic liquid	a_{A-W} / K[a]	b_{A-W}[a]	a_{W-C} / K	b_{W-C}	a_{W-A} / K[a]	b_{W-A}[a]
[C_2mim][NTf_2]	-100.000	-7.650	0.998	-13.500	1.000	-11.650
[C_3mim][NTf_2]	-100.000	-7.650	0.916	-11.248	1.000	-11.650
[C_4mim][NTf_2]	-100.000	-7.650	0.954	-10.648	1.000	-11.650
[C_5mim][NTf_2]	-100.000	-7.650	0.997	-10.004	1.000	-11.650
[C_6mim][NTf_2]	-100.000	-7.650	0.999	-8.751	1.000	-11.650
[C_7mim][NTf_2]	-100.000	-7.650	0.999	-7.877	1.000	-11.650
[C_8mim][NTf_2]	-100.000	-7.650	0.673	-6.840	1.000	-11.650
[C_4py][NTf_2]	-100.000	-7.650	0.895	-10.832	1.000	-11.650
[C_4mim][PF_6]	1.000	-5.1000	0.897	-10.606	1.000	-6.500
[C_6mim][PF_6]	1.000	-5.100	1.103	-8.637	1.000	-6.500
[C_8mim][PF_6]	1.000	-5.100	1.021	-6.754	1.000	-6.500
[C_6mim][BF_4]	-10.000	-3.100	99.991	-8.601	-10.000	-4.000
[C_8mim][BF_4]	-10.000	-3.100	9.998	-6.711	-10.000	-4.000
[C_{10}mim][BF_4]	-10.000	-3.100	-99.782	-3.351	-10.000	-4.000

[a] The parameters that were kept constant were the ones related to the interaction between the anion and water molecules.

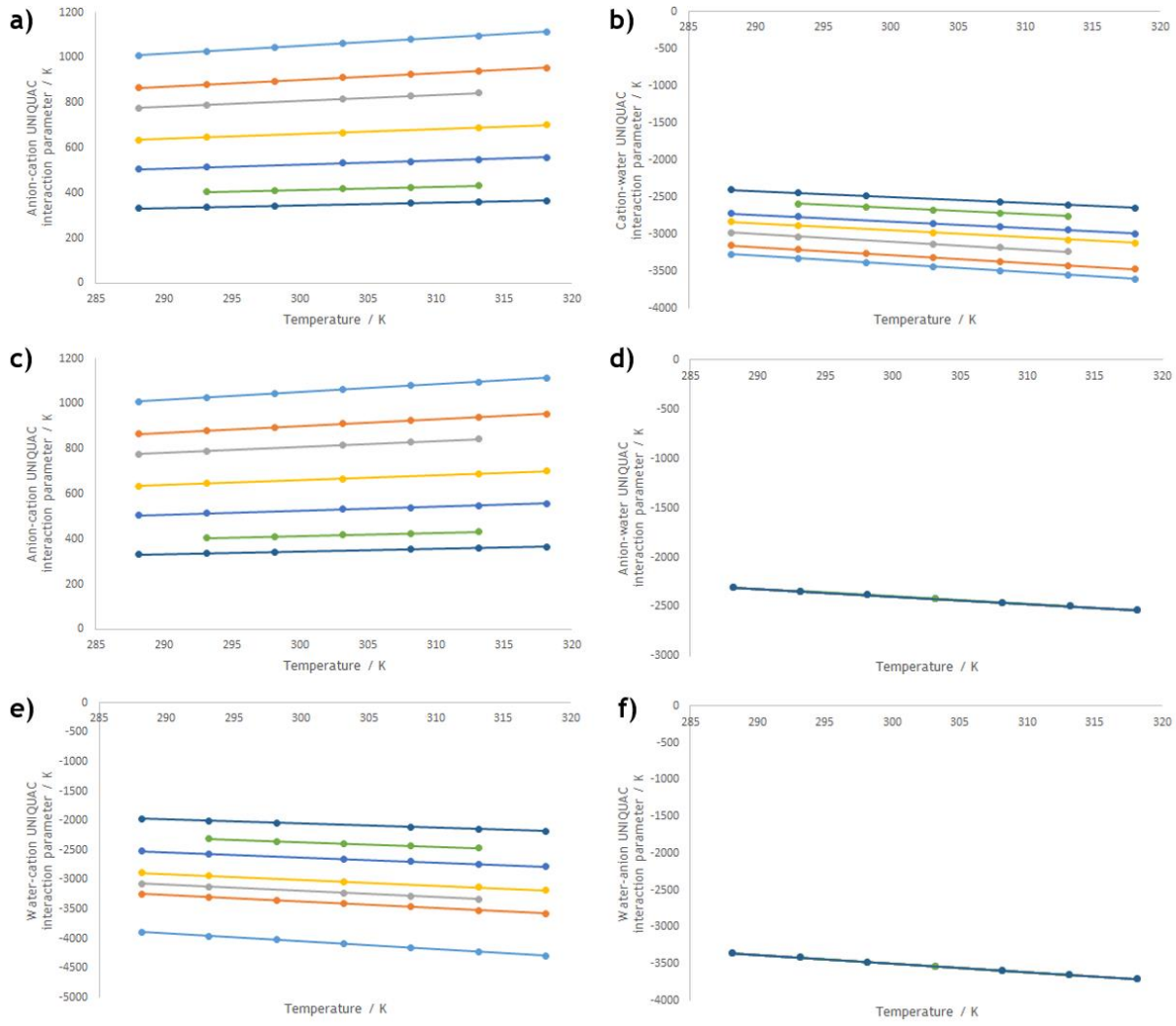


Fig. H.1: Influence of the alkyl chain length on the UNIQUAC interaction parameters for the PDH + UNIQUAC model with 4 parameters of $[NTf_2]^-$-based ionic liquids in water systems. a) cation-anion interactions, b) cation-water interactions, c) anion-cation interactions, d) anion-water interactions, e) water-cation interactions and f) water-anion interactions. The light blue line is the $[C_2mim][NTf_2]$/water, the orange line represents the $[C_3mim][NTf_2]$/water, the grey line displays the $[C_4mim][NTf_2]$/water, the yellow line portrays the $[C_5mim][NTf_2]$/water, the blue line shows the $[C_6mim][NTf_2]$/water, the green line presents the $[C_7mim][NTf_2]$/water and the dark blue line denotes the $[C_8mim][NTf_2]$/water.

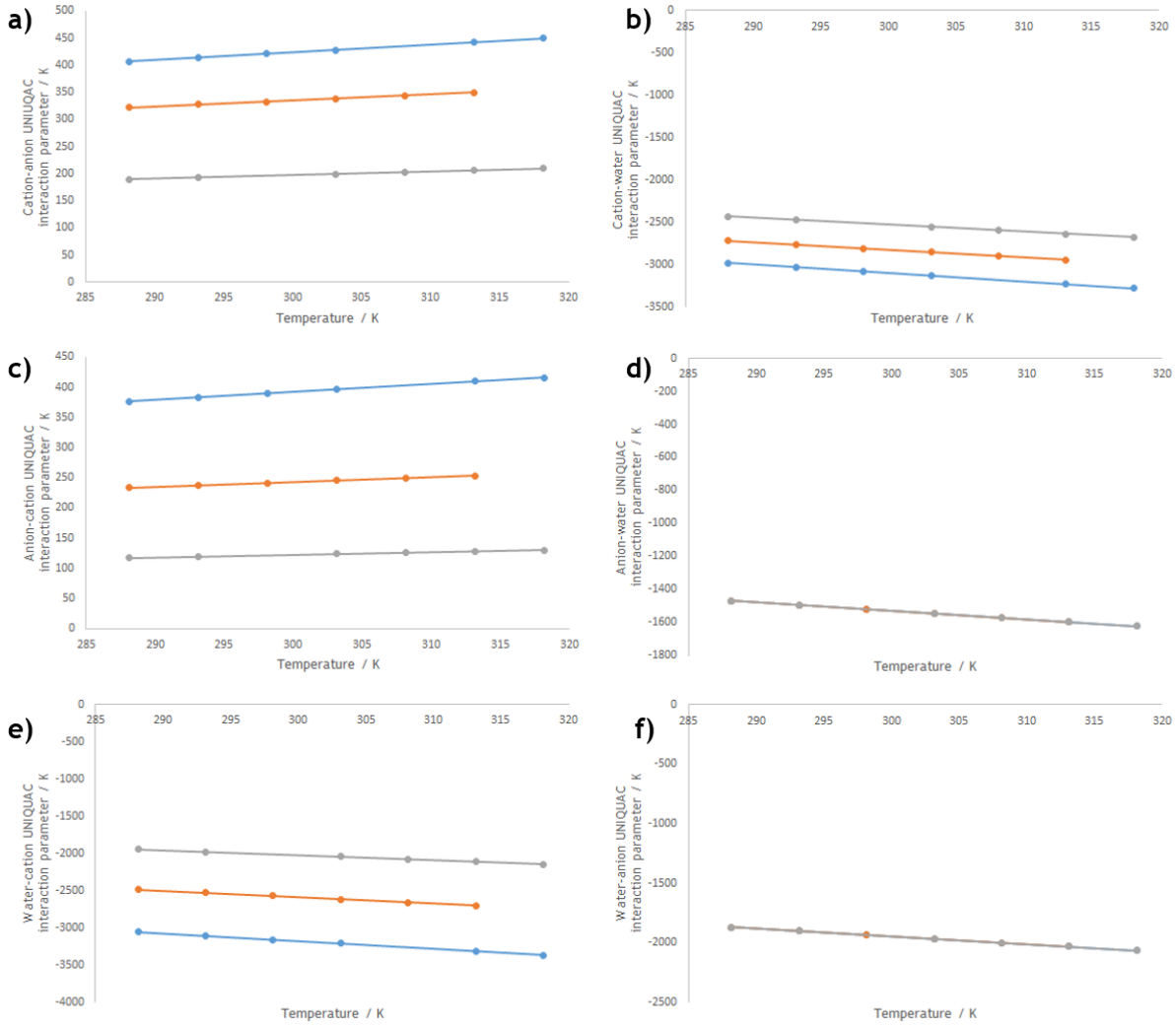


Fig. H.2: Influence of the alkyl chain length on the UNIQUAC interaction parameters for the PDH + UNIQUAC model with 4 parameters of $[PF_6]^-$-based ionic liquids in water systems. a) cation-anion interactions, b) cation-water interactions, c) anion-cation interactions, d) anion-water interactions, e) water-cation interactions and f) water-anion interactions. The light blue line is the $[C_4mim][PF_6]$/water, the orange line corresponds to the $[C_6mim][PF_6]$ and the grey line represents the $[C_8mim][PF_6]$/water.

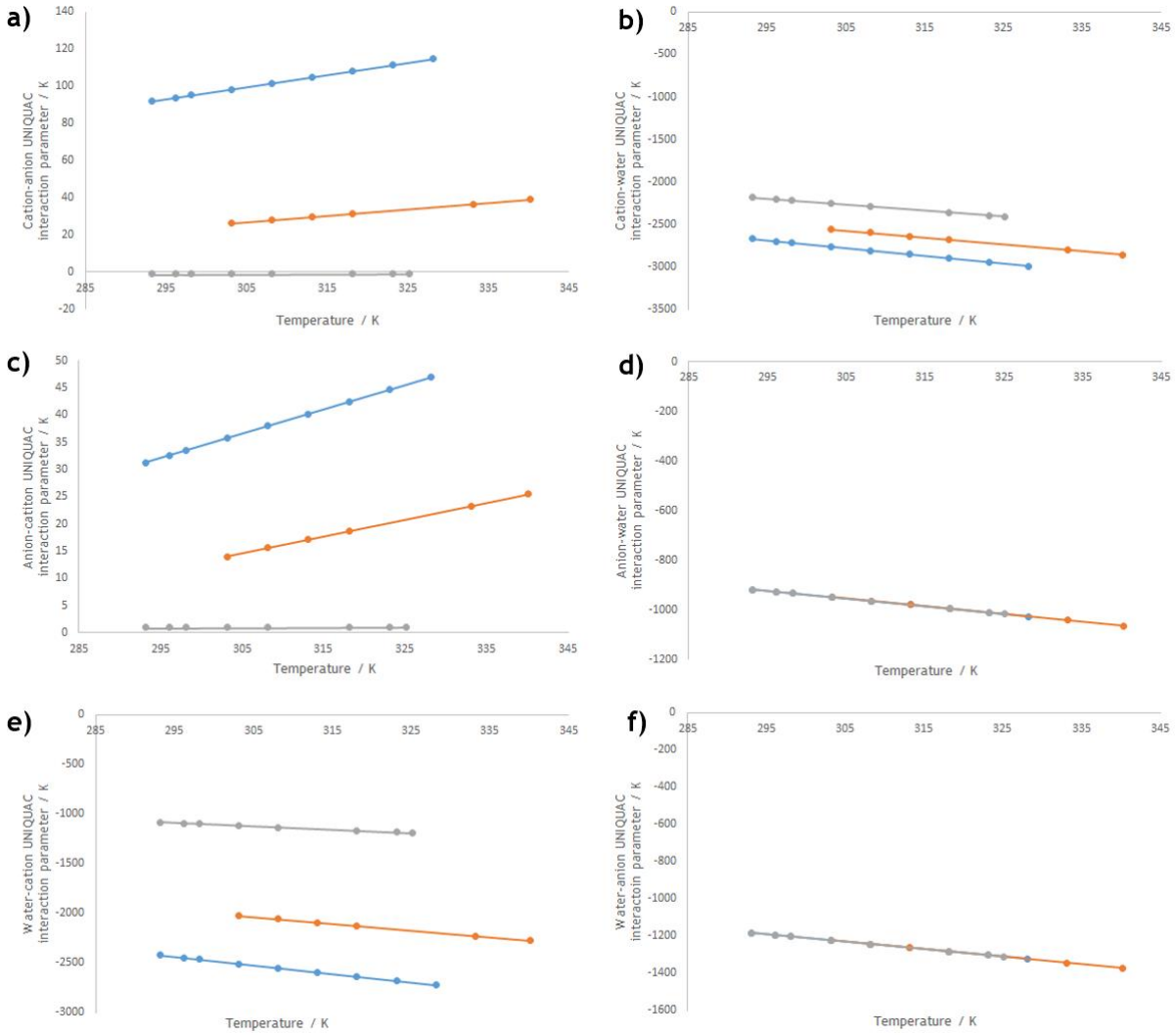


Fig. H.3: Influence of the alkyl chain length on the UNIQUAC interaction parameters for the PDH + UNIQUAC model with 4 parameters of $[BF_4]^-$-based ionic liquids in water systems. a) cation-anion interactions, b) cation-water interactions, c) anion-cation interactions, d) anion-water interactions, e) water-cation interactions and f) water-anion interactions. The light blue line is the $[C_6mim][BF_4]$/water, the orange line corresponds to the $[C_8mim][BF_4]$ and the grey line represents the $[C_{10}mim][BF_4]$/water.

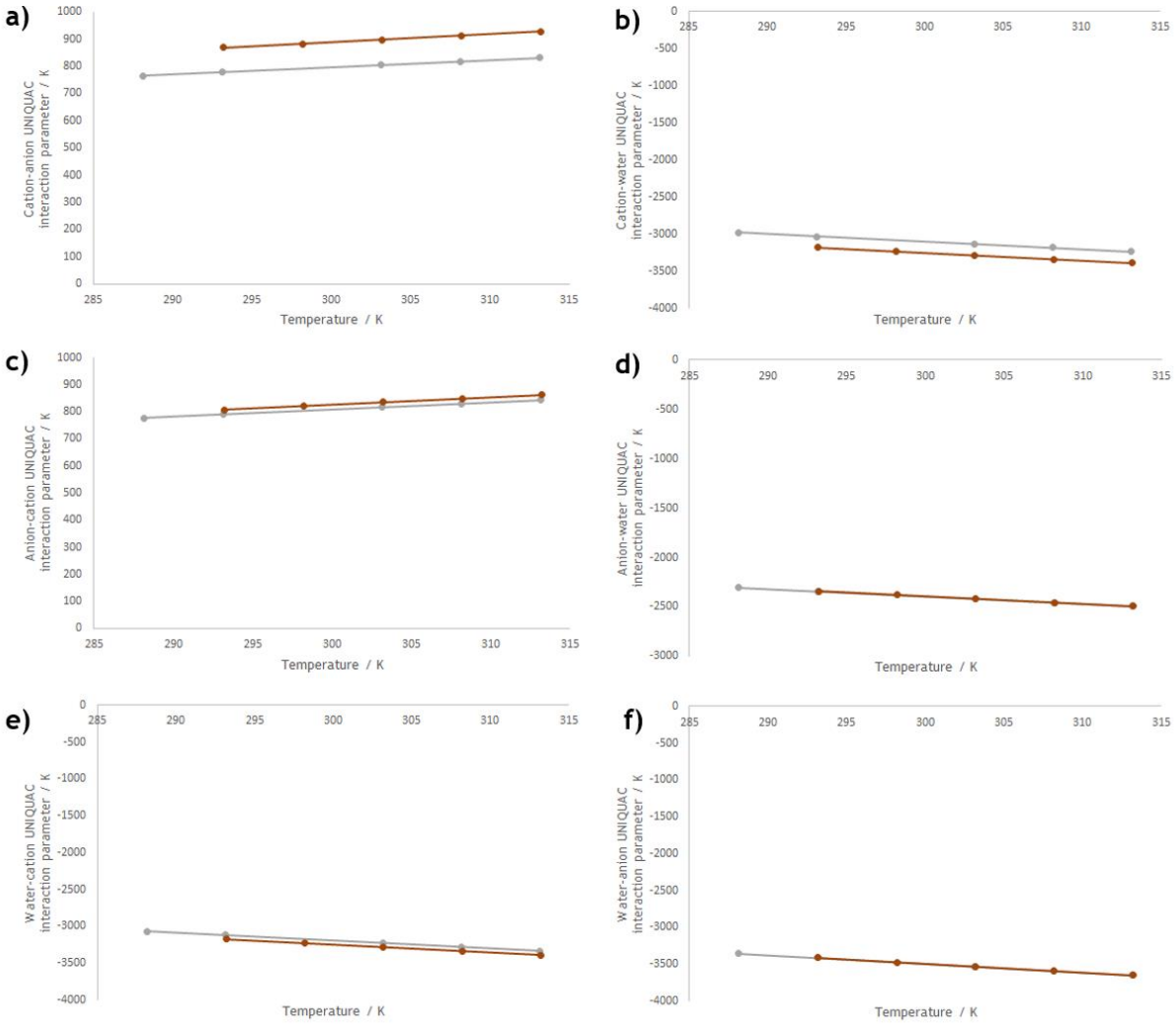


Fig. H.4: Influence of the cation on the UNIQUAC interaction parameters for the PDH + UNIQUAC model with 4 parameters of $[NTf_2]^-$-based ionic liquids in water systems. a) cation-anion interactions, b) cation-water interactions, c) anion-cation interactions, d) anion-water interactions, e) water-cation interactions and f) water-anion interactions. The brown line is the $[C_4py][NTf_2]$/water and the grey line represents the $[C_4mim][NTf_2]$/water.

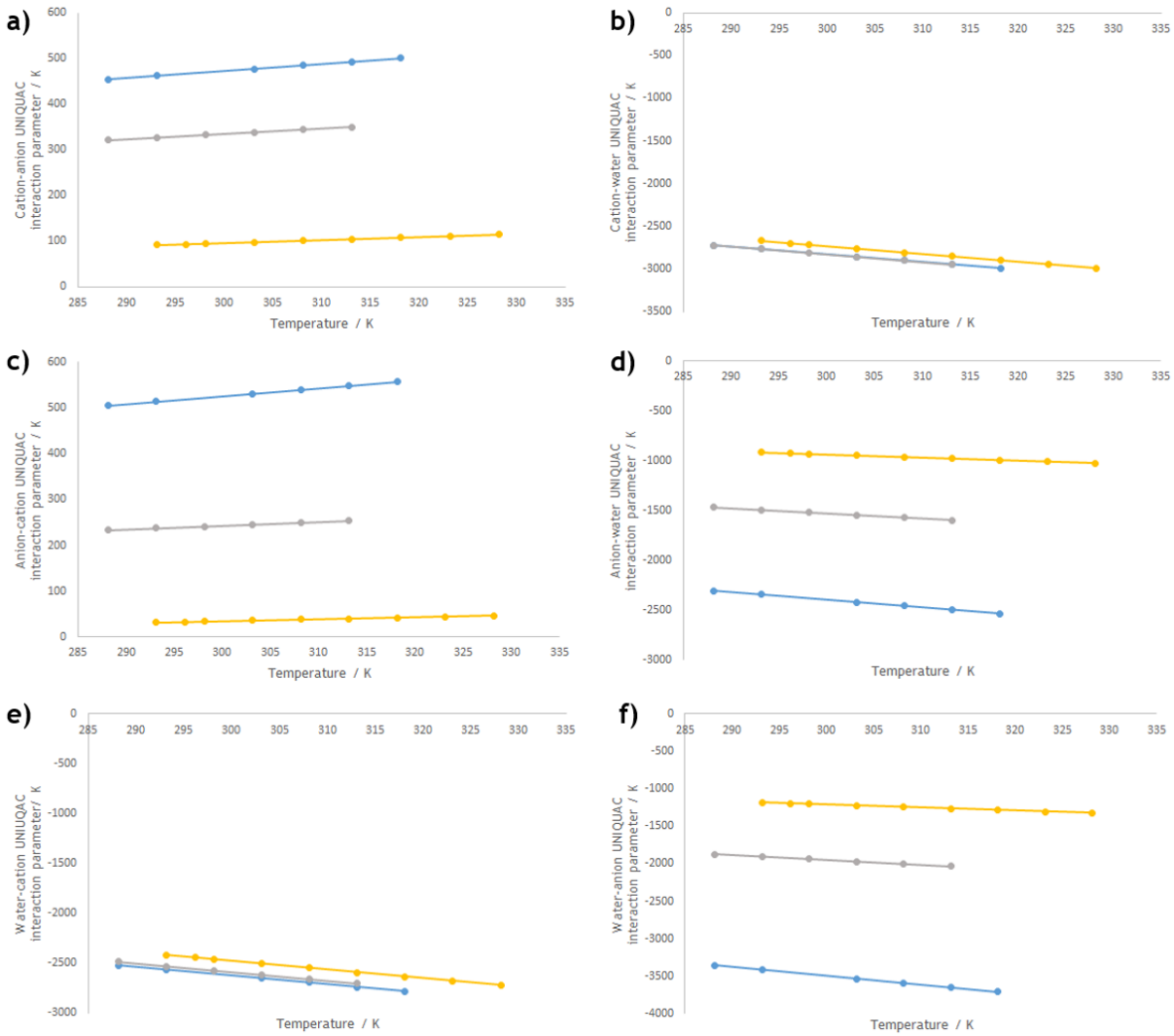


Fig. H.5: Influence of the anion on the UNIQUAC interaction parameters for the PDH + UNIQUAC model with 4 parameters of $[C_6mim]^+$-based ionic liquids in water systems. a) cation-anion interactions, b) cation-water interactions, c) anion-cation interactions, d) anion-water interactions, e) water-cation interactions and f) water-anion interactions. The yellow line is the $[C_6mim][BF_4]$/water, the grey line represents $[C_6mim][PF_6]$/water and the light blue line displays the $[C_6mim][NTf_2]$/water.

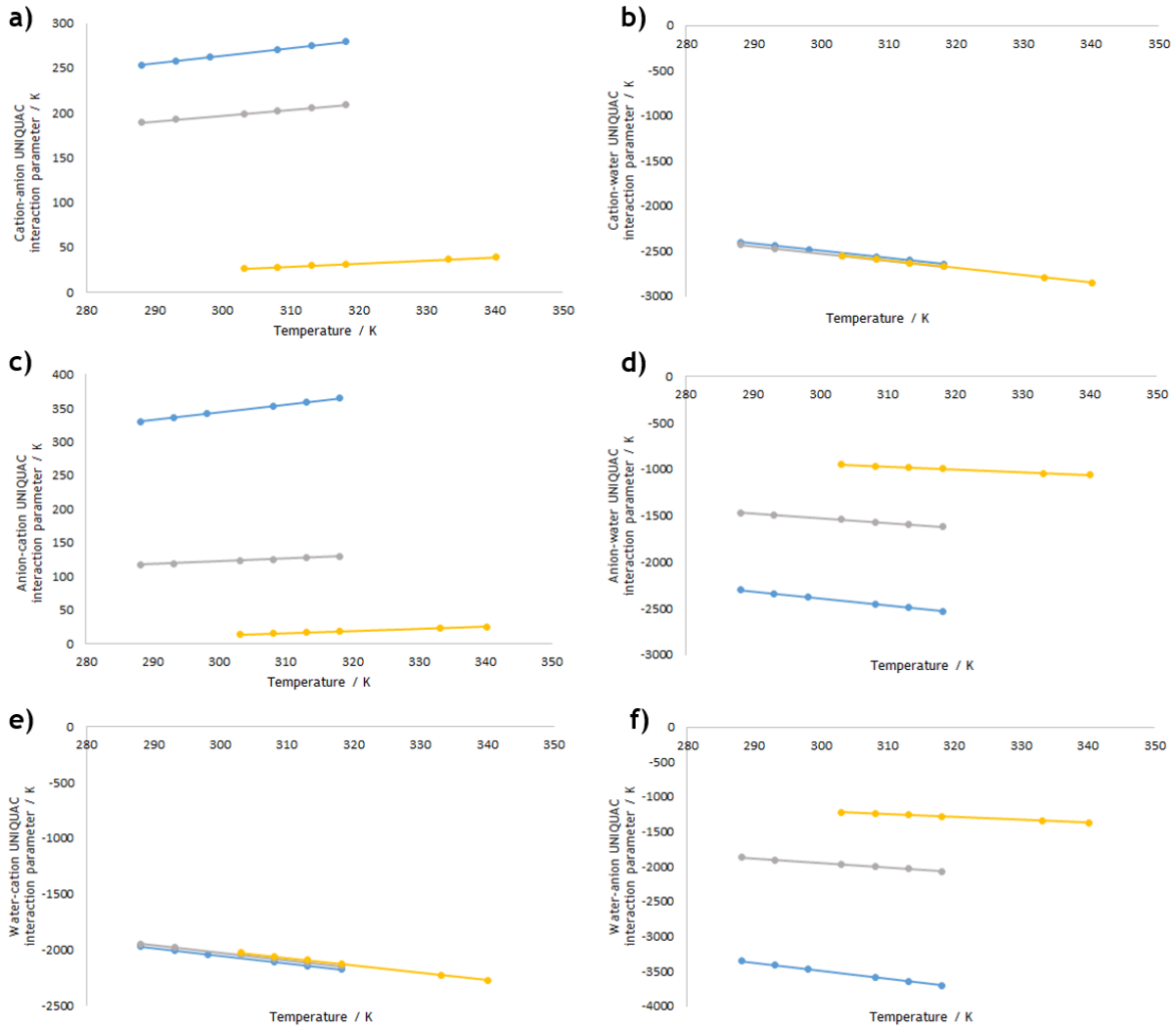


Fig. H.6: Influence of the anion on the UNIQUAC interaction parameters for the PDH + UNIQUAC model with 4 parameters of $[C_8mim]^+$-based ionic liquids in water systems. a) cation-anion interactions, b) cation-water interactions, c) anion-cation interactions, d) anion-water interactions, e) water-cation interactions and f) water-anion interactions. The yellow line is the $[C_8mim][BF_4]$/water, the grey line represents $[C_8mim][PF_6]$/water and the light blue line displays the $[C_8mim][NTf_2]$/water.